



TECHNISCHE  
UNIVERSITÄT  
DARMSTADT

---

# **Studies on the interaction of the inhibitor of apoptosis protein Survivin with DNA-dependent protein kinase to modulate DNA double-strand break repair**

---

Vom Fachbereich Biologie  
der Technischen Universität Darmstadt  
zur Erlangung des akademischen Grades eines

*Doctor rerum naturalium*

genehmigte Dissertation von

**M.Sc. Fabian Weipert**

aus Tübingen

Erstgutachter: Prof. Dr. Bodo Laube

Zweitgutachter: Prof. Dr. Markus Löbrich

Tag der Einreichung: 16.04.2018

Tag der mündlichen Prüfung: 30.05.2018

Darmstadt 2018

D 17

---

---

Weipert, Fabian: Studies on the interaction of the inhibitor of apoptosis protein Survivin with DNA-dependent protein kinase to modulate DNA double-strand break repair

Darmstadt, Technische Universität Darmstadt

Jahr der Veröffentlichung der Dissertation auf TUpriints: 2018

URN: urn:nbn:de:tuda-tuprints-74734

Tag der mündlichen Prüfung: 30.05.2018

Veröffentlicht unter CC BY-NC-ND 4.0 International

<https://creativecommons.org/licenses/>

---

---

---

## Word of Honour

---

Ehrenwörtliche Erklärung:

Ich erkläre hiermit ehrenwörtlich, dass ich die vorliegende Arbeit entsprechend den Regeln guter wissenschaftlicher Praxis selbstständig und ohne unzulässige Hilfe Dritter angefertigt habe.

Sämtliche aus fremden Quellen direkt oder indirekt übernommenen Gedanken sowie sämtliche von Anderen direkt oder indirekt übernommenen Daten, Techniken und Materialien sind als solche kenntlich gemacht. Die Arbeit wurde bisher bei keiner anderen Hochschule zu Prüfungszwecken eingereicht.

---

Fabian Weipert

Darmstadt, den 16.04.2018

---

---

## Contents

---

<b>WORD OF HONOUR .....</b>	<b>I</b>
<b>CONTENTS.....</b>	<b>II</b>
<b>LIST OF FIGURES .....</b>	<b>V</b>
<b>LIST OF TABLES .....</b>	<b>VII</b>
<b>LIST OF ABBREVIATIONS .....</b>	<b>VIII</b>
<b>1. SUMMARY.....</b>	<b>1</b>
<b>2. INTRODUCTION.....</b>	<b>4</b>
2.1. CANCER .....	4
2.2. DNA DAMAGE RESPONSE.....	5
2.2.1. DNA double-strand break repair .....	6
2.3. DNA-DEPENDENT PROTEIN KINASE.....	10
2.3.1. Characterisation of DNA-PK.....	10
2.3.2. Role of DNA-PK in non-homologous end-joining .....	11
2.4. INHIBITOR OF APOPTOSIS PROTEIN FAMILY .....	11
2.5. THE INHIBITOR OF APOPTOSIS PROTEIN SURVIVIN .....	12
2.5.1. Characterisation of Survivin .....	12
2.5.2. Survivin as a molecular target in oncology.....	17
2.6. AIM OF THE THESIS.....	18
<b>3. MATERIALS AND METHODS.....</b>	<b>19</b>
3.1. MATERIALS.....	19
3.1.1. Appliances/Instruments.....	19
3.1.2. Consumables .....	20
3.1.3. Chemicals and media.....	22
3.1.4. Solutions and buffers.....	25
3.1.5. Antibodies .....	29
3.1.6. Expression plasmids.....	31
3.1.7. Specific small interfering RNA.....	35
3.1.8. Commercial kits.....	35
3.1.9. Enzymes and respective buffers.....	35
3.1.10. Electrophoresis markers.....	36
3.1.11. Oligonucleotides.....	36
3.1.12. Cells.....	39
3.2. METHODS .....	41
3.2.1. Cell culture .....	41

3.2.2.	Freezing and thawing of cells .....	41
3.2.3.	Depletion of endogenous Survivin with siRNA .....	41
3.2.4.	Transient transfection of DNA plasmids .....	42
3.2.5.	Stable transfection.....	42
3.2.6.	Irradiation procedure .....	43
3.2.7.	Harvesting and lysis of cells.....	43
3.2.8.	Determination of protein concentration .....	44
3.2.9.	SDS polyacrylamide gel electrophoresis .....	44
3.2.10.	Coomassie Blue staining .....	45
3.2.11.	Western blotting .....	45
3.2.12.	Immunoprecipitation .....	45
3.2.13.	Vector cloning .....	46
3.2.14.	Production of bacterial GST fusion proteins and GST preparation .....	49
3.2.15.	GST pulldown assay .....	49
3.2.16.	NanoLuc Binary Technology (NanoBiT®) complementation assay .....	50
3.2.17.	Förster resonance energy transfer assay .....	51
3.2.18.	Immunofluorescence staining and imaging .....	52
3.2.19.	Homologous recombination assay .....	53
3.2.20.	DNA-PK activity assay.....	54
3.2.21.	Protein docking analysis .....	55
3.2.22.	Data analysis .....	56
<b>4.</b>	<b>RESULTS.....</b>	<b>57</b>
4.1.	THE IMPACT OF SURVIVIN ON THE DNA DOUBLE-STRAND BREAK REPAIR.....	57
4.1.1.	Survivin depletion impacts on the number of DNA double-strand breaks after irradiation with X-rays.....	57
4.1.2.	Involvement of Survivin in the non-homologous end-joining repair pathway .....	59
4.1.3.	Analysis of the involvement of Survivin in the homologous recombination repair pathway	61
4.2.	ESTABLISHMENT OF CELL LINES, STABLY EXPRESSING A SURVIVIN- $\Delta$ XIAP DELETION MUTANT	62
4.3.	INTERACTION OF SURVIVIN WITH DNA-PKCS, A KEY PLAYER OF THE NON-HOMOLOGOUS END-JOINING DNA REPAIR PATHWAY .....	63
4.3.1.	Interaction of the Survivin- $\Delta$ XIAP mutant with DNA-PKcs .....	63
4.3.2.	Interaction of Survivin with the kinase domain (PI3K) of DNA-PKcs.....	65
4.4.	THE IMPACT OF SURVIVIN ON THE ACTIVITY OF DNA-PK .....	73
4.4.1.	Survivin depletion modulates autophosphorylation of DNA-PKcs on serine 2056 .....	74
4.4.2.	XIAP binding site of Survivin is crucial for modulation of DNA-PK kinase activity .....	74
<b>5.</b>	<b>DISCUSSION.....</b>	<b>76</b>

---

<b>6. REFERENCES .....</b>	<b>85</b>
<b>7. APPENDIX .....</b>	<b>101</b>
7.1. DNA SEQUENCES .....	101
7.2. CURRICULUM VITAE.....	103
7.3. OWN WORK.....	104
7.4. ACKNOWLEDGEMENTS .....	105

---

---

## List of Figures

---

Figure 1: Schematic representation of the HR repair pathway.....	7
Figure 2: Schematic representation of the NHEJ repair pathway.....	9
Figure 3: Schematic illustration of the DNA-PKcs protein structure .....	10
Figure 4: Schematic illustration of the Survivin protein structure.....	13
Figure 5: Schematic illustration of Survivin's role in radiation response.....	15
Figure 6: Plasmid map of pEYFP-C1 (Clontech, Mountain View, CA, USA).....	31
Figure 7: Plasmid map of pEYFP-N1 (Clontech, Mountain View, CA, USA) .....	32
Figure 8: Plasmid map of pH3FE .....	33
Figure 9: Plasmid map of pGEX-5X-3 (GE Healthcare, Little Chalfont, UK) .....	34
Figure 10: Treatment with Survivin-specific siRNA results in increased numbers of $\gamma$ H2AX and 53BP1 foci in irradiated SW480 cells.....	58
Figure 11: Treatment with Survivin-specific siRNA results in increased numbers of $\gamma$ H2AX and 53BP1 foci in irradiated A2780 cells.....	59
Figure 12: Treatment with Survivin-specific siRNA results in increased numbers of $\gamma$ H2AX and 53BP1 foci in irradiated OVSAHO cells.....	60
Figure 13: Homologous recombination (HR) assay displays no involvement of Survivin in HR in SW480 cells .....	61
Figure 14: Stable transfection of colorectal cancer (SW480) and glioblastoma (LN-229) cells with Survivin-EGFP fusion constructs .....	63
Figure 15: In immunoprecipitation (IP) experiments with SW480 lysates, DNA-PKcs was found to precipitate with recombinant Survivin wt but not with the $\Delta$ XIAP deletion mutant after irradiation with 4 Gy.....	64
Figure 16: In immunoprecipitation (IP) experiments with LN-229 lysates, DNA-PKcs was found to precipitate with recombinant Survivin wt but not with the $\Delta$ XIAP deletion mutant after irradiation with 4 Gy.....	64
Figure 17: Expression of GST fusion constructs in <i>E. coli</i> BL21 for GST pulldown assay.....	66
Figure 18: GST pulldown assay in SW480 cells shows binding of Survivin to the PI3K domain of DNA-PKcs.....	67
Figure 19: Schematic representation of the NanoBiT complementation assay principle .....	68
Figure 20: Expression of Survivin-LgBiT and Survivin-SmBiT constructs in HEK-293T cells...	68
Figure 21: NanoBiT complementation assay for protein-protein interaction analysis indicates an interaction between Survivin and the PI3K domain of DNA-PKcs .....	69

---

Figure 22: Schematic representation of the Förster resonance energy transfer (FRET) principle .....	70
Figure 23: Expression of CFP/YFP-Survivin/-PI3K fusion constructs in HEK-293T cells .....	71
Figure 24: Exemplary gating strategy for FRET interaction analyses with flow cytometry.....	72
Figure 25: Flow cytometry-based FRET measurements show an interaction between Survivin and the PI3K domain of DNA-PKcs .....	73
Figure 27: Autophosphorylation of serine 2056 of DNA-PKcs is modulated by Survivin.....	74
Figure 28: XIAP binding site deletion mutant of Survivin is not able to restore DNA-PK kinase activity upon knockdown of endogenous Survivin.....	75
Figure 28: Protein docking analysis show an interaction between Survivin and DNA-PKcs ....	81
Figure 29: Survivin as a modulator of the NHEJ double-strand break repair pathway.....	83



---

---

## List of Tables

---

Table 1: Characteristics of primary antibodies used for western immunoblotting, immunoprecipitation and immunofluorescence staining .....	29
Table 2: Characteristics of secondary antibodies used for immunofluorescence staining .....	30
Table 3: Characteristics of secondary antibodies used for western immunoblotting .....	30
Table 4: Primers for cloning of the GST-PI3K construct .....	37
Table 5: Primers for cloning of the NanoBiT® Complementation Assay constructs .....	37
Table 6: Primers for cloning of the FRET constructs .....	37
Table 7: Primers used for sequencing of the cloned constructs .....	38
Table 8: Pipetting scheme for two discontinuous SDS electrophoresis gels.....	44
Table 9: Standard PCR protocol for DNA amplification with PfuUltra HF.....	46
Table 10: Composition of the transfection reagents for single or double transfections for the NanoBiT® complementation assay.....	51
Table 11: Composition of the single or double transfection reaction batches for FRET analysis .....	52
Table 12: Composition of the single or double transfection reactions for the homologous recombination assay .....	53
Table 13: Protocol for real-time PCR used for amplification of the homologous recombination product .....	54

---

---

## List of Abbreviations

---

53BP1	p53-binding protein 1
a-EJ	alternative end-joining
Amp	ampicillin
Apaf1	apoptotic protease-activating factor 1
APC	adenomatous polyposis coli gene
APS	ammonium persulfate
ATM	Ataxia telangiectasia mutated protein kinase
ATR	Ataxia telangiectasia and Rad3 related protein
BCA	bicinchoninic acid
BER	base excision repair
BIR	baculoviral IAP repeat
BLM	Blooms syndrome helicase
bp	base pairs
BRCA1/2	breast cancer type 1/2 susceptibility protein
BSA	bovine serum albumin
CDE	cell cycle-dependent element
CDK1	cyclin-dependent kinase 1
CHR	cell cycle genes homology region
c-H-Ras	v-Ha-ras Harvey rat sarcoma viral oncogene homologue
c-IAP1/2	cellular-IAP1/2
c-Myc	v-myc myelocytomatosis viral oncogene homologue
CPC	chromosomal passenger complex
Crm1	chromosome region maintenance protein 1 homolog
Da	Dalton
DAPI	4',6-Diamidin-2-phenylindol
DCA	dichloroacetic acid
DDR	DNA damage response
DHJ	double Holliday junction

---

D-loop	displacement loop
DMEM	Dulbecco's Modified Eagle Medium
DMSO	dimethyl sulfoxide
DNA	deoxyribonucleic acid
DNA-PKcs	DNA-dependent protein kinase, catalytic subunit
dNTP	deoxynucleotides
DSB	DNA double-strand break
DTT	dithiothreitol
ECFP	enhanced cyan fluorescent protein
ECL	enhanced chemiluminescent
EDTA	ethylenediaminetetraacetic acid
EGFP	enhanced green fluorescent protein
<i>E. coli</i>	<i>Escherichia coli</i>
ESCC	esophageal squamous cell carcinoma
Exo1	Exonuclease1
EYFP	enhanced yellow fluorescent protein
FAK	focal adhesion kinase
FAT	FRAP, ATM, TRRAP domain
FATC	C-terminal of FAT
FBS	fetal bovine serum
FOXO1	forkhead box O1
FRET	Förster resonance energy transfer
GST	glutathione S-transferase
Gy	Gray
HBXIP	hepatitis B X-interacting protein
HEAT	huntingtin, elongation factor 3, regulatory subunit A of PP2A, TOR1
HIF-1 $\alpha$	hypoxia inducible factor 1 $\alpha$
HR	homologous recombination
HRP	horse radish peroxidase
Hsp	heat shock protein
IAP	inhibitor of apoptosis

---

IgG	immunglobulin G
INCENP	inner centromere protein
IP	immunoprecipitation
IR	ionizing radiation
Kan	kanamycin
kb	kilo base pairs
Lig4	DNA ligase IV
MALT	mucosa-associated lymphoid tissue
MCS	multiple cloning site
MDC1	mediator of DNA damage checkpoint protein 1
MMEJ	microhomology-mediated end-joining
MOPS	3-(N-morpholino)propanesulfonic acid
MRN	Mre11/Rad50/Nbs1
MTOC	microtubule organizing centres
mTOR	mammalian target of rapamycin
Neo	neomycin
NER	nucleotide excision repair
NES	nuclear export signal
NLS	nuclear localisation signal
NF- $\kappa$ B	nuclear factor-kappa B
NHEJ	non-homologous end-joining
Notch	neurogenic locus notch homologue
NP-40	Nonidet P-40
NSCLC	non-small cell lung cancer
ori	origin of replication
Parp1	poly (ADP-ribose) polymerase 1
PBS	Dulbecco's Phosphate Buffered Saline
PCR	polymerase chain reaction
PI3K	phosphatidylinositol-3-kinase
PIKK	phosphatidylinositol 3-kinase-related kinases
PKA	protein kinase A

---

Plk1	polo-like kinase 1
PNK	polynucleotide kinase
PTEN	phosphatase and tensin homologue deleted from chromosome ten
RING	really interesting new gene
RIPA	radio-immunoprecipitation assay
RNA	ribonucleic acid
ROS	reactive oxygen species
RPA	replication protein A
RPMI	Roswell Park Memorial Institute
RT	room temperature
S, Ser	serine
SDS	sodium dodecylsulfate
SDS-PAGE	sodium dodecyl sulphate polyacrylamide gel electrophoresis
SEM	standard error of the mean
SIRT1	silent mating type information regulation 2 homologue 2
Smac	second mitochondria derived activator of caspase
Src	c-Sarcoma
SEM	standard error of the mean
STAT3	signal transduction and activator of transcription 3
T, Thr	threonine
TAE	Tris acetate EDTA
TBS	Tris-buffered saline
TBS-T	TBS-Tween 20
TCA	trichloroacetic acid
TCF4	$\beta$ -catenin/transcription factor 4
TEMED	tetramethylethylenediamin
TNF- $\alpha$	tumour necrosis factor- $\alpha$
TRAIL	TNF-related apoptosis-inducing ligand
Tris	tris hydroxymethyl aminomethane
UTR	untranslated region
UV	ultraviolet

---

WNT	wingless-related integration site
wt	wild type
XAF1	XIAP-associating factor 1
XIAP	X-linked inhibitor of apoptosis protein
XLF	XRCC4-like factor
XRCC1/2/4	X-ray cross-complementing protein 1/2/4

---

## 1. Summary

---

During the last years, the ability of tumour cells to evade apoptosis was considered to be an important mechanism to develop resistance against tumour therapies. In this context, members of the inhibitor of apoptosis protein (IAP) family gained increasing attention. Survivin, the smallest member of the IAP family, is a functionally unique protein that is involved in a variety of molecular mechanisms and cellular networks including cell proliferation, regulation of apoptosis and metastasis formation. Furthermore, an overexpression of Survivin in the tumour tissue was correlated with tumour progression as well as a decreased survival of the patients. Besides inhibition of apoptosis and its role as a member of the chromosomal passenger complex, Survivin was also found being accumulated in the nucleus after irradiation. That accumulation was linked to a modulation of DNA double-strand break repair due to its interaction with DNA repair factors such as the catalytic subunit of DNA-dependent protein kinase (DNA-PKcs).

The aim of this thesis was to gain further insight on the molecular mechanisms facilitating a Survivin-mediated regulation of DNA repair by characterising the interaction between Survivin and DNA-PKcs, a major enzyme in the non-homologous end-joining (NHEJ) DNA double-strand break repair pathway, in more detail.

Docking of Survivin wild type (wt) and a X-linked IAP (XIAP) binding site deletion mutant ( $\Delta$ XIAP) of Survivin to DNA-PKcs was evaluated in colorectal cancer SW480 and glioblastoma LN-229 cells via immunoprecipitation experiments. These experiments indicated that recombinant Survivin (wt) was able to co-immunoprecipitate with DNA-PKcs in both lines while the  $\Delta$ XIAP mutant of Survivin did not show complexation to DNA-PKcs. In case of the Aurora-B kinase it has been reported that Survivin stimulates Aurora-B kinase activity by binding to the catalytic domain. In analogy, an interaction of Survivin with the kinase domain of DNA-PKcs (PI3K) was analysed by different methods, including GST pulldown assay, NanoLuc Binary Technology (NanoBiT®) complementation assay and flow cytometry-based Förster resonance energy transfer (FRET). All of these methods confirmed an interaction between Survivin and the PI3K domain of DNA-PKcs, indicating that Survivin is binding directly to the kinase domain but not to other domains like the HEAT1 and FATC domain. Additionally, functional analysis, such as autophosphorylation of serine 2056 of DNA-PKcs, revealed a decreased DNA-PK activity after Survivin knockdown in both SW480 and LN-229 cells. Finally, attenuation of endogenous Survivin in the  $\Delta$ XIAP mutant of Survivin resulted in a decreased DNA-PK activity measured by SignaTECT kinase assay, while recombinant Survivin (wt) rescued DNA-PK activity following irradiation with 4 Gy.

In conclusion these findings for the first time indicate that Survivin not only interacts with DNA-PKcs but directly binds to its kinase domain. Thus, it modulates DNA-PKcs kinase activity and as a consequence repair of radiation induced DNA double-strand breaks. These results add a further facet to the plethora of functions exerted by the nodal protein Survivin in the cellular radiation response in cancer cells.

---

## Zusammenfassung

In den vergangenen Jahren wurde die Fähigkeit von Tumorzellen Apoptose zu umgehen bzw. zu vermeiden als zentraler Mechanismus einer Therapieresistenz erkannt. In diesem Zusammenhang gewannen auch Vertreter der *inhibitor of apoptosis protein* (IAP) Familie immer mehr an Bedeutung. Dabei spielt unter anderem Survivin, der kleinste Vertreter dieser Proteinfamilie, eine bedeutende Rolle aufgrund der universellen Überexpression in Tumorzellen. Survivin ist an einer Vielzahl molekularer Mechanismen und zellulärer Netzwerke wie beispielsweise Zellproliferation, intrazellulärer Signaltransduktion, Apoptoseregulation und Metastasierung beteiligt. Darüber hinaus konnte eine Überexpression von Survivin mit der Tumorprogression und einem schlechteren Überleben der Patienten korreliert werden. Neben der Hemmung von Apoptose und seiner Rolle in der Zellzyklusregulation ist Survivin ebenfalls bekannt dafür nach Bestrahlung im Nukleus zu akkumulieren. Dies steht im Zusammenhang mit der Rolle von Survivin bei der Regulation der DNA-Reparatur als Teil der zellulären Strahlenantwort.

In dieser Arbeit sollte der genaue molekulare Mechanismus einer Survivin-vermittelten Regulation der DNA-Reparatur untersucht werden. Dafür wurde die Interaktion zwischen Survivin und der katalytischen Untereinheit der DNA-abhängigen Proteinkinase (DNA-PKcs), einem wichtigen Faktor im *non-homologous end-joining* (NHEJ) genauer untersucht. Beim NHEJ handelt es sich um einen der beiden Hauptwege der DNA-Doppelstrangbruchreparatur.

Um die Interaktion zwischen Survivin und DNA-PKcs genauer zu verstehen, wurde die Bindung einer Deletionsmutante der *X-linked* IAP-Bindestelle ( $\Delta$ XIAP) von Survivin an DNA-PKcs mittels Immunpräzipitation untersucht. Hierbei zeigte sich sowohl in kolorektalen SW480 Karzinomzellen als auch in LN-229 Glioblastomzellen, eine Bindung des Survivin-Wildtyps an DNA-PKcs, während die Deletionsmutante der XIAP Bindestelle von Survivin nicht mehr mit DNA-PKcs präzipitieren konnte. Im Falle der Aurora-B Kinase ist bekannt, dass Survivin die Kinaseaktivität durch das Binden an deren katalytische Domäne stimuliert. Aus diesem Grund sollte im weiteren Verlauf dieser Studie eine Interaktion von Survivin mit der Kinasedomäne PI3K von DNA-PKcs mittels verschiedener Methoden wie GST *pulldown* Assay, NanoLuc *Binary Technology* (NanoBiT®) Komplementationsassay und Förster-Resonanzenergietransfer (FRET) am Durchflusszytometer untersucht werden. Durch alle verwendeten Analysemethoden konnte eine eindeutige Interaktion zwischen Survivin und der PI3K-Domäne, nicht jedoch mit anderen Domänen wie HEAT1 und FATC gezeigt werden, was auf eine direkte Bindung Survivins an die Kinasedomäne von DNA-PKcs schließen lässt. Zusätzlich zeigten funktionelle Analysen der Interaktion zwischen Survivin und DNA-PKcs, wie zum Beispiel die Detektion der Autophosphorylierung von DNA-PKcs an Serin 2056, eine verminderte Kinaseaktivität von DNA-PK nach Herunterregulation von Survivin in kolorektalen SW480 Karzinomzellen und LN-229 Glioblastomzellen. Eine Herunterregulation des endogenen Survivins in  $\Delta$ XIAP-exprimierenden Zellen und Bestrahlung mit 4 Gy zeigte eine verminderte DNA-PK-Aktivität im SignaTECT Kinase-Assay, wohingegen der rekombinante Survivin Wildtyp die Kinaseaktivität wiederherstellen konnte.

In dieser Studie konnte zum ersten Mal gezeigt werden, dass Survivin nicht nur mit DNA-PKcs interagiert, sondern direkt an dessen Kinasedomäne bindet. Durch diese Interaktion moduliert Survivin die Kinaseaktivität von DNA-PKcs und damit die Reparatur von strahleninduzierten



---

DNA-Doppelstrangbrüchen. Alles in allem wird Survivin einmal mehr seiner Rolle als Knotenpunkt-Protein in der zellulären Strahlenantwort gerecht.

---

## 2. Introduction

---

### 2.1. Cancer

---

With more than 8.8 million deaths, cancer was the second most prevalent cause of death worldwide in 2015. Almost every sixth case of death can be traced back to cancer (WHO, 2018). The number of cancer cases is still increasing due to growth and increasing age of the population (Torre et al., 2015). There are a variety of reasons for the development of cancer, although one third of all cancers are caused by behavioural and dietary reasons, e.g. obesity, low fruit and vegetable consume, lack of physical activity, smoking or alcohol abuse (Risk Factors Collaborators, 2016; Torre et al., 2015; WHO, 2018). Mainly cancer starts with genetic damage. One can discriminate between dominant damage targeting proto-oncogenes and recessive damage, which is targeting tumour suppressor genes or anti-oncogenes. Dominant damage usually leads to a gain of function, whereas recessive damage results in a loss of function. The resulting activation of oncogenes and the inactivation of tumour suppressor genes, respectively, is one basis of the transformation of a normal cell into a tumour cell (Bishop, 1987, 1991). This can be caused by mutations of genes, chromosome aberrations (Bishop, 1987; Holliday, 1979) or hypo-/hypermethylation of CpG islands in promoter regions (Jones and Laird, 1999). However, a single change within a cell is not sufficient for the development of a solid malignancy, instead multiple mutations are necessary (Kinzler and Vogelstein, 1996).

Hanahan and Weinberg first introduced the hallmarks of cancer in 2000. The hallmarks of cancer describe the acquired functional capabilities of (nearly) all human cancers during their development. These capabilities are self-sufficiency in growth signals, insensitivity to anti-growth signals, evading apoptosis, limitless replicative potential, sustained angiogenesis as well as tissue invasion and metastasis (Hanahan and Weinberg, 2000). In 2011 Hanahan and Weinberg added four additional capabilities to the hallmarks of cancer: Genomic instability and mutation can be selectively advantageous to cells, which leads to their dominance in a local tissue environment and therefore benefits tumour progression. The second one is tumour-promoting inflammation, describing an infiltration of the tumour by cells of the immune system. This tumour-associated inflammatory response can supply the tumour development with bioactive molecules like growth factors, enhancing multiple hallmark capabilities (Hanahan and Weinberg, 2011). Two other emerging hallmarks are the deregulation of cellular energetics, which describes the adjustments of the cancer cells in their energy metabolisms in order to produce enough energy for cell growth and division, and the ability of tumour cells to avoid destruction by the immune system (Hanahan and Weinberg, 2011). In contrast to the earlier view of a tumour as a collection of homogeneous cancer cells, they are now considered as complex organs. In order to understand the biology of tumours, one has to study the individual cell types within the tumour as well as its microenvironment. This tumour microenvironment contains a variety of different cell types, e.g. cancer stem cells, immune cells, pericytes, endothelial cells and cancer-associated fibroblasts (Hanahan and Weinberg, 2011).

---

Therapeutic approaches of cancer diseases vary depending on the tumour entity as well as grade and stage of the tumour. More than 60% of all cancer patients receive radiotherapy during their treatment. It can be used in adjuvant and neoadjuvant settings and in most cases radiotherapy is used in a multimodal combination together with chemotherapy and the surgical resection of the tumour. Due to new technologies, radiotherapy has strongly improved in the last years but also approaches combining tumour therapy with molecularly designed agents targeting the hallmarks of cancer have further improved the clinical outcome of the patients (Orth et al., 2014). Another upcoming therapy approach is the combined treatment of the above-mentioned treatments with immunotherapeutic strategies aiming for a stimulation of anti-tumour immune response, which can lead to improved tumour control (Scheithauer et al., 2014).

---

## 2.2. DNA damage response

---

The main goal for every living organism is to deliver intact and unchanged genetic material to its descendants. The genomic integrity is threatened by a permanent occurrence of DNA damage. This DNA damage can be caused by endogenous factors like replication errors or endogenously generated reactive oxygen species (ROS) as well as exogenous factors, for instance environmental caused DNA damage by ultraviolet (UV) light or ionizing radiation (IR). There are a variety of DNA damage lesions, of which the DNA double-strand break (DSB) is the most severe one (Jackson and Bartek, 2009; Khanna and Jackson, 2001). These breaks are more difficult to repair and even though occurring in low numbers, DSB can cause chromosomal aberrations or loss of genetic information what can lead to tumourigenesis (Khanna and Jackson, 2001).

In order to prevent transforming into a tumour cell after DNA damage, cells have developed highly coordinated mechanisms including cell cycle checkpoints, DNA repair and apoptosis, together called the DNA damage response (DDR) (Jackson and Bartek, 2009). To prevent the cells from progressing into synthesis or mitosis with damaged DNA or not fully replicated chromosomes, the progression of the cells to the next cell cycle phase can be arrested by the activation of cell cycle checkpoints. This delay enables the cell to repair DNA damage before progressing in the cell cycle (de la Torre-Ruiz and Lowndes, 2000). Depending on the existing DNA damage as well as the cell cycle phase, DNA repair pathways such as base excision repair (BER), nucleotide excision repair (NER), homologous recombination (HR) and non-homologous end-joining (NHEJ) are used to repair the damage (Branzei and Foiani, 2008; Ciccia and Elledge, 2010). If the DNA is irreparably damaged, the cell can induce the programmed cell death apoptosis in order to prevent the organism from mutations and tumour formation (Sancar et al., 2004). These DDR mechanisms are working hand in hand and their correct functioning is crucial for maintaining the genomic integrity of a cell (Sancar et al., 2004).

---

## 2.2.1. DNA double-strand break repair

---

The two major pathways for the repair of DNA DSBs are homologous recombination (HR) and non-homologous end-joining (NHEJ). HR is a rather slow but error-free DNA repair pathway that does not lose any genetic information. Since it uses homologous sister chromatids as a template for the re-synthesis of the damaged DNA, it can only take place in S and G2 phase when the sister chromatids are present (Beucher et al., 2009; van Gent et al., 2001). In contrast, NHEJ is a fast repair pathway that is not restricted to a specific phase of the cell cycle. Nevertheless the mechanism is error-prone and often results in loss of genetic information or chromosomal aberrations (Branzei and Foiani, 2008; Pfeiffer et al., 2004; Riballo et al., 2004). DNA damage caused by ionizing radiation in G2 phase is mainly repaired by NHEJ (80%) whereas HR repairs approximately 20% of the DSBs (Beucher et al., 2009). However, HR preferably repairs complex DNA damages induced by e.g. carbon ions in S and G2 phase (Shibata et al., 2011).

In the presence of DSBs, the MRN (Mre11/Rad50/Nbs1) complex binds to the break side leading to a recruitment of the ataxia telangiectasia mutated (ATM) protein kinase (Uziel et al., 2003) and its activation via autophosphorylation (Bakkenist and Kastan, 2003). Following activation, ATM phosphorylates the H2A histone variant H2AX to form  $\gamma$ H2AX, which is considered one of the earliest DSB signalling markers (Rogakou et al., 1998). Subsequently,  $\gamma$ H2AX enables the recruitment of other DNA repair factors, such as p53-binding protein 1 (53BP1), mediator of DNA damage checkpoint protein 1 (MDC1), breast cancer type 1 susceptibility protein (BRCA1) etc. to the DSB (Celeste et al., 2002; Lou et al., 2006).

### Homologous recombination

A model for HR was introduced by Robin Holliday and describes the concept of exchanging genetic information between two homologous chromosomes via the formation of so called Holliday junctions. More specifically, HR uses the undamaged sister chromatid as a template for repair by a direct interaction of the two sister chromatids. For that reason, HR is restricted to S and G2 phase of the cell cycle when a sister chromatid is present (San Filippo et al., 2008). According to the double Holliday junction (DHJ) model, HR can be divided into multiple steps. After the induction of a DSB, the 5' ends of the DSB are degraded (resection) to generate single stranded DNA. After finding a homologous region, the single-stranded DNA is invading the homologous DNA sequence, leading to the formation of a displacement loop (D-loop). Then, DNA synthesis is taking place with the homologous DNA sequence as template and thereby DHJ are formed. In the last step, the DHJ are dissolved again, what potentially leads to DNA crossover structures (San Filippo et al., 2008).

A variety of proteins are involved in the different steps of HR. In mammalian cells, resection is initialized by the MRN complex together with CtIP and processed in 3'-5' direction (Garcia et al., 2011; Makharashvili et al., 2014; Symington and Gautier, 2011) as well as the nucleases DNA2 (together with Blooms syndrome helicase, BLM) and Exonuclease1 (Exo1) in 5'-3' direction (Bolderson et al., 2010; Zhu et al., 2008). The generated single stranded DNA is covered by replication protein A (RPA) leading to a recruiting of Rad51 by Breast cancer type 2 susceptibility protein (BRCA2) to the resected DNA regions (Sorensen et al., 2005). Rad51

together with Rad54 are then catalysing the search for homology and the invasion of the homologous DNA strand (Baumann et al., 1996; Renkawitz et al., 2014). After Rad51 has been removed, synthesis of the new DNA can be started (Terasawa et al., 2007). The process ends by dissolution of DHJ (San Filippo et al., 2008). A schematic overview of the HR repair pathway is shown in Figure 1.

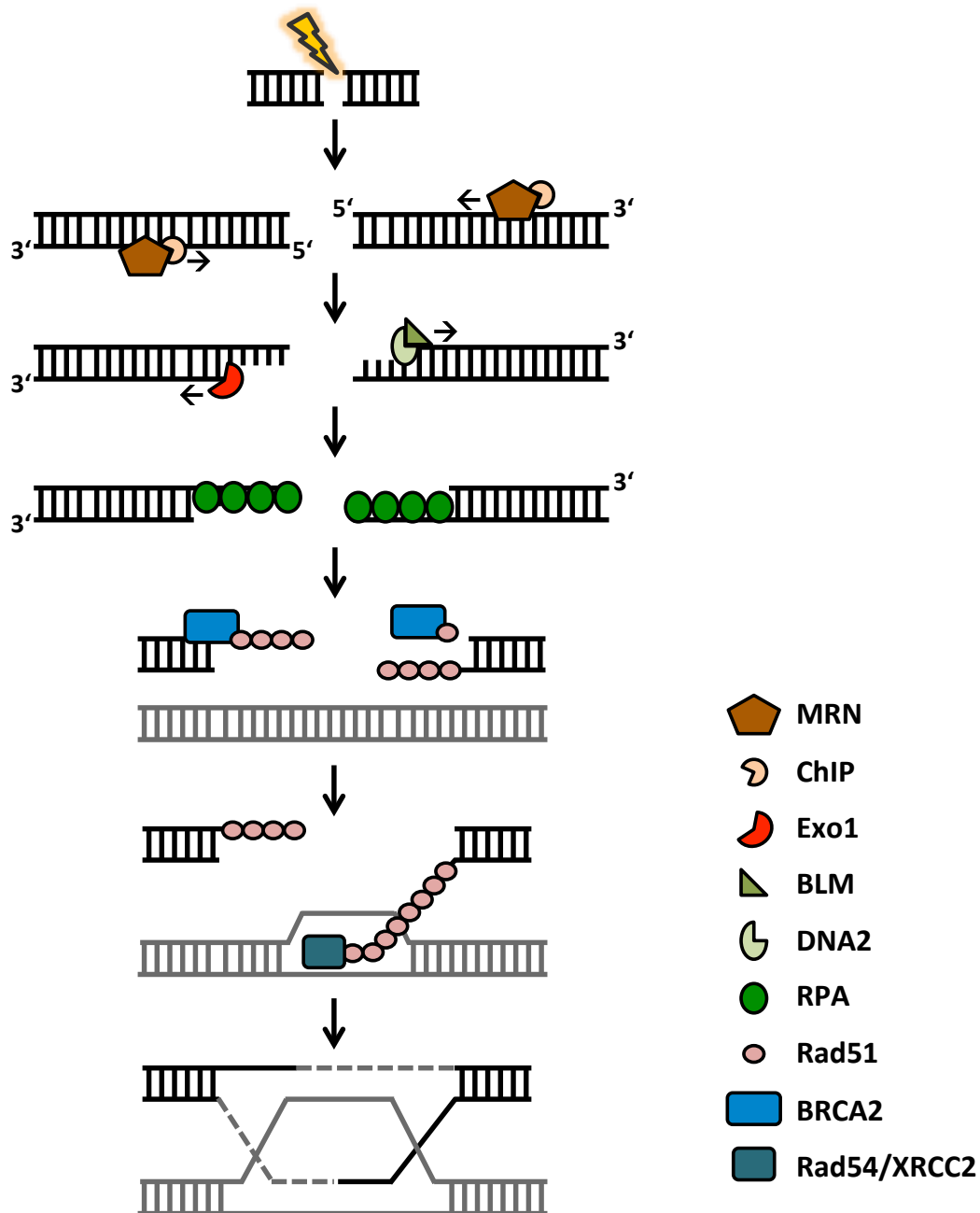


Figure 1: Schematic representation of the HR repair pathway. The first step of HR is resection, which is initialized by the MRN complex together with CtIP as well as the nucleases DNA2 (together with Blooms syndrome helicase, BLM) and Exo1 (Exonuclease 1). The generated single stranded DNA is covered by RPA (replication protein A) followed by recruitment of Rad51 by BRCA2 (Breast cancer type 2 susceptibility protein) to the resected DNA regions. Rad51 together with Rad54 are then catalysing the search for homology and the invasion of the homologous DNA strand. Following DNA synthesis, the process ends by dissolution of DHJ (double Holliday junctions). (Figure modified according to (Beucher et al., 2009))

---

## Non-homologous end-joining

Non-homologous end-joining is the predominant pathway for the repair of DSB in mammalian cells. This end-joining repair can be further divided into the canonical non-homologous end-joining (NHEJ) and alternative end-joining (a-EJ) also called microhomology-mediated end-joining (MMEJ). As suggested by their terms, NHEJ and MMEJ require no or very little homologous sequences, instead they are directly ligating the two DSB ends without the need of a sister chromatid. Therefore, NHEJ and MMEJ are independent of the cell cycle phase (Ranjha et al., 2018).

During the NHEJ, the Ku70/80 heterodimer binds to the broken DNA ends and recruits the catalytic subunit of DNA-dependent protein kinase (DNA-PKcs) generating the DNA-PK holoenzyme (Jette and Lees-Miller, 2015). Ligation of the compatible DNA ends is performed by a complex of DNA ligase IV (Lig4), X-ray cross-complementing protein 4 (XRCC4) and XRCC4-like factor (XLF). Human PAXX, a XRCC4 and XLF paralog, is interacting with Ku in order to stabilize the repair machinery (Iliakis et al., 2015; Mahaney et al., 2009; Ochi et al., 2015). Depending on the source of DNA damage, DNA ends are not compatible and cannot be ligated until processed. IR, for instance, often induces DNA ends containing damaged bases and/or backbone sugars and these must be processed before ligation. This process is executed by the nuclease Artemis, the DNA polymerases Pol  $\gamma$  and Pol  $\lambda$  or the polynucleotide kinase (PNK) (Iliakis et al., 2015; Lieber, 2010; Mahaney et al., 2009). A schematic overview of the NHEJ procedure is depicted in Figure 2.

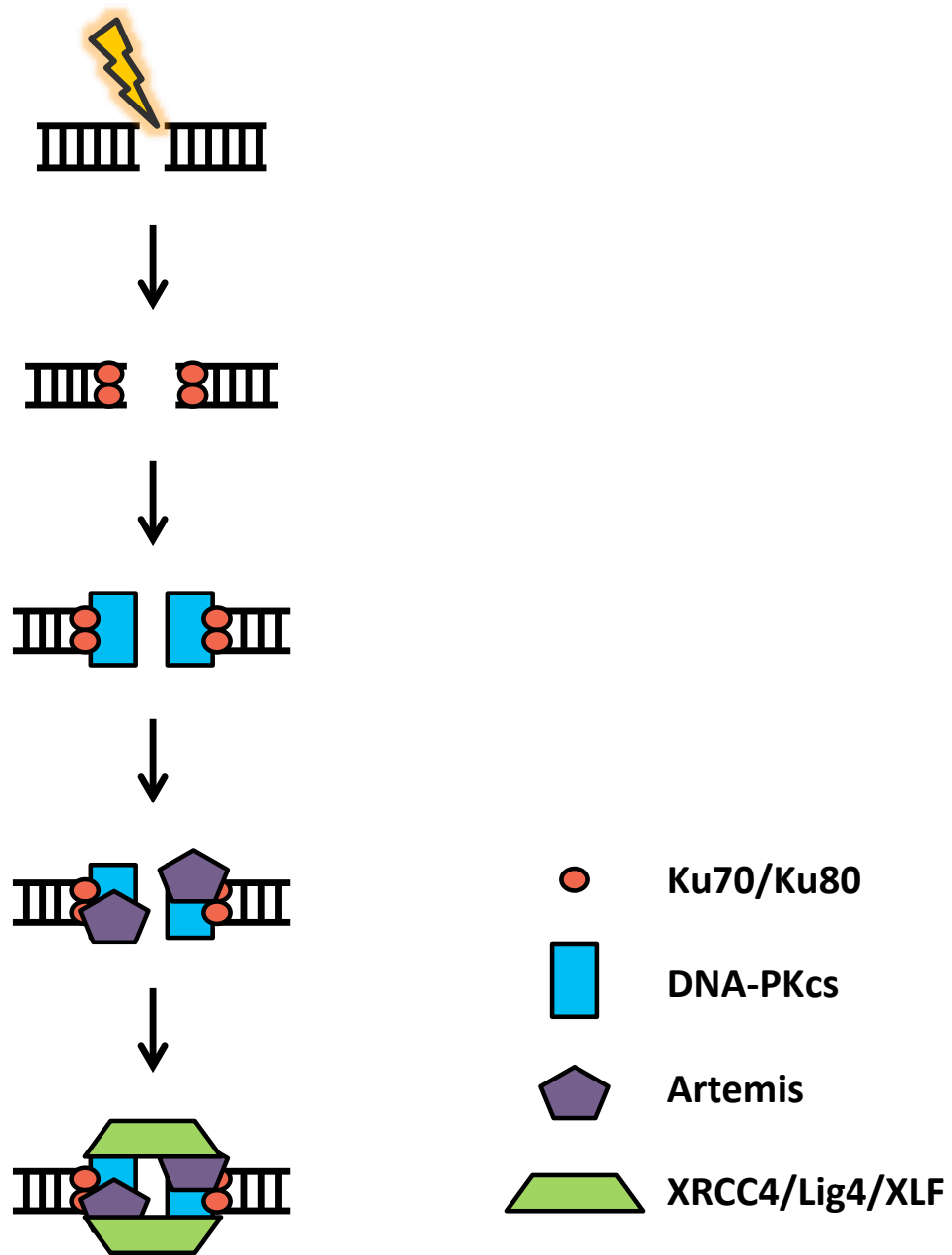


Figure 2: Schematic representation of the NHEJ repair pathway. Ku70/80 heterodimer binds to the broken DNA ends and recruits DNA-PKcs (DNA-dependent protein kinase, catalytic subunit). After minimal processing of the DNA ends by the nuclease Artemis, ligation is performed by a complex of Lig4 (DNA ligase IV), XRCC4 (X-ray cross-complementing protein 4) and XLF (XRCC4-like factor). (Figure modified according to (Beucher et al., 2009))

MMEJ is another very fast DNA DSB repair pathway that operates as a backup to the canonical NHEJ or HR in G2 phase cells. However, this backup comes at the cost of increased formation of chromosome translocations (Iliakis et al., 2015). There are a variety of proteins involved in MMEJ, including poly (ADP-ribose) polymerase 1 (Parp1), Lig1 and Lig3, XRCC1

---

and Histone H1. CtIP and Mre11 are involved in DNA end resection. Polymerase  $\theta$  is promoting MMEJ in a Parp1 dependent manner (Iliakis et al., 2015).

---

## 2.3. DNA-dependent protein kinase

---

---

### 2.3.1. Characterisation of DNA-PK

---

Anderson and colleagues first described a human DNA-activated protein kinase in 1985 (Walker et al., 1985). This serine/threonine protein kinase consists of a catalytic subunit (DNA-PKcs, 470 kDa), encoded by the *PRKDC* gene, and the heterodimer Ku70/80 ( $\approx$  150 kDa) (Collis et al., 2005; Goodwin and Knudsen, 2014; Jette and Lees-Miller, 2015). Along with ATM and Ataxia telangiectasia and Rad3 related protein (ATR), DNA-PKcs belongs to the phosphatidylinositol 3-kinase-related kinases (PIKK), a sub-family of the phosphatidylinositol-3-kinase (PI3K) group (Collis et al., 2005; Hill and Lee, 2010; Shiloh, 2003). DNA-PKcs consists of a large N-terminal  $\alpha$ -helical region including the HEAT (huntingtin, elongation factor 3, regulatory subunit A of PP2A, TOR1) repeats and the DNA interacting region, as well as a C-terminal region including the Ku interacting region and the FAT (FRAP, ATM, TRRAP), kinase and FATC (C-terminal of FAT) domain (Figure 3) (Jette and Lees-Miller, 2015). The HEAT repeats probably mediate protein-protein interactions (Andrade and Bork, 1995; Brewerton et al., 2004; Jiang et al., 2006) and facilitate bending to allow folding of the polypeptide chain into a hollow circular structure (Sibanda et al., 2010), whereas the functions of the FAT and FATC domains remain unclear. Though it is presumed, that the two domains are interacting, since they always co-occur (Bosotti et al., 2000) and that the FATC domain is required for kinase activity (Beamish et al., 2000). The amino acid sequence also contains multiple phosphorylation sites including the PQR cluster and the ABCDE cluster (Figure 3) (Cui et al., 2005; Meek et al., 2007). ATM and ATR primarily target the ABCDE cluster with the threonine (Thr, T) 2609 phosphorylation site in response to DSBs and replication stress. However, serine (Ser, S) 2056 is an autophosphorylation site in response to DSBs (Davis et al., 2014).

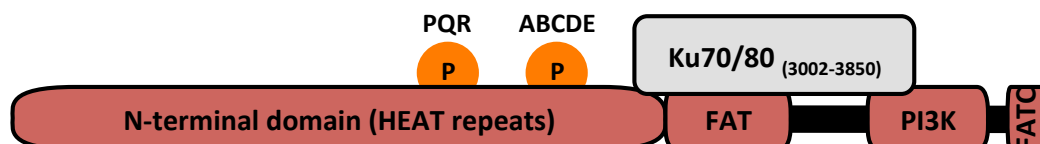


Figure 3: Schematic illustration of the DNA-PKcs protein structure. This illustration shows the functional domains of DNA-PKcs, the phosphorylation clusters PQR and ABCDE and the binding region for the heterodimer Ku70/80. HEAT (huntingtin, elongation factor 3, regulatory subunit A of PP2A, TOR1); FAT (FRAP, ATM, TRRAP); PI3K: kinase domain; FATC (C-terminal of FAT). (Figure modified according to (Jette and Lees-Miller, 2015))



---

### 2.3.2. Role of DNA-PK in non-homologous end-joining

---

The holoenzyme DNA-PK is the key enzyme of the NHEJ DNA DSB repair pathway. In the first step that triggers NHEJ, the heterodimer Ku70/80 binds to the break ends due to its high affinity to DNA ends (Critchlow and Jackson, 1998; Weterings and van Gent, 2004). Ku70/80 acts as a nodal point where the nuclease, polymerases and the ligase of the NHEJ can bind (Lieber, 2008). The recruitment of DNA-PKcs by Ku is DNA-dependent and in order to facilitate the recruitment of DNA-PKcs to the break, the Ku molecule induces an inward translocation (Lieber, 2008). This holoenzyme of Ku and DNA-PKcs is forming a DNA-binding tunnel that holds the broken DNA to protect it from unnecessary processing (Yin et al., 2017) but allows necessary modifications for the ligation (Lieber, 2010; Mahaney et al., 2009; Weterings and van Gent, 2004). The accumulation of DNA-PKcs at the break site is not influenced by its kinase activity or phosphorylation status, although an impairment of both leads to a deficient repair (Uematsu et al., 2007). Altogether DNA-PKcs has very limited kinase activity in the absence of Ku and DNA (Davis et al., 2014) and its function in NHEJ is tightly linked to its kinase activity (Jette and Lees-Miller, 2015).

DNA-PKcs can phosphorylate all of the NHEJ factors, including Ku, XRCC4, Lig4 and XLF *in vitro*, interestingly though none of these phosphorylations are actually required for NHEJ (Davis et al., 2014). However, phosphorylation of the Thr2609 cluster and autophosphorylation of Ser2056 are important for the execution of NHEJ. Upon ablation of these phosphorylation sites, cells end up with severe radiosensitization and less efficient NHEJ repair *in vitro* (Davis et al., 2014). On the other hand, autophosphorylation may also lead to a loss of kinase activity and a dissociation of DNA-PKcs from Ku (Chan and Lees-Miller, 1996; Merkle et al., 2002). A model by Uematsu and colleagues proposed that autophosphorylation of DNA-PKcs is required for destabilization of the protein-DNA complex to make the DNA ends accessible which is important to facilitate ligation of the DNA strands (Uematsu et al., 2007).

---

### 2.4. Inhibitor of apoptosis protein family

---

In 1993 an apoptosis inhibiting baculovirus gene was discovered in virally infected *Spodoptera frugiperda* insect cells (Crook et al., 1993). Since then cellular homologs have been discovered in yeast, nematodes, flies and higher vertebrates (Srinivasula and Ashwell, 2008). These members of the inhibitor of apoptosis (IAP) protein family are characterised by the existence of one, two or three baculoviral IAP repeat (BIR) motifs at their N-terminus. The BIR motif is a sequence of approximately 70 amino acids including the signature sequence CX<sub>2</sub>CX<sub>16</sub>HX<sub>6</sub>C with C=cysteine, H=histidine and X=any amino acid. It folds as three-stranded  $\beta$ -sheets surrounded by four  $\alpha$ -helices (Hinds et al., 1999; Sun et al., 1999; Sun et al., 2000; Verdecia et al., 2000), forming a hydrophobic core. At the centre of this core is a zinc ion, which is coordinated by cysteine and histidine residues (Srinivasula and Ashwell, 2008). The BIR domains function as mediators of protein-protein interactions, whereby the presence of more copies per molecule can increase the affinity for the interaction (Srinivasula and Ashwell, 2008). Regarding this, it is also known that the members of the IAP protein family bind to each other via their BIR domains. For example, the BIR domain of Survivin and two BIR domains of X-linked inhibitor of apoptosis protein (XIAP) are responsible for the formation of

---

a complex with increasing stability against proteasomal degradation, which enables them to inhibit apoptosis (Dohi et al., 2004; Srinivasula and Ashwell, 2008). In addition to the BIR domain, the majority of IAPs contain another domain that is widely distributed, the RING (really interesting new gene) domain. It contains two zinc ions that are coordinated by six or seven cysteines and one or two histidines (Weissman, 2001). RING domains can catalyse the transfer of ubiquitin to target proteins in conjunction with ubiquitin activating enzyme (E1) and ubiquitin conjugating enzyme (E2) (Lorick et al., 1999) and by providing ubiquitin protein ligase (E3) activity (Srinivasula and Ashwell, 2008).

The functions of IAPs go beyond inhibiting apoptosis. They are also known to be involved in mitotic chromosome segregation, cellular morphogenesis, copper homeostasis and intracellular signalling. The different functions are not only depending on the respective domains but also on changes in their expression level as well as on posttranslational modifications (Srinivasula and Ashwell, 2008). In particular, phosphorylation of IAPs can influence their stability, localisation within the cell and interactions with other proteins (Kuranaga et al., 2006; Oshima et al., 2006; Samuel et al., 2005). Interactions among IAPs can also affect their expression levels (Arora et al., 2007; Conze et al., 2005; Dohi et al., 2004; Silke et al., 2005).

As inhibition of apoptosis plays a major role in the formation of cancer by enabling survival in delicate conditions, it is not surprising that IAPs have been found to be overexpressed in many different tumour entities. For instance, Survivin has been shown to be highly expressed in most hematologic and solid human tumours (Altieri, 2003b; Miura et al., 2011) and elevated levels are associated with a poor prognosis of patients. This led to the hypothesis, that an overexpression of IAPs might comprise an oncogenic event (Altieri, 2003b; Duffy et al., 2007). Besides Survivin also other IAPs play a role in mammalian cancers: cellular-IAP1 (c-IAP1) promotes carcinogenesis (Hunter et al., 2007; Zender et al., 2006) and c-IAP2 is correlated with mucosa-associated lymphoid tissue (MALT) lymphoma (Inagaki, 2007). In addition to overexpression of IAPs to evade apoptosis, tumour cells can also down-regulate factors like XIAP-associating factor 1 (XAF1) that suppresses the caspase-inhibitory activity of XIAP (Liston et al., 2001; Plenchette et al., 2007).

The participation of IAPs in tumourigenesis by helping the malignant cell to avoid apoptosis, together with the discovery of IAP-regulating proteins has put this protein family in the focus of many research groups aiming for IAP-targeting strategies in order to target their function to improve cancer therapy (Wright and Duckett, 2005).

---

## **2.5. The inhibitor of apoptosis protein Survivin**

---

---

### **2.5.1. Characterisation of Survivin**

---

Survivin was first described by Ambrosini and colleagues in 1997. It was found to have a BIR domain and therefore was dedicated to the inhibitor of apoptosis protein family. The human *BIRC5* gene encodes the Survivin protein with 142 amino acids and with 16.5 kDa it is the

smallest member of the IAP protein family (Ambrosini et al., 1997). Survivin can be organized as a monomer (Altieri, 2010; Bourhis et al., 2007) or a stable homodimer (Chantalat et al., 2000; Verdecia et al., 2000). In contrast to other IAP members, Survivin has only one BIR domain and is lacking the RING domain (Ambrosini et al., 1997; Verdecia et al., 2000). At its C-terminus Survivin has an extended  $\alpha$ -helical coiled-coil domain (Ambrosini et al., 1997). Besides, Survivin contains different phosphorylation and protein binding sites, enabling interactions with a large numbers of different protein partners and being involved in multiple activities (Colnaghi and Wheatley, 2010; Dohi et al., 2007; O'Connor et al., 2002; Wheatley et al., 2007) (Figure 4).

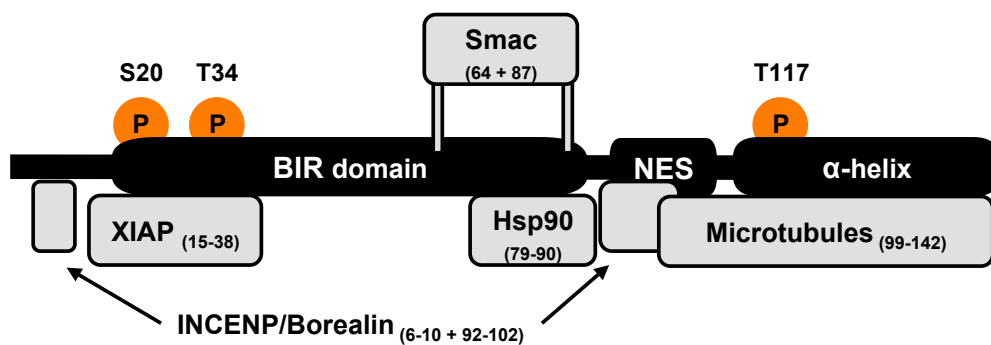


Figure 4: Schematic illustration of the Survivin protein structure. The illustration shows functional domains, binding sites and phosphorylation sites of Survivin. INCENP: inner centromere protein; XIAP: X-linked inhibitor of apoptosis protein; Smac: Second mitochondria-derived activator of caspase; Hsp90: Heat shock protein 90; NES: nuclear export signal; S20: serine 20; T34: threonine 34; T117: threonine 117. (Figure modified according to (Rodel et al., 2011))

Survivin was first described as a bifunctional protein involved in apoptosis and cell division (Altieri, 2003a; Li et al., 1998). Nowadays it is known to be a multifunctional protein, interacting with a variety of proteins in order to coordinate its function within different cellular processes (Figure 5).

When inhibiting apoptosis, Survivin, in line with most IAPs, does not bind directly to caspases (Srinivasula and Ashwell, 2008). Although the exact mechanism of apoptosis inhibition by Survivin is not entirely clear, it is believed that apoptosis inhibition is induced by a complex formation of XIAP (which can bind to caspases) and Survivin (Dohi et al., 2004). In order to form this complex, the residues 15-38 of the Survivin BIR domain (Dohi et al., 2007) interact with BIR1 and BIR3 of XIAP (Dohi et al., 2004). The Survivin-XIAP complex promotes both, Survivin and XIAP stability against proteasomal degradation leading to increased suppression of caspase-9 activity (Dohi et al., 2004). Other than that, Survivin binds to hepatitis B X-interacting protein (HBXIP) and although neither of the two proteins can interact with caspases individually, the complex is able to bind pro-caspase-9 in order to suppress apoptosis by preventing its recruitment to apoptotic protease-activating factor 1 (Apaf1) (Marusawa et al., 2003). Survivin localised in the mitochondria was found to be interacting with second mitochondria derived activator of caspase (Smac). Through binding of Smac, IAPs are losing

---

their inhibitory activity because they can no longer bind to caspase-9 leading to an activation of the latter (Du et al., 2000).

Apart from inhibiting apoptosis, the Survivin-XIAP complex is further participating in intracellular signalling pathways. The complex is directly involved in the activation of the transcription factor nuclear factor-kappa B (NF- $\kappa$ B), which leads to an increased transcription of the extracellular matrix protein fibronectin. The latter engages  $\beta$ 1 integrins at the cell surface and activation of the cell motility kinases, proto-oncogene c-Sarcoma (Src) and focal adhesion kinase (FAK). This leads to increased tumour cell migration, invasion and metastatic dissemination (Mehrotra et al., 2010).

In the nucleus, Survivin, together with the mitotic kinase Aurora-B, Borealin and the inner centromere protein (INCENP), acts as a member of the chromosomal passenger complex (CPC) (Gassmann et al., 2004; Honda et al., 2003) (Figure 5). The CPC is essential for the coordination of proper chromosome segregation and cytokinesis (Lens et al., 2006; Ruchaud et al., 2007; Yang et al., 2004). Survivin is concentrated at the inner centromeres in prophase and metaphase of mitosis, relocates to the central spindle in anaphase and accumulates at the midbody during cytokinesis (Beardmore et al., 2004; Skoufias et al., 2000; Uren et al., 2000; Wheatley et al., 2001). By interacting with the other members of the CPC, Survivin regulates chromosomal alignment, cytokinesis and chromatin-associated spindle assembly (Lens et al., 2006). Besides it stabilizes the mitotic spindle by binding to the microtubules with its C-terminal  $\alpha$ -helix and modulating microtubule dynamics (Giodini et al., 2002; Rosa et al., 2006). While Aurora-B is the enzymatic core of the CPC (Ditchfield et al., 2003; Hauf et al., 2003), Survivin directs the complex to its correct localisation (Vader et al., 2006), making it an important mitotic regulator. Accordingly, it is not surprising, that inhibition of Survivin expression result in cell division defects (Chen et al., 2000; Li et al., 1999) and homozygous deletion of the Survivin gene leads to early embryonic death (Uren et al., 2000).

Besides inhibiting apoptosis and its part in the CPC, Survivin was also found being accumulated in the nucleus following irradiation and that was linked to an involvement of Survivin in DNA double-strand break repair (Figure 5). It has been shown that Survivin interacts with DNA-PK, a major repair factor in DNA double-strand break repair, as well as MDC1,  $\gamma$ H2AX and 53BP1 in colorectal cancer cells and glioblastoma (Capalbo et al., 2010; Reichert et al., 2011).

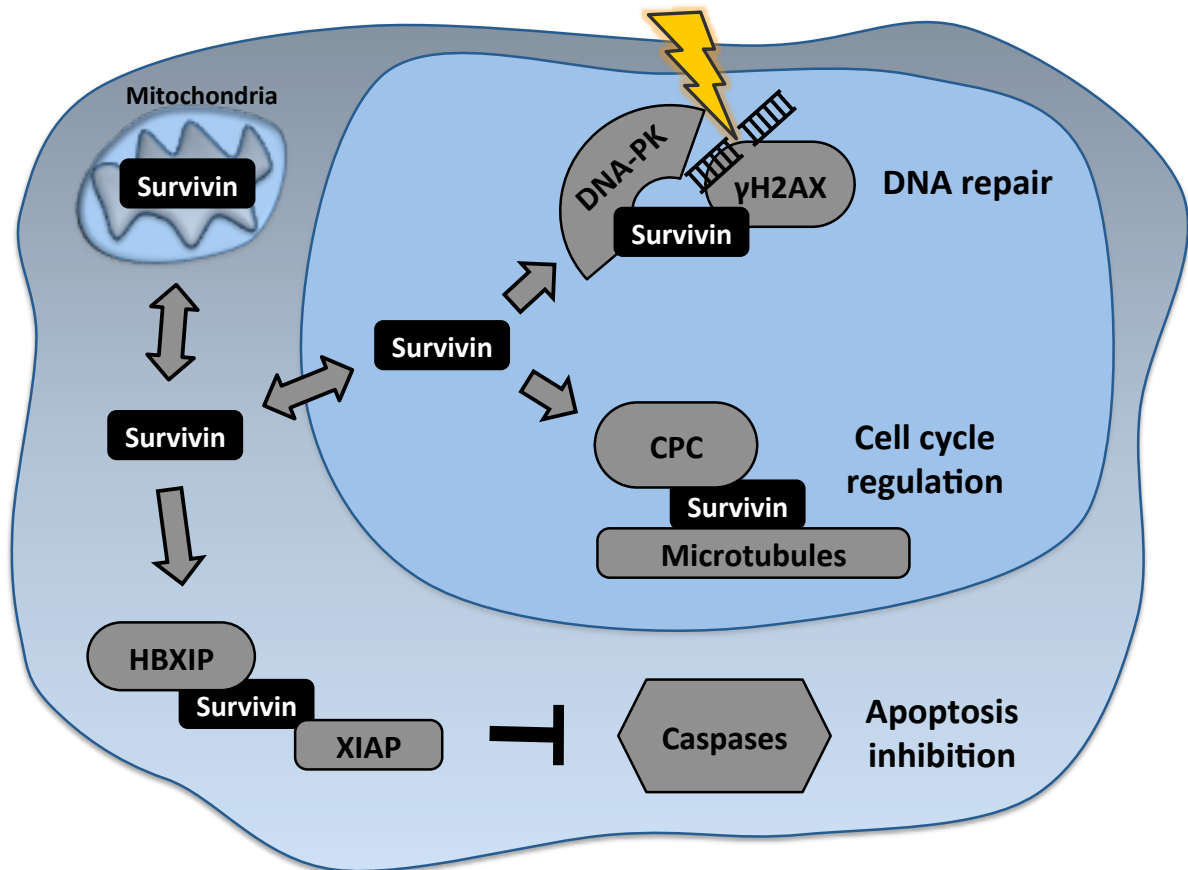


Figure 5: Schematic illustration of Survivin's role in radiation response. In the cytoplasm Survivin interacts with HBXIP or other members of the IAP family such as XIAP to inhibit apoptosis. In the nucleus it participates in cell cycle regulation as a part of the CPC. Besides it modulates DNA repair by interacting with DNA repair factors. HBXIP: hepatitis B X-interacting protein; XIAP: X-linked IAP; CPC: chromosomal passenger complex; DNA-PK: DNA-dependent protein kinase.

In line with the presence of Survivin in different subcellular pools in cytoplasm, mitochondria and nucleus, a leucine-rich nuclear export signal (NES) was described. Moreover, an interaction of this NES of Survivin with the nuclear export receptor chromosome region maintenance protein 1 homolog (Crm1) is involved in the intracellular localisation as well as cancer-relevant functions of Survivin (Colnaghi et al., 2006; Knauer et al., 2006; Stauber et al., 2006).

Interference with expression or functions of Survivin as well as other IAPs can affect cellular homeostasis leading to cancer or other human diseases. In genome wide studies comparing normal and cancer tissues, Survivin has been found to be the fourth top transcript uniformly elevated in cancers of colon, lung, breast, brain and melanoma while not or less expressed in the corresponding non-cancerous tissues (Velculescu et al., 1999). However, expression of Survivin is upregulated by various oncogenic pathways, whereas silencing of the Survivin gene is achieved by several tumour suppressor networks (Guha and Altieri, 2009). In non-cancerous cells, Survivin levels can be kept low due to the activated tumour suppressor machinery while the activation of oncogenes is associated with an inactivation of tumour

---

suppression, which is then accompanied by an induction of Survivin expression (Guha and Altieri, 2009).

In non-cancerous cells, Survivin expression is controlled in a cell cycle-dependent manner with a peak in mitosis (Li et al., 1998) and a pronounced increase in G2/M phase (Altieri, 2001; Lens et al., 2006). The regulation also involves CDE/CHR (cell cycle-dependent element/cell cycle genes homology region) elements located within the Survivin promoter (Li and Altieri, 1999).

In tumour cells, gene expression of Survivin is additionally mediated by cell cycle-independent mechanisms (Li et al., 2010; Xia and Altieri, 2006). Such mechanisms are the demethylation of CpG islands in the promoter region of Survivin (Hattori et al., 2001) or increased promoter activity (Li and Altieri, 1999) by oncologic transcription factors like v-Harvey rat sarcoma viral oncogene homologue (c-H-Ras) (Sommer et al., 2003), v-myc myelocytomatosis viral oncogene homologue (c-Myc) (Fang et al., 2009), wingless-related integration site (WNT)/ $\beta$ -catenin/transcription factor 4 (TCF4) (Kim et al., 2003), neurogenic locus notch homologue (Notch) (Lee et al., 2008), signal transduction and activator of transcription 3 (STAT3) (Gritsko et al., 2006), hypoxia inducible factor 1 $\alpha$  (HIF-1 $\alpha$ ) (Wu et al., 2010) and E2F transcription factors (Jiang et al., 2004). Besides, Survivin is a downstream target of NF- $\kappa$ B (Kawakami et al., 2005), which can be activated by growth factors, e.g. mammalian target of rapamycin (mTOR) and insulin (Vaira et al., 2007). While the above mentioned factors result in transcriptional activation, a decrease of Survivin transcript level can be mediated by wild type tumour suppressor p53 (Xia and Altieri, 2006), wild type adenomatous polyposis coli gene (APC) (Zhang et al., 2001) or phosphatase and tensin homologue deleted from chromosome ten (PTEN) (Guha et al., 2009).

The exact mechanisms of the repression or up-regulation of Survivin transcription are not yet fully understood. For p53 it is assumed that it is binding directly to the promoter region of Survivin (Hoffman et al., 2002) and that chromatin modifications within the Survivin promoter (Mirza et al., 2002) and epigenetic modifications by DNA cytosine methyltransferase 1 (Esteve et al., 2005) lead to repressed Survivin transcription by p53. In case of PTEN, repression of Survivin transcription is caused by occupation of the promoter by the transcription factors forkhead box O1 (FOXO1) and FOXO3a (Guha et al., 2009). Another Survivin promoter binding protein which represses Survivin transcription by epigenetic chromatin modifications is histone deacetylase silent mating type information regulation 2 homologue 2 (SIRT1). SIRT1 is transcribed via Breast cancer type 1 susceptibility protein (BRCA1) (Wang et al., 2008).

In addition to wild type Survivin mRNA that is predominantly present, there are at least four alternative splicing variants of Survivin mRNA (Badran et al., 2004; Caldas et al., 2005; Mahotka et al., 1999). These splicing variants differ in their cellular localisation as well as in their function in apoptosis regulation (Krieg et al., 2002; Mahotka et al., 2002).

But regulation of Survivin is not restricted to a transcriptional level. Post-transcriptional regulations of Survivin can be ubiquitylation, de-ubiquitylation (Vong et al., 2005; Zhao et al., 2000) and phosphorylation. There are three known phosphorylation sites in Survivin that are involved in different functions and phosphorylated by different kinases: Ser20 (protein kinase

---

A, PKA and polo-like kinase 1, Plk1), Thr34 (cyclin dependent kinase 1, CDK1) and Thr117 (aurora kinase B) (Colnaghi and Wheatley, 2010; Dohi et al., 2007; O'Connor et al., 2002; Wheatley et al., 2007). These post-transcriptional modifications have been implicated in protein trafficking through different cellular compartments as well as protein stabilization. Binding to the heat shock protein (Hsp) 90 chaperone stabilizes Survivin and prevents it from ubiquitin-proteasomal degradation (Fortugno et al., 2003; Zhao et al., 2000).

---

### 2.5.2. Survivin as a molecular target in oncology

---

Survivin expression has been shown to be low in most terminally differentiated tissues (Altieri, 2003b). Nonetheless, Survivin expression was found in endothelial cells, CD34 positive hematopoietic progenitor cells, basal keratinocyte stem cells and kidney tubuli cells (Fukuda and Pelus, 2006; Lechler et al., 2007). However, in most solid and liquid human tumours Survivin is highly expressed (Altieri, 2003b; Miura et al., 2011). These elevated levels of Survivin expression in tumours were associated with more aggressive clinicopathologic features, an increased risk of tumour recurrences and shortened overall survival of the patients in many different tumour entities (Altieri, 2003b; Capalbo et al., 2007; Mita et al., 2008; Rodel et al., 2012; Sprenger et al., 2011). Due to the different expression in normal tissue and cancer cells as well as the involvement in apoptosis inhibition and maintaining cancer cell viability, Survivin was supposed to be a promising target for molecular cancer therapy (Mita et al., 2008; Pennati et al., 2008). According to this, a variety of Survivin-targeting strategies have been developed including mRNA antagonization with antisense oligonucleotides, siRNAs, small molecule inhibitors or Survivin-based immunotherapy (Mita et al., 2008).

A multitude of preclinical studies performed in different cancer cell lines could show that targeting of Survivin resulted in inhibition of tumour cell proliferation and increased apoptosis along with increased sensitivity to TNF-related apoptosis-inducing ligand (TRAIL), tumour necrosis factor- $\alpha$  (TNF- $\alpha$ ) and chemotherapeutic drugs in cell culture and xenograft models (Kelly et al., 2011; Miura et al., 2011). Survivin is further known to be a radio-resistance factor, leading to a radiation sensitization effect on tumour cells upon Survivin down-regulation (Asanuma et al., 2000; Chakravarti et al., 2004; Rodel et al., 2003). A reduced clonogenic survival *in vitro* in different tumour entities as well as tumour growth retardation in xenograft models were found after Survivin depletion combined with ionizing radiation (Rodel et al., 2011). The complex mechanisms behind these findings far exceed a mere radiation-induced apoptosis (Rodel et al., 2011). Additionally, inability to repair irradiation-induced DNA damage after Survivin depletion can decrease tumour cell survival (Chakravarti et al., 2004). Besides, Survivin-specific siRNA, a small molecule inhibitor of Survivin expression (YM155) or antisense oligonucleotides showed a decreased DNA repair (Iwasa et al., 2008; Rodel et al., 2008; Rodel et al., 2005).

In addition to that, several phase I and II clinical trials targeting Survivin were performed, applying the small molecule inhibitor YM155 (Astellas Pharma Inc., Tokyo, Japan), a second generation 2'-O-methoxy-methyl modified antisense oligonucleotide (LY2181308/Gataparsen, Eli Lilly and Company, Indianapolis, IN, USA) or immunotherapeutic approaches (Rodel et al.,

---

2012). These immunotherapeutic approaches suppose that Survivin might be recognized as a “non-self” protein in cancer patients leading to an immune response against it (Andersen and Thor, 2002). Such an anti-Survivin T-cell reactivity has been detected in patients suffering from a variety of tumour entities (Schmidt et al., 2003).

---

## **2.6. Aim of the thesis**

---

As reported before, besides its role in the regulation of apoptosis and cell cycle progression, Survivin is reported to be involved in DNA double-strand break repair most likely by its interaction with DNA repair factors such as the catalytic subunit of DNA-dependent protein kinase (DNA-PKcs). The aim of the thesis was to gain further insight on the molecular mechanisms facilitating a Survivin-mediated regulation of DNA repair by further characterising the interrelationship between Survivin and DNA-PKcs, a major enzyme in the non-homologous end-joining (NHEJ) DNA double-strand break repair pathway.

For this purpose the interrelationship of Survivin and DNA-PKcs was analysed by immunoprecipitation, GST pulldown assay, NanoLuc Binary Technology (NanoBiT®) complementation assay and flow cytometry-based Förster resonance energy transfer (FRET) assay. Functional properties were analysed by autophosphorylation of serine 2056 of DNA-PKcs and kinase assays.



---

### 3. Materials and Methods

---

#### 3.1. Materials

---

##### 3.1.1. Appliances/Instruments

---

<u>Appliance/Instrument</u>	<u>Model/Description</u>	<u>Company</u>
Agarose gel electrophoresis chamber		peQLab Biotechnologie, Erlangen
Centrifuges	Mini Spin UNIVERSAL 329R MEGA STAR 1.6R	Eppendorf AG, Hamburg Hettich, Tuttlingen VWR, Darmstadt
Electrophoresis chamber for SDS gels + accessories	Mini-PROTEAN® Tetra Vertical Electrophoresis Cell	Bio-Rad, Munich
ELISA reader	TECAN infinite M200 pro	TECAN, Männedorf, Switzerland
Flow cytometer	CytoFLEX S	Beckman Coulter, Krefeld
Freezing container	Mr. Frosty™	Thermo Fisher Scientific, Dreieich
Gel electrophoresis power supply	Power Pack P25 T	Biometra, Göttingen
Heat sealer	Futura Junior	Audion, Weesp, the Netherlands
Hotplate/stirrer		VWR, Darmstadt
Imaging System	Odyssey® Fc Imaging System	LI-COR, Lincoln, NE, USA
Incubator	HERA cell 240 + 240i	Thermo Fisher Scientific, Dreieich
Laminar flow hood	HERA safe	Thermo Fisher Scientific, Dreieich
Linear accelerator	Synergy	Elekta, Crawley, UK
Magnet for Dynabeads	DynaMag™-2 Magnet	Thermo Fisher Scientific, Dreieich

Microscopes	AxioVert A1	Zeiss, Jena
	AxioManager Z1 with Axio Vision Imager Software 4.6.2. and AxioCam MRc	Zeiss, Jena
pH meter	pH Meter 765 Calimatic	Knick, Berlin
Photometer	Bio Photometer	Eppendorf, Hamburg
Real time PCR	Step One Plus	Applied Biosystems, Darmstadt
Scales	CP324S	Sartorius, Göttingen
	PRACTUM612-1S	
Semi-dry transfer system	Trans-Blot® Turbo™ Transfer System	Bio-Rad, Munich
Shakers	IKA® shaker MTS 4	IKA Labortechnik, Staufen
	IKA® KS 260 basic	IKA Labortechnik, Staufen
	IKA® LOOPSTER digital	IKA Labortechnik, Staufen
	Mixer HC	STARLAB, Hamburg
	ES-20	BioSan, Riga, Latvia
Shaker for bacteria	MaxQ 4450	Thermo Fisher Scientific, Dreieich
Thermocycler	Primus 96 advanced	PEQLab Biotechnologie, Erlangen
Ultrasonic bath	Bandelin Sonorex RK 31	BANDELIN electronic, Berlin
Vortex-Genie 2		Scientific Industries, Bohemia, NY, USA
Water bath	Typ W/B 5	Gesellschaft für Labortechnik, Burgwedel

### 3.1.2. Consumables

Description	Company
15 ml tubes	Greiner Bio-One, Frickenhausen

50 ml tubes	Greiner Bio-One, Frickenhausen
60 mm cell culture dishes	Sarstedt, Nümbrecht
100 mm cell culture dishes	Sarstedt, Nümbrecht
96-well micro-plates	Greiner Bio-One, Frickenhausen
Cell scraper M	TPP, Trasadingen, Switzerland
CELLSTAR® 6-well cell culture plates	Greiner Bio-One, Frickenhausen
CELLSTAR® 12-well cell culture plates	Greiner Bio-One, Frickenhausen
CELLSTAR® 24-well cell culture plates	Greiner Bio-One, Frickenhausen
CELLSTAR® 96-well cell culture plates	Greiner Bio-One, Frickenhausen
CELLSTAR® 96-well cell culture plates, white polystyrene wells flat bottom	Greiner Bio-One, Frickenhausen
CELLSTAR® Filter Top cell culture flasks	Greiner Bio-One, Frickenhausen
C-Chip Disposable Hematocytometer, Digital Bio	NanoEnTek, Seoul, South Korea
Cover foil, Easy seal (80x140 mm)	Greiner Bio-One, Frickenhausen
CryoPure Tube 1.8 ml	Sarstedt, Nümbrecht
Culture slides 8 chambers	BD Falcon, Erembodegem, Belgium
FACS tubes, flow cytometry	Sarstedt, Nümbrecht
Filter paper	Whatman, Kent, UK
Glass beakers	Schott, Mainz
Insulin syringes	B. Braun, Melsungen
Microscope cover glasses (24x60 mm)	Marienfeld, Lauda-Königshofen
Microscopic slides	Thermo Fisher Scientific, Dreieich
Mini-PROTEAN® TGX™ Precast Gels	Bio-Rad, Munich
Petri dish (sterile, 92x16 mm)	Sarstedt, Nümbrecht
Pipette-tips, TipOne®, graduated, blue/yellow/white	Starlab, Hamburg
Pipette-tips, TipOne®, graduated, filter tips	Starlab, Hamburg
Polystyrene Round-Bottom tubes (14 ml)	Becton Dickinson, Heidelberg

Reaction tubes (0.5 ml)	Eppendorf, Hamburg
Reaction tubes (1.5 ml)	Sarstedt, Nümbrecht
Reaction tubes (2.0 ml)	Sarstedt, Nümbrecht
LoBind reaction tubes (1.5 ml)	Eppendorf, Hamburg
Trans-Blot® Turbo™ Mini Nitrocellulose Transfer Packs	Bio-Rad, Munich

### 3.1.3. Chemicals and media

<u>Description</u>	<u>Company</u>
3-(N-morpholino)propanesulfonic acid (MOPS)	Carl Roth, Karlsruhe
4',6-Diamidin-2-phenylindol (DAPI)	Molecular Probes, Eugen, OR, USA
Agarose NEEO Ultra-Quality	Carl Roth, Karlsruhe
Acetic acid	J. T. Baker (Fisher Scientific), Schwerte
Albumin Fraction V (pH 7)	AppliChem, Darmstadt
Ammonium peroxodisulfate (APS)	Carl Roth, Karlsruhe
Ampicillin	Carl Roth, Karlsruhe
<sup>32</sup> P ATP (250 μCi)	PerkinElmer, Waltham, MA, USA
Benzonase® Nuclease	Sigma-Aldrich, St. Louis, MO, USA
Bromophenol blue	AppliChem, Darmstadt
No-Weigh™ BS <sup>3</sup>	Thermo Fisher Scientific, Dreieich
Bovine Serum Albumin (BSA)	AppliChem, Darmstadt
Calcium chloride	AppliChem, Darmstadt
CellLytic™ B Cell Lysis Reagent (2x)	Sigma-Aldrich, St. Louis, MO, USA
Coomassie Brilliant Blue G-250	Thermo Fisher Scientific, Dreieich
CytoFLEX Sheath Fluid	Beckman Coulter, Brea, CA, USA
Distilled water	Thermo Fisher Scientific, Dreieich

Deoxynucleotides (dNTP) (10 mM)	Thermo Fisher Scientific, Dreieich
Dichloroacetic acid (DCA)	AppliChem, Darmstadt
Dulbecco's Phosphate Buffered Saline (PBS)	Thermo Fisher Scientific, Dreieich
Dulbecco's Modified Eagle Medium (DMEM)	Thermo Fisher Scientific, Dreieich
Dithiothreitol (DTT)	Sigma-Aldrich, St. Louis, MO, USA
Dimethyl sulfoxide (DMSO)	AppliChem, Darmstadt
Dynabeads™ Protein G	Thermo Fisher Scientific, Dreieich
Effectene transfection reagent	QIAGEN, Hilden
Ethanol	Sigma-Aldrich, St. Louis, MO, USA
Ethylenediaminetetraacetic acid (EDTA)	AppliChem, Darmstadt
Ethidium bromide (EtBr)	Carl Roth, Karlsruhe
Fetal bovine serum (FBS)	Thermo Fisher Scientific, Dreieich
Geneticin (G418)	AppliChem, Darmstadt
Glycerine	Carl Roth, Karlsruhe
Glutathione Sepharose™ 4 Fast Flow	GE Healthcare, Little Chalfont, UK
Glycine	AppliChem, Darmstadt
Halt™ Protease Inhibitor Single-Use Cocktail	Thermo Fisher Scientific, Dreieich
Hydrogen chloride (HCl)	AppliChem, Darmstadt
IPTG BioChemica	AppliChem, Darmstadt
Isopropanol	Sigma-Aldrich, St. Louis, MO, USA
K2 transfection system	Biontex, Munich
Kanamycin	Carl Roth, Karlsruhe
LB medium	Carl Roth, Karlsruhe
LB agar	Carl Roth, Karlsruhe
Lysozyme	Sigma-Aldrich, St. Louis, MO, USA
Methanol	Sigma-Aldrich, St. Louis, MO, USA
Methylene blue C.I. 52015	AppliChem, Darmstadt
Milk powder	Carl Roth, Karlsruhe

Nonidet P-40	AppliChem, Darmstadt
Non-reducing Lane Marker, Sample Buffer	Thermo Fisher Scientific, Dreieich
Opti-MEM I	Thermo Fisher Scientific, Dreieich
Penicillin 10.000 Units, Streptomycin 10 mg/ml	Sigma-Aldrich, St. Louis, MO, USA
PerfeCTa® SYBR® Green SuperMix, ROX	Quantabio, Beverly, MA, USA
peqGREEN DNA/RNA Dye	PEQLab Biotechnologie, Erlangen
Pierce® ECL, Western Blotting Substrate	Thermo Fisher Scientific, Dreieich
Ponceau S	AppliChem, Darmstadt
Propidium iodide	Thermo Fisher Scientific, Dreieich
Ribonuclease A (RNase A; 100 mg/ml)	QIAGEN, Hilden
RNase/DNase-free water	Thermo Fisher Scientific, Dreieich
Roti-Fect PLUS	Carl Roth, Karlsruhe
Rotiphoresis gel 30	Carl Roth, Karlsruhe
Roswell Park Memorial Institute (RPMI)- 1640 medium	Thermo Fisher Scientific, Dreieich
Rubidium chloride	Sigma-Aldrich, St. Louis, MO, USA
Silicon for cloning cylinders	Momentive performance materials, Albany, NY, USA
Sodium hydroxide (NaOH)	Sigma-Aldrich, St. Louis, MO, USA
Sodium chloride (NaCl)	Sigma-Aldrich, St. Louis, MO, USA
Sodium dodecylsulfate (SDS) pellets	Carl Roth, Karlsruhe
Sodium dodecylsulfate (SDS) 20% solution	AppliChem, Darmstadt
Sodium fluoride	Sigma-Aldrich, St. Louis, MO, USA
Sodium orthovanadate	Sigma-Aldrich, St. Louis, MO, USA
Tetramethylethylenediamin (TEMED)	Carl Roth, Karlsruhe
Trichloroacetic acid (TCA)	AppliChem, Darmstadt
Trypan Blue Stain 0.4%	Thermo Fisher Scientific, Dreieich
Trypsin/Ethylene diamine tetraacetic acid	Thermo Fisher Scientific, Dreieich

(EDTA, 0.25%)	
Tween® 20	AppliChem, Darmstadt
Tris hydroxymethyl aminomethane (Tris)	Carl Roth, Karlsruhe
Triton X-100	AppliChem, Darmstadt
Vectashield® Mounting Medium	Vector, Burlingame, CA, USA
WesternSure® PREMIUM Chemiluminescent Substrate	LI-COR, Lincoln, NE, USA

---

### 3.1.4. Solutions and buffers

---

#### Immunofluorescence

DAPI staining solution	600 ng/ml in PBS
Fixing/permeabilisation solution	3.7% Formaldehyde/0.25% Triton X-100 in PBS
Blocking/antibody dilution solution	5% BSA in PBS

#### SDS-PAGE and western blotting

Radio-immunoprecipitation assay (RIPA) buffer (10x)

1.752 g	NaCl
2 ml	NP-40
1 g	DCA
1 ml	SDS (20% solution)
6.67 ml	1.5 M Tris, pH 8.0
adjust volume to 20 ml distilled water	

IP lysis buffer (1x)

2 ml	1 M Tris, pH 8.2
15 ml	1 M NaCl
1 ml	Triton X-100

---

adjust volume to 100 ml distilled water

1 M Tris HCl, pH 8.8

121.2 g      Tris

adjust volume to 1 l with distilled water

adjust pH 8.8 with HCl

1 M Tris HCl, pH 6.8

60.6 g      Tris

adjust volume to 500 ml with distilled water

adjust pH 6.8 with HCl

SDS electrophoresis buffer (10x)

30.3 g      Tris

144 g      Glycine

10 g      SDS pellets

adjust volume to 1 l with distilled water

Tris-buffered saline (TBS, 10x), pH 7.5

87.7 g      NaCl

12.1 g      Tris

adjust volume to 1 l with distilled water

adjust pH 7.5 with HCl

TBS-Tween 20 (TBS-T)

100 ml      TBS (10x)

1 ml      Tween 20

adjust volume to 1 l with distilled water



---

#### Antibody diluent

0.5 g            BSA

adjust volume to 10 ml with TBS-T

#### Milk powder solution

0.5 g            milk powder

adjust volume to 10 ml with TBS-T

#### Ponceau solution

0.5 g            Ponceau S

37.5 ml        TCA

adjust volume to 250 ml with distilled water

#### Reducing electrophoresis buffer (6x)

25 ml           Glycerol

4.63 g          DTT

5.14 g          SDS pellet

17.5 ml        1 M Tris/HCl, pH 6.8

0.25 mg        Bromophenol blue

adjust volume to 50 ml with distilled water

#### Coomassie staining solution

2.5 g            Coomassie Brilliant Blue G-250

454 ml        Methanol

92 ml          Acetic acid

adjust volume to 1 l with distilled water

mix 30 min on magnetic stirrer then filter with pleated filter

---

### Coomassie destaining solution

400 ml      Methanol

100 ml      Acetic acid

adjust volume to 1 l with distilled water

### Agarose gel electrophoresis

#### DNA loading dye Blue Run (5x)

1.25 ml      1 M Tris/HCl, pH 7.0

15 ml        0.5 M EDTA

25 mg        Bromophenol blue

12.5 ml      Glycerol

adjust volume to 50 ml with distilled water

#### Tris acetate EDTA (TAE) buffer (50x)

242 g        Tris (in 500 ml distilled water)

100 ml      0.5 M Na<sub>2</sub>EDTA, pH 8.0

57.1 ml      glacial acetic acid

adjust volume to 1 l with distilled water

### Growth media for bacteria

#### LB medium

20 g        LB medium

adjust volume to 1 l with distilled water

#### LB agar plates

35 g        LB agar

adjust volume to 1 l with distilled water

---

## Preparation of competent *Escherichia coli* (*E. coli*)

### MOPS I solution

10 ml          0.5 M MOPS  
5 ml          0.1 M RbCl  
adjust volume to 50 ml with distilled water  
adjust pH 7.0 with 1 M NaOH

### MOPS II solution

10 ml          0.5 M MOPS  
5 ml          0.1 M RbCl  
5 ml          0.7 M CaCl<sub>2</sub>  
adjust volume to 50 ml with distilled water  
adjust pH 6.5 with 1 M NaOH

---

## 3.1.5. Antibodies

---

Table 1: Characteristics of primary antibodies used for western immunoblotting, immunoprecipitation and immunofluorescence staining.

Target	Host	Type	Stock solution [ $\mu$ g/ml]	Dilution	Molecular weight [kDa]	Company	Catalogue number
Anti- $\beta$ -Actin	mouse	IgG	1000	1:10 000	42	Sigma-Aldrich	A5441
Anti-Lamin B1	mouse	IgG1-Kappa	200	1:200	68	MBL	JM-3046-100
Anti-Calnexin	mouse	IgG	250	1:500	90	BD Biosciences	610524
Anti-Survivin	rabbit	IgG	200	1:750	16.5	R&D Systems	AF886
Anti-phospho-H2AX (Ser139)	mouse	IgG1	1000	1:1000	17	Millipore	05-636

Anti-53BP1	rabbit	IgG	1	1:1000	250	Novus Biologicals	NB100-304
Anti-GFP	mouse	IgG	2000	1:1000	27	Abcam	ab1218
Anti-GFP	rabbit	IgG	2000	1:1000	27	Abcam	ab290
Anti-GST	mouse	IgG	200	1:8000	26	Santa Cruz	sc-138
Anti-DNA-PKcs	mouse	IgG	200	1:500	470	Thermo	MS-370-P0
Anti-DNA-PKcs	mouse	IgG	200	1:500	470	Abcam	ab44815
Anti-pDNA-PKcs S2056	rabbit	IgG	600	1:500	470	Abcam	ab18192
Isotype control	rabbit	IgG	2500	1:100	-	Cell Signaling	3900
Isotype control	mouse	IgG	2500	1:100	-	Cell Signaling	5415

Table 2: Characteristics of secondary antibodies used for immunofluorescence staining.

Target	Host	Type	Dilution	Label	Company	Catalogue number
Anti-rabbit	goat	IgG	1:500	Alexa Fluor <sup>R</sup> 488	Life technologies	A11034
Anti-mouse	goat	IgG	1:500	Alexa Fluor <sup>R</sup> 594	Life technologies	A11032

Table 3: Characteristics of secondary antibodies used for western immunoblotting.

Coupled enzyme	Specificity	Host	Type	Dilution	Company	Catalogue number
Horse radish peroxidase	rabbit	goat	IgG	1:1000	Southern Biotech	4050-05
Horse radish peroxidase	mouse	goat	IgG	1:1000	Southern Biotech	1030-05

### 3.1.6. Expression plasmids

#### pEYFP-C1

In addition to pEYFP-C1, pECFP-C1 was used, too. It is based on the exact same plasmid backbone, the only difference is the included fluorescence gene.

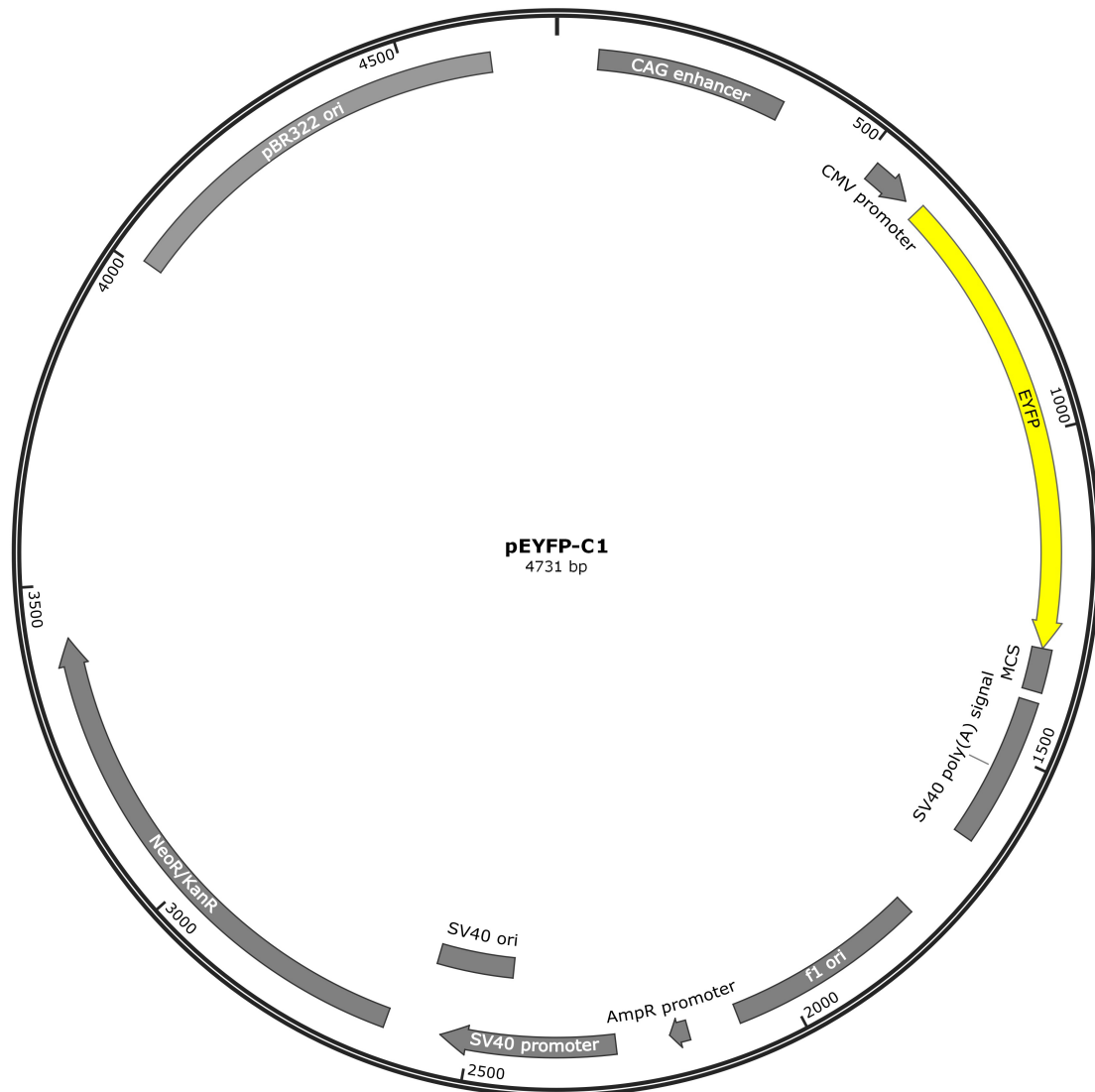


Figure 6: Plasmid map of pEYFP-C1 (Clontech, Mountain View, CA, USA). The map of the 4731 bp long plasmid shows characteristic vector elements like promoters, origins of replication (ori), a resistance gene against Neomycin/Kanamycin as well as the EYFP reporter gene (yellow) followed by the multiple cloning site (MCS) including restriction sites. The plasmid map was created with SnapGene (GSL Biotech LLC, Chicago, IL, USA).

## pEYFP-N1

In addition to pEYFP-N1, pECFP-N1 and pEGFP-N1 were used, too. They are based on the exact same plasmid backbone, the only difference is the included fluorescence gene.

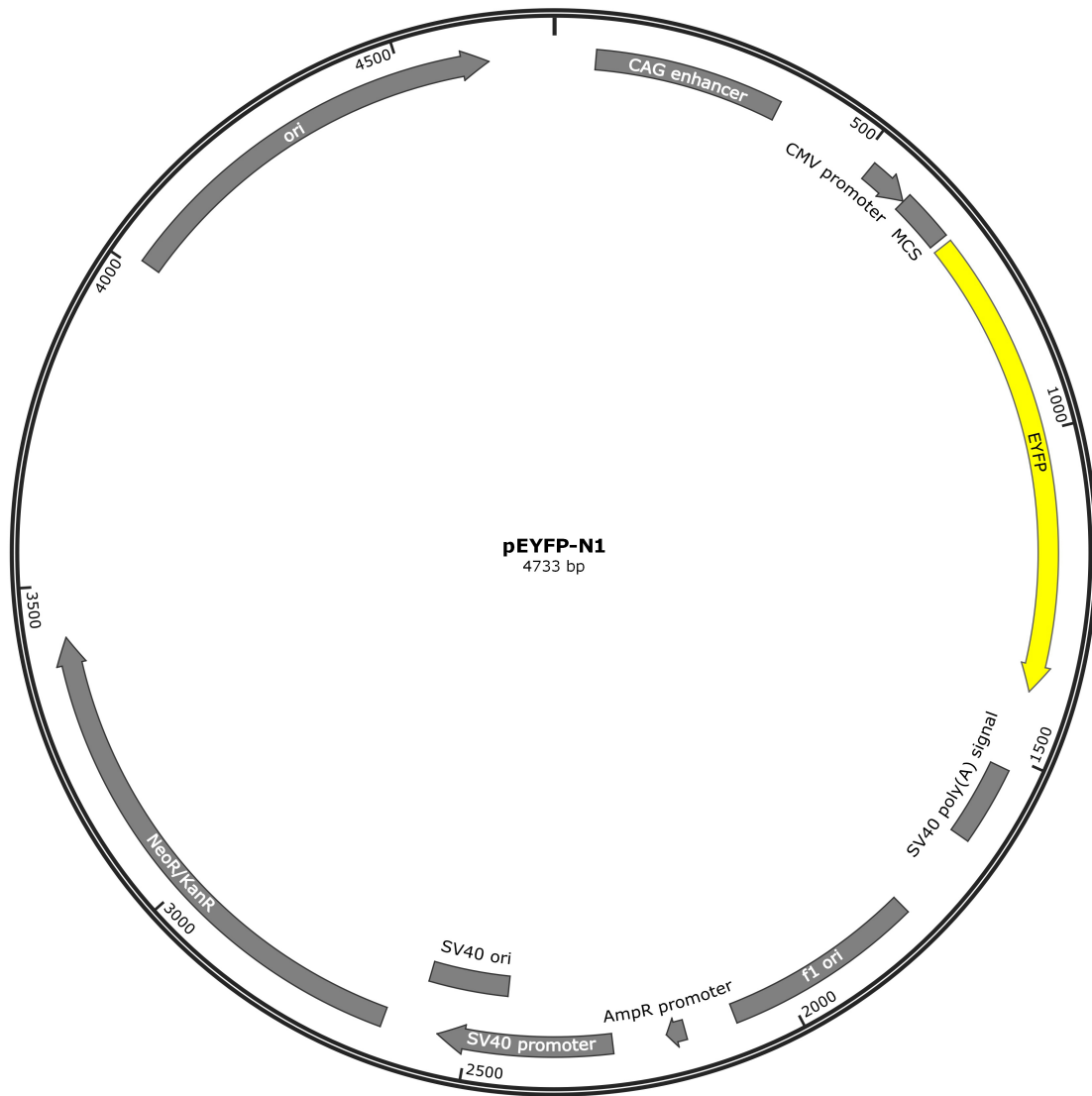


Figure 7: Plasmid map of pEYFP-N1 (Clontech, Mountain View, CA, USA). The map of the 4733 bp long plasmid shows characteristic vector elements like promoters, origins of replication (ori), a resistance gene against Neomycin/Kanamycin as well as the multiple cloning site (MCS) including restriction sites followed by the EYFP reporter gene (yellow). The plasmid map was created with SnapGene (GSL Biotech LLC, Chicago, IL, USA).

## pH3FE

This plasmid was kindly provided by Dr. Yves Matthes, AG Prof. Strebhardt, Goethe-University Frankfurt. It is derived of the pcDNA3.1/Hygro(+) plasmid (Invitrogen, Carlsbad, CA, USA) where a FLAG tag was inserted into its NheI/HindIII sites. Also the EcoRI site in this plasmid was mutated.

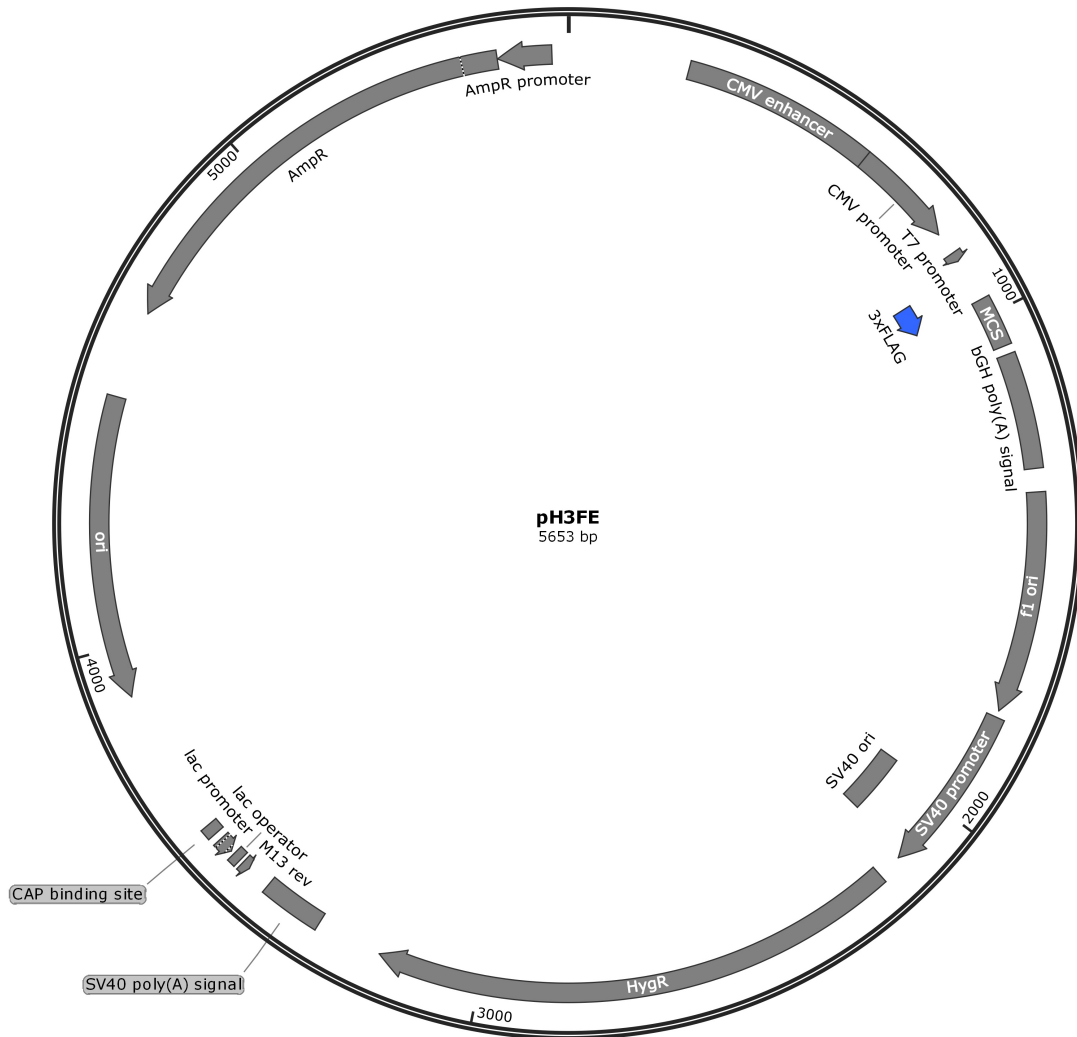


Figure 8: Plasmid map of pH3FE. This 5653 bp long plasmid is derived from the pcDNA3.1/Hygro(+) plasmid where a FLAG tag was inserted into its NheI/HindIII sites and the EcoRI site was mutated. The map shows characteristic vector elements like promoters, origins of replication (ori), a resistance gene against Ampicillin as well as the FLAG reporter gene (blue) followed by the multiple cloning site (MCS) including restriction sites. The plasmid map was created with SnapGene (GSL Biotech LLC, Chicago, IL, USA).

## pGEX-5X-3

The pGEX-5X-3 plasmid (GE Healthcare, Little Chalfont, UK) was kindly provided by Dr. Yves Matthes, group of Prof. Strebhardt, Goethe-University Frankfurt. He additionally included a KpnI restriction site to the multiple cloning site (MCS) of the plasmid.

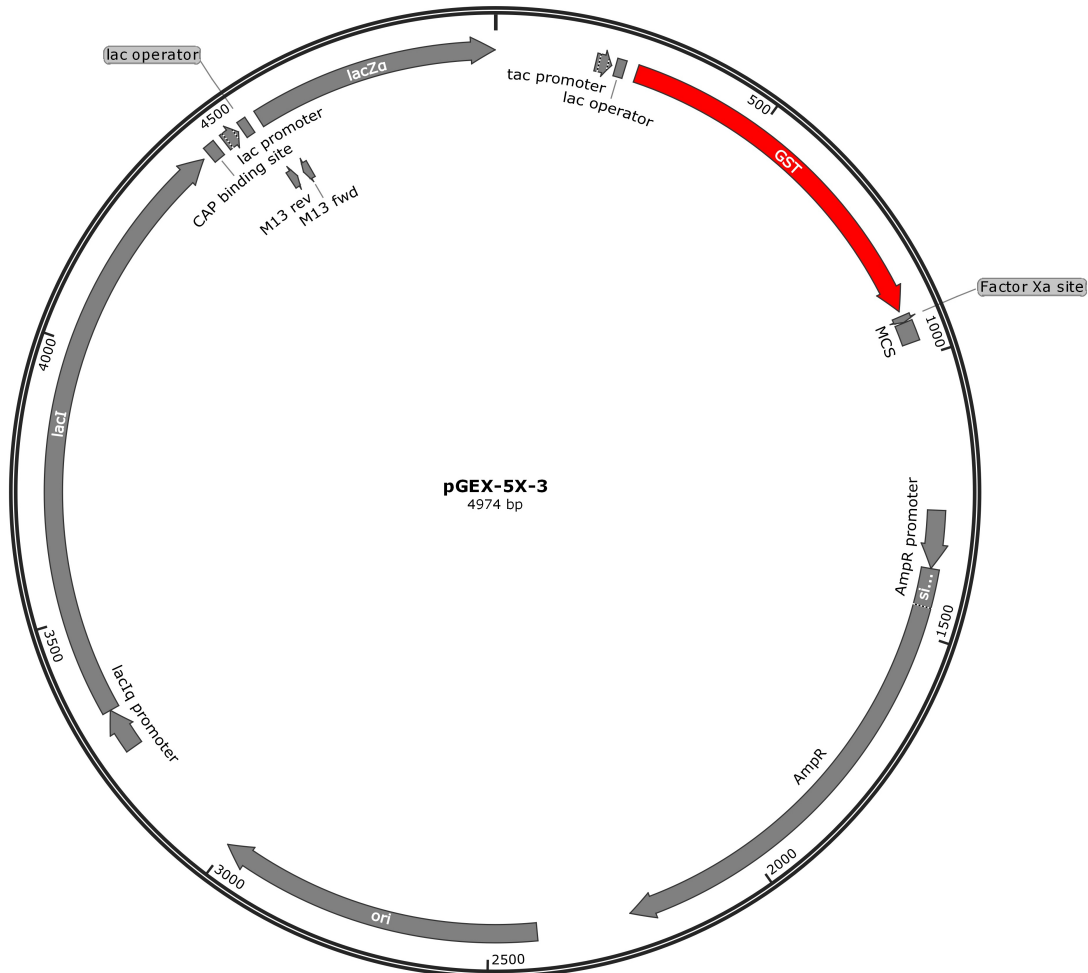


Figure 9: Plasmid map of pGEX-5X-3 (GE Healthcare, Little Chalfont, UK). The map of the 4974 bp long plasmid shows characteristic vector elements like promoters, origins of replication (ori), a resistance gene against Ampicillin as well as the GST reporter gene (red) followed by the multiple cloning site (MCS) including restriction sites. A KpnI restriction site was additionally added to the MCS. The plasmid map was created with SnapGene (GSL Biotech LLC, Chicago, IL, USA).



---

### 3.1.7. Specific small interfering RNA

---

#### Survivin specific small interfering RNA (siRNA)

Negative control siRNA	QIAGEN, Hilden
<i>BIRC5</i> Survivin 3 siRNA (#s1458)	Ambion, Austin, TX, USA
Sequence (5' → 3')	Sense: GCAGGUUCCUUAUCUGUCAtt
	Antisense: UGACAGAU AAGGAACCUGCag

---

### 3.1.8. Commercial kits

---

<u>Description</u>	<u>Company</u>
Homologous Recombination Assay Kit	Norgen Biotek, Thorold, Ontario, Canada
Micro BCA™ Protein Assay Kit	Thermo Fisher Scientific, Dreieich
NanoBiT Complementation Assay	Promega, Madison, WI, USA
Nuclear Complex Co-IP Kit	Active Motif, La Hulpe, Belgium
NucleoBond® Xtra Midi Plus EF	Macherey-Nagel, Dueren
NucleoSpin® Plasmid Kit	Macherey-Nagel, Dueren
NucleoSpin® Gel and PCR Clean-Up Kit	Macherey-Nagel, Dueren
NucleoSpin® RNA	Macherey-Nagel, Dueren
NucleoSpin® Tissue	Macherey-Nagel, Dueren
PCR Mycoplasma Test Kit	AppliChem, Darmstadt
SignaTECT® DNA-Dependent Protein Kinase Assay	Promega, Madison, WI, USA

---

### 3.1.9. Enzymes and respective buffers

---

<u>Description</u>	<u>Company</u>
PfuUltra High-Fidelity DNA Polymerase	Stratagene, La Jolla, CA, USA
PfuUltra HF Reaction Buffer (10x)	Stratagene, La Jolla, CA, USA

T4 DNA Ligase	New England Biolabs, Frankfurt
T4 DNA Ligase Buffer (10x)	New England Biolabs, Frankfurt
Taq DNA Polymerase	Sigma-Aldrich, St. Louis, MO, USA
10x PCR Reaction Buffer	Sigma-Aldrich, St. Louis, MO, USA
M-MLV Reverse Transcriptase	Promega, Madison, WI, USA
M-MLV Reaction Buffer (5x)	Promega, Madison, WI, USA
ApaLI, 10 U/ $\mu$ l	New England Biolabs, Frankfurt
EcoRI, 20 U/ $\mu$ l	New England Biolabs, Frankfurt
KpnI, 10 U/ $\mu$ l	New England Biolabs, Frankfurt
NheI, 10 U/ $\mu$ l	New England Biolabs, Frankfurt
SacI, 20 U/ $\mu$ l	New England Biolabs, Frankfurt
NEB Buffer 10x	New England Biolabs, Frankfurt

### 3.1.10. Electrophoresis markers

<u>Description</u>	<u>Company</u>
ProSieve QuadColor Protein Marker	Lonza, Cologne
GelPilot 1kb Plus Ladder	QIAGEN, Hilden

### 3.1.11. Oligonucleotides

The melting temperature ( $T_m$ ) of the oligonucleotides was calculated according to the formula from Nelson and Brutlag (1979):  $T_m = 4\text{ }^\circ\text{C} \times (G + C) + 2\text{ }^\circ\text{C} \times (A + T)$ . The oligonucleotides were ordered from Eurofins Genomics (Ebersberg, Germany). Concentration of the oligonucleotides was first adjusted to 100 pmol/ $\mu$ l and then diluted to a working concentration of 10  $\mu$ M. Oligonucleotides were stored at -20  $^\circ$ C.

## Primers for cloning of GST-PI3K

Table 4: Primers for cloning of the GST-PI3K construct. The protein of interest sequence is labelled in cyan, stop codon in red and restriction sites in yellow. fw = forward, rv = reverse.

Primer	Sequence 5' → 3'	Restriction site
PI3K_KpnI_fw	ACTGGTACCGAACACCCTTTCCTGGTGA	KpnI
PI3K_EcoRI_rv	ACTGAATTCCTTAATTTTTCCAATCAAAGGAGGG	EcoRI

## Primers for cloning of the NanoBiT® Complementation Assay constructs

Table 5: Primers for cloning of the NanoBiT® Complementation Assay constructs. The protein of interest sequences are labelled in cyan, start/stop codons in red, restriction sites in yellow and kozak sequence in grey. fw = forward, rv = reverse.

Primer	Sequence 5' → 3'	Restriction site
1.1-C-PI3K-fw	ATCTAGCTAGCGGCGGCATCGAACACCCTTTCCTGGTGAAG	NheI
1.1-C-PI3K-rv	ACTGGGAGCTCCATTTTTCCAATCAAAGGAGGGC	SacI
1.1-N-PI3K-fw	ACTGCGAGCTCAGAACACCCTTTCCTGGTGAAG	SacI
1.1-N-PI3K-rv	TACTAGCTAGCTTAATTTTTCCAATCAAAGGAGGGC	NheI
1.1-C-Surv-fw	ATCTAGCTAGCGGCGGCATGGTGCCCCGACGTTGC	NheI
1.1-C-Surv-rv	ACTGGGAGCTCCATCCATGGCAGCCAGCTGC	SacI
1.1-N-Surv-fw	ACTGCGAGCTCAGGGTGCCCCGACGTTGCC	SacI
1.1-N-Surv-rv	TACTAGCTAGCTCAATCCATGGCAGCCAGCTG	NheI

## Primers for cloning of the Förster resonance energy transfer (FRET) constructs

Table 6: Primers for cloning of the FRET constructs. The protein of interest sequences are labelled in cyan, start/stop codons in red, restriction sites in yellow and kozak sequence in grey. fw = forward, rv = reverse.

Primer	Sequence 5' → 3'	Restriction site
pECFP-C1-PI3K_fw	CGGAATTCCTGAACACCCTTTCCTGGTGAAG	EcoRI
pECFP-C1-PI3K_rev	GGGGTACCTTAATTTTTCCAATCAAAGGAGGG	KpnI

pECFP-N1-PI3K_fw	CGGAATTCGGCGGCATGGAACACCCTTTCCTGGTGAAAG	EcoRI
pECFP-N1-PI3K_rev	GGGGTACCGTATTTTTCCAATCAAAGGAGGGC	KpnI
pECFP/YFP-C1-HEAT1_fw	CGGAATTCGCGGGCTCCGGAGCCGGT	EcoRI
pECFP/YFP-C1-HEAT1_rev	GGGGTACCTTAGTTTATAACCTTGCACGG	KpnI
pECFP/YFP-N1-HEAT1_fw	CGGAATTCGGCGGCATGGCGGGCTCCGGAGCCGGT	EcoRI
pECFP/YFP-N1-HEAT1_rev	GGGGTACCGTGTTTATAACCTTGCACGGTCC	KpnI
pECFP/YFP-C1-FATC_fw	CGGAATTCCTGAAAAAAGGAGGGTCATGG	EcoRI
pECFP/YFP-C1-FATC_rev	GGGGTACCTTACATCCAGGGCTCCCAT	KpnI
pECFP/YFP-N1-FATC_fw	CGGAATTCGGCGGCATGCTGAAAAAAGGAGGGTCATGG	EcoRI
pECFP/YFP-N1-FATC_rev	GGGGTACCGTCATCCAGGGCTCCCATCCT	KpnI
pECFP-C1-Survivin_fw	CGGAATTCGGTGCCCCGACGTTGCC	EcoRI
pECFP-C1-Survivin_rev	GGGGTACCTCAATCCATGGCAGCCAGCTGC	KpnI
pECFP-N1-Survivin_fw	CGGAATTCGGCGGCATGGGTGCCCC	EcoRI
pECFP-N1-Survivin_rev	GGGGTACCGTATCCATGGCAGCCAGCTGCT	KpnI

## Primers for sequencing

Table 7: Primers used for sequencing of the cloned constructs. fw = forward, rv = reverse.

Primer	Sequence 5' → 3'	Application
pGex for	ATAGCATGGCCTTTCAGG	GST-PI3K construct
pGex rev	GAGCTGCATGTGTCAGAGG	GST-PI3K construct
Forward TK	CACCGAGCGACCCTGCAGC	NanoBiT constructs
pBiT1.1-C	TCATCCACAGGGTACACCAC	NanoBiT constructs
pBiT2.1-C + 2.1-N	CTGCATTCTAGTTGTGTTTGTCC	NanoBiT constructs
pBiT1.1-N	TCACTGCATTCTAGTTGTGG	NanoBiT constructs

pEGFPC1for	GATCACTCTCGGCATGGAC	FRET constructs
pEGFPC1rev	CATTTTATGTTTCAGGTTTCAGGG	FRET constructs
CMVfor	CGCAAATGGGCGGTAGGCGTG	FRET constructs
pEGFPN1rev	GTCCAGCTCGACCAGGATG	FRET constructs

### 3.1.12. Cells

#### Bacteria

*Escherichia coli* (*E. coli*) DH5 $\alpha$  (Promega, Madison, WI, USA) were used for all cloning procedures. For the expression of GST fusion proteins, the IPTG inducible strain *E. coli* BL21 One Shot™ BL21 Star™ (DE3) (Thermo Fisher Scientific, Dreieich) was used.

#### Human cell lines

HEK-293T: The HEK-293T cell line is a highly transfectable derivative of human embryonic kidney 293 cells. They contain the SV40 T-antigen and are competent to replicate vectors carrying the SV40 region of replication. Originally, 293T cells were referred to as 293tsA1609neo. The cells were cultured in Dulbecco's Minimal Essential Medium (DMEM) supplemented with 10% FBS, 50 U/ml penicillin and 50  $\mu$ g/ml streptomycin at 37 °C in a humidified atmosphere containing 5% CO<sub>2</sub>.

A2780: The A2780 cell line was established from human ovarian endometroid adenocarcinoma tumour tissue of an untreated patient. A2780 cells are p53 wild type. The cells were cultured in Roswell Park Memorial Institute (RPMI)-1640 medium supplemented with 10% FBS, 50 U/ml penicillin and 50  $\mu$ g/ml streptomycin at 37 °C in a humidified atmosphere containing 5% CO<sub>2</sub>.

LN-229: The LN-229 cell line was established from a right frontal parieto-occipital glioblastoma in 1979. It has a C/T mutation at codon 98 of p53. The cells were cultured in DMEM supplemented with 10% FBS, 50 U/ml penicillin and 50  $\mu$ g/ml streptomycin at 37 °C in a humidified atmosphere containing 5% CO<sub>2</sub>. LN-229 cells stably transfected with plasmids encoding different Survivin mutants were created within this work. These mutant cell lines were cultivated in DMEM supplemented with 10% FBS, 50 U/ml penicillin, 50  $\mu$ g/ml streptomycin and 750  $\mu$ g/ml G418.

---

**OVSAHO:** The OVSAHO cell line was established from a human ovarian tumour. Its p53 is mutated and BRCA2 homozygously deleted (Domcke et al., 2013). The cells were cultured in RPMI-1640 medium supplemented with 10% FBS, 50 U/ml penicillin and 50  $\mu\text{g}/\text{ml}$  streptomycin at 37 °C in a humidified atmosphere containing 5% CO<sub>2</sub>.

**SW480:** The SW480 cell line was established from a primary adenocarcinoma of the colon by A. Leibovitz in the 1970s. It has two p53 mutations, a G/A mutation at codon 273 and a C/T mutation at codon 309. The cells were cultured in DMEM supplemented with 10% FBS, 50 U/ml penicillin and 50  $\mu\text{g}/\text{ml}$  streptomycin at 37 °C in a humidified atmosphere containing 5% CO<sub>2</sub>. SW480 cells stably transfected with plasmids encoding different Survivin mutants were kindly provided by Dr. Chrysi Petraki. These mutant cell lines were cultivated in DMEM supplemented with 10% FBS, 50 U/ml penicillin, 50  $\mu\text{g}/\text{ml}$  streptomycin and 750  $\mu\text{g}/\text{ml}$  G418.

---

## 3.2. Methods

---

### 3.2.1. Cell culture

---

The respective cell lines were passaged every 3 to 4 days at a confluency of about 90%. Therefore, the cell culture medium was removed, cells were washed with 10 ml PBS and detached using 2 ml trypsin/EDTA and incubation for approximately 5 min at 37 °C and 5% CO<sub>2</sub>. The trypsin/EDTA reaction was stopped and the cells resuspended by adding the respective cell culture medium. The cell suspension was then diluted 1:4 – 1:12 according to the different cell lines and plated on T-75 flasks with 12 ml of the respective medium (3.1.12).

Depending on the experiments, different numbers of cells were seeded. Therefore, they were counted in chamber slides (NanoEnTek) following trypsinization. Trypan blue staining was used to differentiate between living and dead cells. The number of viable cells was quantified according to the manufacturers instructions.

Cell culture supernatants were regularly checked for contaminations with mycoplasma via a PCR-based mycoplasma test kit.

---

### 3.2.2. Freezing and thawing of cells

---

For freezing, cells were washed with PBS, trypsinized, centrifuged (100 x g, 5 min, room temperature (RT)), resuspended in precooled cryomedium (DMEM/RPMI + 20% FBS + 5% DMSO) and 1 ml, including 1 x 10<sup>6</sup> cells, was transferred into each cryotube. Those were then stored in a freezing container at -80 °C to allow gentle cooling by 1 °C per hour. The next day, the cryotubes were transferred into storage boxes and kept at -80 °C.

For thawing, cells were transferred into 5 ml of the respective prewarmed medium as fast as possible. After centrifugation (100 x g, 5 min, RT) cells were resuspended in 12 ml fresh medium and plated on a T-75 flask.

---

### 3.2.3. Depletion of endogenous Survivin with siRNA

---

Transfection of cells with siRNA using Roti-Fect PLUS is transient and therefore of limited duration. The reagent uses the principle of importing siRNA into the cell by the formation of DNA lipid complexes. Once in the cell, the siRNA is interacting with the complement mRNA, leading to a suppression of the corresponding protein production. For the attenuation of endogenous Survivin, siRNA targeting the 3'-untranslated region (UTR) of Survivin mRNA was used.

For transfection with Roti-Fect PLUS, cells were seeded aiming for a confluency of approximately 40% at 24 h after plating in 6-wells. Control siRNA and Survivin siRNA were diluted in serum-free Opti-MEM to a final concentration of 20 nM and a volume of 125 µl for

---

each well. Roti-Fect PLUS transfection reagent was also diluted in serum-free Opti-MEM (5  $\mu$ l Roti-Fect PLUS + 120  $\mu$ l Opti-MEM per well). After incubation at RT for 5 min, the diluted siRNA was added to the Roti-Fect PLUS dilution and incubated at RT for 20 min. In the meantime, cells were washed with PBS once and 1 ml of pre-warmed serum-free Opti-MEM was added. Afterwards, the siRNA/Roti-Fect PLUS solution was mixed and 250  $\mu$ l were added dropwise to each well. After incubation for 8 h at 37 °C and 5% CO<sub>2</sub>, 1.25 ml Opti-MEM/20% FBS was added to stop transfection. The transfected cells were then incubated for at least another 16 h at 37 °C and 5% CO<sub>2</sub> prior to any further experiments.

---

### 3.2.4. Transient transfection of DNA plasmids

---

For the transient transfection of cells with plasmid DNA, two different transfection reagents were used, depending on the further experiments. Both reagents use the principle of the uptake of DNA into the cell by the formation of DNA lipid complexes.

The K2 Transfection System was used for transient transfection of SW480 cells for GST pull-down assays as well as stable transfection of LN-229 cells with EGFP constructs. Effectene transfection reagent was used for protein-protein interaction studies with the NanoBiT® complementation assay and Förster resonance energy transfer (FRET) assay, as well as homologous recombination assay. In all three experiments, single and double transfections with one or two plasmids were performed, though different DNA concentrations were used depending on the conducted assay.

---

### 3.2.5. Stable transfection

---

For the stable transfection of LN-229 cells, the constructs first had to be linearized using 30  $\mu$ g of plasmid DNA, 10  $\mu$ l 10x NEBuffer, 4  $\mu$ l ApaLI enzyme (10 U/ $\mu$ l), 1  $\mu$ l BSA (100x) and volumes were adjusted to 100  $\mu$ l with RNase/DNase-free water in 1.5 ml tubes. After incubation at 37 °C overnight, linearization was confirmed via agarose gel electrophoresis and subjected to PCR clean-up using the NucleoSpin® Gel and PCR Clean-Up Kit (Macherey-Nagel) following manufacturer's instructions. LN-229 cells were then stably transfected with pEGFP-N1, Survivin-EGFP or Survivin $\Delta$ XIAP-EGFP using the K2 Transfection System. Therefore, cells were seeded aiming for a confluency of approximately 80% at 24 h after plating in 6-wells. Before transfection, medium was exchanged with 1125  $\mu$ l fresh medium (+ 20% FBS + 1% P/S) and 11.25  $\mu$ l K2 Multiplier was added to each 6-well, followed by an incubation for 2 h at 37 °C and 5% CO<sub>2</sub>. Meanwhile, 4  $\mu$ g of the linearized plasmid DNA was mixed with 67.5  $\mu$ l serum-free Opti-MEM per transfected 6-well (solution A) and 4.5  $\mu$ l K2 transfection reagent was mixed with 67.5  $\mu$ l serum-free Opti-MEM per transfected 6-well (solution B). Both solutions were carefully mixed and solution A was added to solution B respectively, followed again by careful mixing. After 20 min incubation at RT and 2 h incubation of the cells with K2 Multiplier, 142  $\mu$ l of the DNA lipid complexes were added to the 6-wells and mixed by careful pivoting. Following transfection in 6-well plates and further incubation at 37 °C and 5% CO<sub>2</sub>, cells were transferred to 100 mm petri dishes where colonies



---

were allowed to grow. For selection of transfected cells, the DMEM medium supplemented with 10% FBS and 1% P/S was enriched with 750  $\mu\text{g}/\text{ml}$  G418.

Clones were isolated from 100 mm petri dishes when some colonies were large enough to be visible by naked eye. Therefore, the dishes were washed with PBS and transferred to a fluorescence microscope where fluorescent colonies were selected. The dishes were then taken back under the laminar flow hood and silicon-embedded cloning cylinders were carefully placed on the selected colonies. Cells within the cloning cylinders were detached with 60  $\mu\text{l}$  trypsin/EDTA, incubated for 5 min at 37 °C and 5% CO<sub>2</sub>, resuspended with 60  $\mu\text{l}$  DMEM (+ 10% FBS + 1% P/S) and transferred into 12-well plates (one clone per well) along with 1 ml medium (DMEM + 10% FBS + 1% P/S + 750  $\mu\text{g}/\text{ml}$  G418). When cells were grown to a confluency of approximately 60-80% they were transferred to T-25 flasks and later (when 80-100% confluent) harvested for cryostocks.

EGFP expression of the different stably transfected clones was verified via western blotting as well as fluorescence microscopy using an Axiovert 40 CFL microscope after staining the nuclei with DAPI.

---

### **3.2.6. Irradiation procedure**

---

For irradiation with X-rays, cells were exposed to single doses from 1 to 4 Gy photons using a linear accelerator (Synergy, Elekta, Crawley, UK) with 6 MeV/100 cm focus-surface distance and a dose rate of 6 Gy/min. Non-irradiated controls were kept in parallel at ambient temperature in the accelerator control room. Medical physics experts of the Department of Radiotherapy and Oncology performed regular dosimetry.

---

### **3.2.7. Harvesting and lysis of cells**

---

For cell lysis using radioimmunoprecipitation assay buffer (RIPA), cells were washed once with ice-cold PBS and scraped in RIPA buffer on ice at the respective time points after irradiation. The lysates were transferred to a precooled 1.5 ml tube and incubated on ice for 30 min, followed by centrifugation at 14000 x g for 15 min at 4 °C. The supernatant containing the proteins was then transferred into a new precooled 1.5 ml tube and stored at -80 °C.

For cell lysis for immunoprecipitation, IP lysis buffer (1x) was used. Cells were washed with PBS, scraped in PBS and transferred to a precooled 1.5 ml tube. After centrifugation at 400 x g for 5 min at 4 °C, the pellet was resuspended in IP lysis buffer, followed by sonification twice for 1 min and incubation on a rotator for 1 h at 4 °C. Then, the lysates were centrifuged at 14000 x g for 15 min at 4 °C and the supernatant containing the proteins was transferred into a new precooled 1.5 ml tube. Protein samples were stored at -80 °C.

---

### 3.2.8. Determination of protein concentration

---

Protein concentrations of the lysates were determined with the Micro BCA™ Protein Assay Kit. This assay is based on the formation of a purple-coloured reaction product by two molecules bicinchoninic acid (BCA) with a cuprous cation ( $\text{Cu}^{1+}$ ).  $\text{Cu}^{1+}$  originates from the reduction of  $\text{Cu}^{2+}$  by proteins in an alkaline medium. The BCA- $\text{Cu}^{1+}$  complex is water-soluble and can be detected with an ELISA reader at 562 nm (Smith et al., 1985). The intensity of the purple reaction product is proportional to the protein concentration which can be determined by comparing its absorbance to a BSA standard curve, measured in parallel in the range of 0-40  $\mu\text{g}/\text{ml}$  protein. The protein samples were diluted 1:150 in ddH<sub>2</sub>O and the concentrations determined in triplicates. As for the rest, the BCA assay was performed according to manufacturer's instructions.

---

### 3.2.9. SDS polyacrylamide gel electrophoresis

---

With sodium dodecyl sulphate polyacrylamide gel electrophoresis (SDS-PAGE), proteins can be separated by their molecular weight due to the SDS in the gel and the reducing electrophoresis buffer, which is denaturing the proteins leading to an evenly distributed negative charge. The gels were prepared according to the pipette scheme in Table 8. Prior to electrophoresis, protein extracts including 6x reducing electrophoresis buffer were heated at 99 °C for 10 min. Per lane, 20-30  $\mu\text{g}$  total protein extract were loaded on the gel and separated by 25 mA per gel.

Table 8: Pipetting scheme for two discontinuous SDS electrophoresis gels (8.3 cm x 7.3 cm x 1 mm).

	Separation gel 6%	Separation gel 10%	Separation gel 12%	Collection gel 5%
Distilled water	6.9 ml	4.7 ml	3.6 ml	3.52 ml
Rotiphoresis gel 30	3.2 ml	5.4 ml	6.5 ml	0.836 ml
Tris HCl (pH 8.8)	6.0 ml	6.0 ml	6.0 ml	-
Tris HCl (pH 6.8)	-	-	-	0.626 ml
10% SDS	0.162 ml	0.162 ml	0.162 ml	0.05 ml
20% APS	0.054 ml	0.054 ml	0.054 ml	0.04 ml
TEMED	0.012 ml	0.012 ml	0.012 ml	0.005 ml

---

### 3.2.10. Coomassie Blue staining

---

For Coomassie Blue staining, the SDS gel was incubated in Coomassie Blue solution for 1 h at RT while shaking, leading to a fixation and staining of the separated proteins. Afterwards the gel was destained with destaining solution for approximately 10 min at RT while shaking, followed by 10 min washing with distilled water. These two steps were repeated five times. Afterwards, the gel was ready for evaluation.

---

### 3.2.11. Western blotting

---

For western blotting, SDS-PAGE (3.2.9) with 6%, 10% or 12% gels was performed. For proteins with a higher molecular weight like DNA-PKcs (470 kDa), lower percentage gels (6%) were used and for small proteins like Survivin (16.5 kDa), higher percentage gels (12%) were used. Following SDS-PAGE, filter papers and a nitrocellulose membrane soaked in transfer buffer were placed in a blotting cassette. Then, the SDS gel was placed on top of the membrane followed by more filter papers soaked in transfer buffer. After the blotting cassette was locked, protein transfer was performed at 1.3 A and up to 25 V per gel for 10 min or 15 min for DNA-PKcs. To confirm the correct protein transfer and equal loading of the SDS gel, the membranes were incubated in Ponceau S solution for 2 min, subsequently washed with distilled water and destained with TBS-T. For blocking, the membranes were incubated in 5% milk powder/TBS-T at RT for 1 h, followed by an overnight incubation at 4 °C with the respective primary antibodies (Table 1), diluted in 5% BSA/TBS-T. After incubation with the primary antibodies, the membranes were washed three times with TBS-T for 10 min at RT. Thereafter, horseradish peroxidase-conjugated goat anti-rabbit and goat anti-mouse secondary antibodies (Table 3), diluted in 5% milk powder/TBS-T were applied to the membranes for 1 h at RT. Membranes were washed again three times with TBS-T and once with TBS for 10 min at RT before they were ready for detection. Next, the membranes were placed on an imaging tray and incubated for 2 min with working solutions of an enhanced chemiluminescent (ECL) substrate. Odyssey Fc Imaging System and Image Studio Version 5.2 Software were used for detection of the chemiluminescent signal.

---

### 3.2.12. Immunoprecipitation

---

For co-immunoprecipitation 50  $\mu$ l of the magnetic beads were washed once with PBS, before 3  $\mu$ g of the respective antibody diluted in PBS was added, followed by incubation on a rotator at 4 °C for 6 h. A non-specific mouse mAb IgG1 isotype antibody was used as a control. In the meantime, cells were harvested on ice (3.2.7) and protein concentrations were determined using BCA (3.2.8). After the 6 h incubation, the antibodies bound to the magnetic beads were cross-linked using BS<sup>3</sup>. Therefore, the Ig-coupled antibody was washed twice with 200  $\mu$ l conjugation buffer (20 mM sodium phosphate, 0.15 M NaCl), followed by incubation in 250  $\mu$ l BS<sup>3</sup> (5 mM in conjugation buffer) for 30 min at RT while rotating. Adding 12.5  $\mu$ l quenching buffer (1 M Tris HCl, pH 7.5) and incubating for 15 min at RT while rotating quenched the cross-linking reaction. Beads were then washed three times with 200  $\mu$ l PBS-T, before 2 mg of the respective protein was added. After incubation overnight at 4 °C while

---

rotating and washing three times with ice-cold PBS, beads were resuspended in 26  $\mu$ l lysis buffer and 9  $\mu$ l loading buffer. The samples were heated for 10 min at 99 °C with thorough mixing in between prior to SDS-PAGE and western blotting.

---

### 3.2.13.Vector cloning

---

#### Polymerase chain reaction (PCR)

Either existing plasmids encoding the gene of interest or cDNA were used as templates for insertion of the genes of interest into the plasmids. 50 ng of plasmid or 2.5  $\mu$ l of cDNA were used as template along with 5  $\mu$ l 10x Buffer plus 2.5  $\mu$ l forward and reverse primers (10  $\mu$ M, 3.1.11) plus 1  $\mu$ l dNTPs (10 mM each) plus 1  $\mu$ l PfuUltra HF adjusting to a total volume of 50  $\mu$ l with RNase/DNase-free water per reaction. The PCR conditions are shown in Table 9. Annealing temperature and elongation time were adjusted according to primer melting temperature and length of template respectively. The annealing temperature was set at the lowest melting temperature of one of the primers, elongation time was calculated with 1 min per kb of the amplified template.

Table 9: Standard PCR protocol for DNA amplification with PfuUltra HF. Annealing temperature and elongation time were adjusted according to primer melting temperature and length of template respectively.

Temperature [°C]	Time [min:sec]	
95	2:00	
95	0:30	35x
According to melting temp.	1:00	
72	1:00/kb	
72	15:00	
4	$\infty$	

The PCR samples were purified using the NucleoSpin® Gel and PCR Clean-Up Kit following manufacturer's instructions.

#### Agarose gel electrophoresis

DNA fragments were separated via agarose gel electrophoresis. The agarose gels were prepared using 60 ml of a 1% agarose gel/TAE buffer solution, supplemented with 5  $\mu$ l

---

peqGREEN in order to visualize DNA. Before loading on the gel, DNA was mixed with an appropriate volume of DNA loading dye (5x). Gel electrophoresis was performed at 80 V for approximately 1 h. Thereafter, DNA was visualized using the Odyssey Fc Imaging System and Image Studio Version 5.2 Software. The size of the DNA was determined with the GelPilot 1kb Plus DNA ladder.

### Restriction enzyme digestion

For restriction enzyme digestion approximately 10  $\mu\text{g}$  of the purified PCR samples and the respective plasmids were used with 20 U of each restriction enzyme, 5  $\mu\text{l}$  NEBuffer #1 (10x) and 0.5  $\mu\text{l}$  BSA (100x) and adjusted to a total volume of 50  $\mu\text{l}$  with RNase/DNase-free water. The digestions were incubated at 37 °C overnight.

The digested inserts were purified using the NucleoSpin® Gel and PCR Clean-Up Kit following the manufacturer's instructions and eluted in 30  $\mu\text{l}$  RNase/DNase-free water. For purification of the linearized plasmid backbones, the digestion reaction batches were loaded and separated on a 1% agarose gel. The plasmid of the correct size was then extracted from the gel and also purified by using the NucleoSpin® Gel and PCR Clean-Up Kit and eluted in 50  $\mu\text{l}$  RNase/DNase-free water.

### Ligation

Ligation reactions contained the plasmid backbone DNA and the respective insert, 1  $\mu\text{l}$  T4 DNA ligase and 1  $\mu\text{l}$  T4 ligase buffer (10x) adjusted to a total volume of 10  $\mu\text{l}$  with RNase/DNase-free water per reaction, followed by incubation overnight at 14 °C. Equimolar ratios for vector and insert were calculated as follows:

$$ng\ insert = \frac{ng\ vector \times size\ of\ insert\ (bp)}{size\ of\ vector\ (bp)}$$

For ligations, an insert to vector ratio of 3:1 was used.

### Preparation of competent *Escherichia coli* (*E. coli*)

For the preparation of competent *E. coli* DH5 $\alpha$ , 5 ml LB medium were inoculated with a cryo stock of *E. coli* DH5 $\alpha$ , followed by overnight incubation at 37 °C while shaking at 250 rpm. The following day, 400  $\mu\text{l}$  of the overnight culture was transferred into 200 ml LB medium. Incubation at 37 °C while shaking at 250 rpm was continued until an OD<sub>600</sub> of 0.2 was reached. The cells were then pelleted at 4100 x g and 4 °C for 10 min and resuspended in 20 ml MOPS I buffer. After 10 min incubation on ice, the cells were centrifuged again at 4100 x g and 4 °C for 10 min, followed by resuspension of the pellet in 20 ml MOPS II buffer. Due to the CaCl<sub>2</sub>, the membrane permeability is changed which leads to the possibility of DNA uptake through the membrane (Mandel and Higa, 1970). After another incubation at 4 °C for 30 min and centrifugation at 4100 x g and 4 °C for 10 min, the pellet was resuspended in 2 ml

---

MOPS II buffer and aliquoted into 200  $\mu$ l portions in precooled 1.5 ml tubes containing 50  $\mu$ l glycerol. After mixing carefully, the competent cells were snap frozen in liquid nitrogen and stored at -80 °C.

### **Transformation**

For the transformation of chemically competent *E. coli* DH5 $\alpha$  cells with plasmids, 50  $\mu$ l cells per transformation were thawed on ice and mixed with plasmid DNA. In case of previously ligated plasmids, 3  $\mu$ l of the ligation reaction batch was used, for retransformation of plasmids, 50 ng DNA was used. DNA and cells were mixed carefully and incubated on ice for 20 min, followed by a heat-shock for 45 sec at 42 °C in a water bath. After that, the cells were cooled on ice for 2 min, before 200  $\mu$ l sterile LB medium was added. Prior to plating on LB-agar plates containing the appropriate antibiotics, the cells were regenerated for 60 min at 37 °C while shaking. The plates were incubated overnight at 37 °C.

### **Plasmid mini-preparation**

For plasmid mini-preparation, 5 ml LB medium was inoculated with one colony of the transformed *E. coli* DH5 $\alpha$  cells. After overnight incubation at 37 °C with agitation, plasmid isolation with 4 ml from the overnight culture was performed, using the NucleoSpin® Plasmid Kit and following the manufacturer's instructions. For each transformation approach, at least three colonies were used. After that, the concentrations of the isolated plasmids were measured using spectrophotometry. The plasmids were stored at -20 °C.

### **Control digestion and sequencing**

To test whether the isolated plasmids have incorporated the correct insert, a control digestion was performed using the same restriction enzymes as for the cloning. After incubation overnight at 37 °C, the resulting fragments were analysed via agarose gel electrophoresis. The plasmids showing the correct band pattern were sent for sequencing. Sequencing was performed by Eurofins Genomics (Ebersberg), the primers used are shown in Table 7.

### **Plasmid midi-preparation**

The plasmids with the correct sequence were then produced in a higher scale using midi-preparation. Therefore, 100  $\mu$ l of the remaining bacteria culture of the mini-preparation was used to inoculate 100 ml LB medium containing the appropriate antibiotics. After incubation overnight at 37 °C with agitation, the plasmids were isolated using the NucleoBond® Xtra Midi Plus EF Kit following manufacturer's instructions. Thereafter, the DNA concentrations were measured using spectrophotometry. The plasmids were stored at -20 °C.

---

### 3.2.14. Production of bacterial GST fusion proteins and GST preparation

---

With glutathione S-transferase (GST) fusion proteins protein-protein interactions can be verified. Consequently, the GST encoding sequence is linked directly to the sequence of the protein of interest. After transcription and translation in bacteria, a GST fusion protein is produced and can be isolated for interaction studies. Due to the high binding affinity of GST to glutathione, glutathione coupled sepharose beads can be used for purification of the GST fusion protein.

In this study, the kinase domain of DNA-PKcs was fused to a GST protein. Hence RNA was isolated from SW480 cells using the NucleoSpin® RNA kit following the manufacturer's instructions. Next, cDNA was created using an oligo-dT primer and the enzyme reverse transcriptase. From this cDNA, PI3K was amplified using PCR and inserted into the KpnI/EcoRI restriction sites of the pGEX-5X-3 (including a KpnI restriction site, 3.1.6) vector. A detailed cloning procedure was described earlier (3.2.13). *E. coli* BL-21 transformed with the GST fusion proteins was cultivated in 10 ml of selective LB medium over night at 37 °C while shaking at 250 rpm. The next day, the overnight culture was transferred into 100 ml selective LB medium and incubated for 75 min while shaking at 250 rpm, followed by induction with 50 µl IPTG to a final concentration of 1 mM. The interaction of IPTG with the *lac* repressor leads to the expression of the T7 polymerase gene, which then recognises its specific promotor resulting in the production of GST fusion protein. After further incubation for 1 h while shaking at 250 rpm, bacteria were collected by centrifugation (4100 x g, 15 min, 4 °C). The pellet was resuspended in 2 ml cold CelLytic B (2x) lysis buffer supplemented with 1 µl PMSF (0.2 M), 1 µl Na<sub>3</sub>VO<sub>4</sub> (100 mM), 10 µl protease inhibitor (100x), 10 µl lysozyme (100 mg/ml), 1 µl Benzonase (250 U/µl) and transferred into a 2 ml tube, followed by rotation for 15 min at RT. After centrifugation at 18000 x g for 15 min at 4 °C, the supernatant containing the protein fraction was transferred to a new precooled 2 ml tube. To isolate the GST fusion proteins, 100 µl of a 50% glutathione sepharose beads suspension were added to the protein solution and incubated for 30 min at 4 °C while rotating. The beads were ready to use after washing twice with PBS. By centrifugation (2000 x g, 3 min, 4 °C) GST fusion protein bound to the beads was isolated, followed by three washing steps with PBS and mixing thoroughly to remove unspecific bound proteins. After resuspension in 50 µl PBS, the amount of GST fusion protein was determined by SDS-PAGE (3.2.9) and Coomassie Blue staining (3.2.10).

---

### 3.2.15. GST pulldown assay

---

With a pulldown assay, direct interactions between proteins can be detected. Accordingly, the protein-coupled GST beads are incubated with cell lysate containing the potential interaction partner of the GST fusion protein. Here, the kinase domain of DNA-PKcs (PI3K) was fused to GST and investigated regarding an interaction with Survivin which was linked to either an EGFP- or a FLAG tag.

At first, SW480 cells were seeded aiming for a confluency of approximately 80% at 24 h after plating in 6-well plates. Before transfection with the K2 Transfection System, medium was

---

exchanged with 1125  $\mu$ l fresh medium (+ 20% FBS + 1% P/S) and 11.25  $\mu$ l K2 Multiplier were added to each well, followed by incubation for 2 h at 37 °C and 5% CO<sub>2</sub>. Meanwhile, 1.6  $\mu$ g of plasmid DNA were mixed with 67.5  $\mu$ l serum-free Opti-MEM per transfected 6-well (solution A) and 4.5  $\mu$ l K2 transfection reagent were mixed with 67.5  $\mu$ l serum-free Opti-MEM per transfected well (solution B). Both solutions were carefully mixed and solution A was added to solution B respectively followed again by careful mixing. After 20 min incubation at RT and 2 h incubation of the cells with K2 Multiplier, 142  $\mu$ l of the DNA lipid complexes was added to the 6-wells and mixed by careful pivoting. The transfected cells were then incubated for another 24 h at 37 °C and 5% CO<sub>2</sub> prior to seeding in 100 mm dishes for further growth of the cells for another 24 h. At 1 h after IR with 4 Gy, SW480 cells were harvested (3.2.7) and the lysates were incubated together with the GST fusion protein overnight at 4 °C while rotating. Unspecific binding was blocked by addition of 10% BSA (10 mg/ml). After the incubation, the glutathione sepharose beads were washed three times with IP lysis buffer. Then, beads were resuspended in 24  $\mu$ l IP lysis buffer and 6x reducing electrophoresis buffer, followed by separation via SDS-PAGE (3.2.9). GST fusion proteins or interacting proteins were detected with specific antibodies via western blotting (3.2.11).

---

### **3.2.16. NanoLuc Binary Technology (NanoBiT®) complementation assay**

---

The NanoBiT® assay is based on a two-subunit NanoLuc luciferase that can be used for intracellular detection of protein-protein interactions. This luciferase consists of a large subunit (LgBiT, 17.6 kDa) and a small subunit (SmBiT, 1.3 kDa). The two subunits are fused to two interaction partners and when expressed in cells, the interaction of the proteins brings the two subunits into close proximity. This leads to the structural complementation of LgBiT and SmBiT, generating a functional enzyme that is producing a luminescent signal, which can be detected with an ELISA reader. Because of the subunits low affinity to each other, their interaction is driven by the behaviour of the fusion partners.

In order to test all possible combinations, constructs were made encoding LgBiT and SmBiT fusions to the N- and C-termini of Survivin and the kinase domain of DNA-PKcs (PI3K), resulting in eight different expression constructs. Subsequently, Survivin and PI3K were amplified from existing plasmids, using the primers given in Table 5. Standard cloning procedure was used as described earlier (3.2.13).

For the NanoBiT complementation assay HEK-293T cells were transiently transfected with one or two plasmids encoding the different NanoBiT constructs. As a transfection reagent, Effectene was used. The transfection approaches were set up in 1.5 ml tubes as shown below.



Table 10: Composition of the transfection reagents for single or double transfections for the NanoBiT® complementation assay.

Plasmid DNA	Conc. plasmid DNA	$\mu\text{l}$ DNA	$\mu\text{l}$ EC buffer	$\mu\text{l}$ Enhancer	$\mu\text{l}$ Effectene	$\mu\text{l}$ EC buffer
Mock	50 ng/ $\mu\text{l}$	-	29.2	0.8	1.5	18.5
Single transfection	50 ng/ $\mu\text{l}$	1.0	28.2	0.8	1.5	18.5
Double transfection	50 ng/ $\mu\text{l}$	1.0 + 1.0	27.2	0.8	1.5	18.5

At first, the plasmid DNA was diluted with EC buffer, followed by the addition of enhancer and thorough mixing. After incubation at RT for 5 min, 1.5  $\mu\text{l}$  Effectene was diluted in a total volume of 20  $\mu\text{l}$  EC buffer for each reaction, mixed thoroughly and added to the DNA solutions, followed by 20 min incubation at RT. In the meantime, cells were harvested and counted. After the incubation, 50  $\mu\text{l}$  of each transfection reaction was pipetted into a 96-well plate and 100  $\mu\text{l}$  of cell suspension including  $6 \times 10^4$  HEK-293T cells were added and carefully mixed. The transfected cells were then incubated for another 24 h at 37 °C and 5% CO<sub>2</sub> prior to irradiation. 1 h after IR with 4 Gy, cell culture medium was carefully replaced by 100  $\mu\text{l}$  serum-free Opti-MEM. To start the luminescence reaction, 25  $\mu\text{l}$  of the Nano-Glo Live Cell Reagent (1 volume of Nano-Glo Live Cell Substrate with 19 volumes of Nano-Glo LCS Dilution Buffer) was added and mixed by gentle shaking for 10 sec. A 10 min incubation step at 37 °C within the TECAN ELISA reader was followed by the luminescence measurement for 2 sec/well. Analysis of the resulting data was performed using Microsoft EXCEL.

### 3.2.17. Förster resonance energy transfer assay

The Förster resonance energy transfer (FRET) was introduced by Theodor Förster in 1948. He described that an energy transfer between two fluorophores is possible through non-radiative dipol-dipol coupling. Thereby, an excited donor fluorophore can transfer energy to an acceptor fluorophore (Förster, 1948; Jares-Erijman and Jovin, 2003; Sun et al., 2013). An essential prerequisite is that the two fluorophores have to be within a distance of 10 nm or less. In addition, the emission spectrum of the donor fluorophore and the absorption spectrum of the acceptor fluorophore have to be overlapping (Clegg, 1995; Jares-Erijman and Jovin, 2003; Sun et al., 2013). This makes FRET a powerful research tool for measurements of protein-protein interactions (Patterson et al., 2000). As fluorophores, green fluorescent protein (GFP) colour variants like cyan fluorescent protein (CFP) or yellow fluorescent protein (YFP) can be used. By coupling the fluorophores to proteins, interactions of both proteins can be investigated in living cells (Selvin, 2000).

For FRET analysis, HEK-293T cells were transiently transfected with one or two plasmids encoding the different CFP/YFP constructs. As a transfection reagent, Effectene was used. The transfection approaches were set up in 1.5 ml tubes as described below.

Table 11: Composition of the single or double transfection reaction batches for FRET analysis.

Plasmid DNA	Conc. plasmid DNA	$\mu\text{l}$ DNA	$\mu\text{l}$ EC buffer	$\mu\text{l}$ Enhancer	$\mu\text{l}$ Effectene
Mock	300 ng/ $\mu\text{l}$	-	96.8	3.2	10
Single transfection	300 ng/ $\mu\text{l}$	1.4	95.4	3.2	10
Double transfection	300 ng/ $\mu\text{l}$	0.7 + 0.7	95.4	3.2	10

First, the plasmid DNA was diluted with EC buffer, followed by the addition of enhancer and thorough mixing. After incubation at RT for 5 min, 10  $\mu\text{l}$  Effectene was added to each reaction, mixed thoroughly and incubated for 20 min at RT. In the meantime, cells were harvested and counted. After the incubation, 110  $\mu\text{l}$  of each transfection reaction was pipetted into a 6-well plate and cell suspension including  $5 \times 10^5$  HEK-293T cells in 2 ml medium was added and carefully mixed. The transfected cells were then incubated for another 48 h at 37 °C and 5% CO<sub>2</sub> prior to irradiation. 1 h after IR with 4 Gy, cells were harvested for flow cytometry measurements. Thus, cells were washed once with PBS, detached from the cell culture plates with trypsin/EDTA and transferred to a 1.5 ml reaction tube. After centrifugation (400 x g, 5 min, 4 °C) and washing once with PBS, cells were resuspended in 200  $\mu\text{l}$  PBS and stored on ice protected from light until flow cytometry measurement.

Flow cytometry measurements were performed with the CytoFLEX-S flow cytometer. To measure CFP or FRET signals, cells were excited with a laser wavelength of 405 nm and the emission was detected with a 450/45 filter for CFP and a 525/40 filter for FRET. For YFP measurement, cells were excited with the 488 nm laser and the emission was detected with a 525/40 filter. To exclude overlapping emission spectra of CFP and YFP fluorescence, a compensation matrix was generated before every experiment. For each sample, 100000 events were measured. The gates were set according to flow cytometry-based FRET described by Banning and colleagues (Banning et al., 2010). Analysis of the resulted data was performed with CytExpert software version 1.2.11.0.

### 3.2.18. Immunofluorescence staining and imaging

Cells were seeded on glass coverslips in 6-well plates and transfected with siRNA 24 h later. 48 h after siRNA transfection, the 6-well plates were irradiated with doses ranging from 1-4 Gy. At different time points (15 min, 30 min and 24 h) after irradiation, cells were washed with ice cold PBS and fixed/permeabilized for 15 min with 3.7% formaldehyde/0.25% Triton X-100 in PBS. After three washing steps with PBS for 10 min each, cells were blocked with 5%

BSA in PBS for 60 min. Primary antibodies (Table 1) were diluted in blocking solution and incubated for 1 h followed by three 10 min washing steps with PBS. Appropriate secondary antibodies (Table 2) were also diluted in blocking solution and incubated for 1 h in the dark. Subsequently, the coverslips were washed three times with PBS, the nuclei were counterstained with DAPI solution (600 ng/ml) and were mounted onto glass slides with Vectashield. Images were acquired using an AxioImager Z1 microscope, equipped with an AxioCam MRc camera and Axio Vision Imager Software 4.6.2. For quantification, 40 nuclei were evaluated from at least three independent experiments and unified to one data point.

### 3.2.19. Homologous recombination assay

With the Homologous Recombination Assay Kit, HR efficiency in Survivin depleted cells was quantified in a non-radioactive, real-time PCR-based approach. Therefore, cells were co-transfected with two different plasmids each with a different mutation in its lacZ coding region. A recombination of these two plasmids leads to a recombined plasmid with a functional lacZ sequence (Ohba et al., 2014). This recombined plasmid can be quantified with specific primers by real-time PCR using isolated genomic DNA of the co-transfected cells as template.

For the assay,  $0.5 \times 10^5$  cells were seeded in 24-well plates and transfected with Survivin siRNA (3.2.3) 24 h later. 12 h before the highest degree of Survivin depletion, the cells were transfected with the HR assay plasmids using Effectene transfection reagent. The transfection reaction batches were set up in 1.5 ml tubes as shown in Table 12. As positive control, a plasmid encoding the functional lacZ gene was used and as negative control, the cells were transfected with just one of the lacZ-mutated plasmids.

Table 12: Composition of the single or double transfection reactions for the homologous recombination assay.

	Plasmid	$\mu\text{l}$ DNA	$\mu\text{l}$ EC buffer	$\mu\text{l}$ Enhancer	$\mu\text{l}$ Effectene
Positive control		10	50	1.6	5
Negative control	dl-1 / dl-2	10	50	1.6	5
Double transfection	dl-1 + dl-2	10	40	1.6	5

First,  $0.5 \mu\text{g}$  plasmid DNA was diluted in EC buffer, followed by the addition of enhancer and thorough mixing. After incubation at RT for 5 min,  $5 \mu\text{l}$  Effectene were added to each reaction and mixed thoroughly. Following 20 min incubation at RT, cells were supplied with fresh medium before adding the transfection complexes dropwise to the cells. Cells were irradiated with 4 Gy directly after plasmid transfection and genomic DNA was isolated from the transfected cells after 12 h incubation using the standard protocol for human or animal tissue

and cultured cells of the NucleoSpin® Tissue Kit. The genomic DNA was eluted in 25  $\mu$ l RNase/DNase-free water and the concentrations were measured using spectrophotometry.

For detection of the relative plasmid quantity, real-time PCR was performed using 50 ng DNA diluted in 8  $\mu$ l RNase/DNase-free water, 2  $\mu$ l primers (concentration was not specified by the manufacturer) and 10  $\mu$ l PerfeCTa® SYBR® Green SuperMix. The “universal primers” were used for amplification of the plasmid backbone which served as normalization, whereas the “assay primers” amplified the recombined plasmid. The real-time PCR protocol for amplification is given in Table 13.

Table 13: Protocol for real-time PCR used for amplification of the homologous recombination product.

Step	Temperature [°C]	Time [min:sec]	
1	95	3:00	
2	95	0:15	40x
3	61	0:30	
4	72	1:00	
Detection of fluorescence			
Detection of melting curves			

$C_T$  values were exported to Microsoft Excel and the HR efficiency was calculated as normalized fold expression using the  $\Delta\Delta C_T$  method (Livak and Schmittgen, 2001). The  $C_T$  of the negative control siRNA treated cells was used to calculate  $\Delta C_T$ .  $\Delta C_T$  of the recombined plasmids amplified with “assay primers” was normalized to the  $\Delta C_T$  of the backbone plasmids amplified with “universal primers”.  $\Delta\Delta C_T$  was calculated using the following formula:

$$\Delta\Delta C_T = \frac{2^{C_T(\text{control assay primer}) - C_T(\text{sample assay primer})}}{2^{C_T(\text{control universal primer}) - C_T(\text{sample universal primer})}}$$

### 3.2.20. DNA-PK activity assay

For analysis of DNA-PK activity, two different methods were applied: the SignaTECT® DNA-Dependent Protein Kinase Assay and the autophosphorylation measurement of DNA-PKcs at its Ser2056 phosphorylation site.

#### SignaTECT® DNA-Dependent Protein Kinase Assay

This kinase assay is based on the phosphorylation of a biotinylated p53-derived peptide substrate by DNA-PK with [ $\gamma$ - $^{32}$ P] ATP. This biotinylated peptide substrate can then be spotted

---

on a biotin capture membrane for detection of the incorporated  $^{32}\text{P}$  into the p53-derived peptide.

The SignaTECT® DNA-Dependent Protein Kinase Assay was performed following the manufacturer's instructions. For each reaction, 25  $\mu\text{g}$  protein from nuclear extracts was used. Nuclear extracts were prepared with the Nuclear Complex Co-IP Kit according to manufacturer's protocol and protein concentrations were determined (3.2.8). The amount of incorporated  $^{32}\text{P}$  into the p53-derived peptide substrate was determined by liquid scintillation counting.

### **Autophosphorylation of DNA-PKcs**

S2056 is an autophosphorylation site of DNA-PK that was shown to be autophosphorylated in response to ionizing radiation (Chen et al., 2005; Wechsler et al., 2004). To analyse this autophosphorylation site, the respective cell lysates were subjected to SDS-PAGE (3.2.9) and western blotting (3.2.11), using antibodies directed against DNA-PKcs and pDNA-PKcs S2056 (Table 1).

---

#### **3.2.21. Protein docking analysis**

---

To predict the interaction interfaces between Survivin and DNA-PKcs, the docking programs Schrödinger Suite (Schrödinger, LLC, New York City, NY, USA) and PatchDock (Schneidman-Duhovny et al., 2005) have been used. PIPER is the protein-protein docking module of Schrödinger Suite and its methodology is carried out in two steps: conformational sampling followed by structural clustering to identify and rank the probability of docked protein poses.

For the first step, PIPER employs an efficient FFT (Fast Fourier Transform) approach that makes it possible to evaluate a high number of poses. Generated and scored poses simple use atomistic energy function that can efficiently separate potentially acceptable poses from those that are very unlikely. Typically, 70000 poses are evaluated, and from these the 1000 best scoring poses are kept for the second step. In the second step, the 1000 poses are clustered based on structure. Then, the member of each cluster with the nearest neighbours is taken as representative of that cluster.

The second docking program used was PatchDock, a geometry-based molecular docking algorithm. The aim of this algorithm is to find docking transformations that yield good molecular shape complementarity. When applied, such transformations induce wide interface areas and small amounts of steric clashes. A wide interface is ensured to include several matched local features of the docked molecules that have complementary characteristics. Each candidate of the docked molecules is further evaluated by a scoring function that considers geometric fit and atomic desolvation energy.

Pre-processing steps such as filling the missing hydrogen atoms, side chains, loops, cap-termini, creation of disulphide bonds and energy minimizations were performed before the docking analyses in order to obtain more native structures of the proteins.

---

The top 100 docked poses were then post-processed and refined by the FireDock program (Andrusier et al., 2007; Mashiach et al., 2008) in order to generate a near-native docking structure. The FireDock algorithm performs side-chain optimization and rigid-body minimization. After refinement, the interactions between residues were determined according to their binding energies ( $\Delta G$ ) by using the GROMOS96 (BIOMOS b.v, Zürich, Switzerland) and PocketQuery (Camacho Lab, University of Pittsburgh, PA, USA) programs as well as their distances by DeepView–Swiss-PDBViewer (Guex and Peitsch, 1997). The interaction pairs with higher  $\Delta G$  values and distances  $< 5 \text{ \AA}$  between side chain hydrogen atoms were qualified as potential interactors.

---

### **3.2.22. Data analysis**

---

Experimental data are presented as mean  $\pm$  standard error of the mean (SEM). At least three independent experiments were performed. A two-sided unpaired Student's t-test was performed using Microsoft Excel software to test statistical significance. Results were considered statistically significant when a p-value less than 0.05 was reached, more significant with  $p < 0.01$  and highly significant with  $p < 0.001$ , respectively.

---

## 4. Results

---

---

### 4.1. The impact of Survivin on the DNA double-strand break repair

---

Previous work has shown a decreased DNA double-strand break repair after Survivin knockdown in colorectal cancer and glioblastoma cell lines (Capalbo et al., 2010; Reichert et al., 2011). One aim of this study was to further investigate which DNA DSB repair pathway is affected by Survivin as well as the exact molecular mechanism underlying this inhibition.

---

#### 4.1.1. Survivin depletion impacts on the number of DNA double-strand breaks after irradiation with X-rays

---

To analyse the impact of Survivin on radiation induced DNA damage induction and repair, immunofluorescence analysis of the phosphorylation of the histone variant H2AX on serine 139 ( $\gamma$ H2AX) and the recruiting of p53-binding protein 1 (53BP1) as markers for the presence of DNA DSBs were applied. For that purpose, SW480 colorectal and A2780 ovarian cancer cell lines were plated onto glass coverslips and transfected with Survivin siRNA or control siRNA. As a control, mock treated cells were analysed. 48 h after transfection, cells were irradiated with single doses of 1 or 4 Gy.  $\gamma$ H2AX and 53BP1 foci formation was quantified 15 min and 30 min after IR with 1 Gy and residual foci were counted 24 h after irradiation with 4 Gy.

In SW480 colorectal cancer cells, the number of  $\gamma$ H2AX/53BP1 foci at early time points (15 min, 30 min) was significantly increased after irradiation with 1 Gy upon knockdown of Survivin (Figure 10C). Residual DNA damage (24 h) was also significantly increased in SW480 cells upon Survivin knockdown and irradiation with 4 Gy (Figure 10B). The siRNA-mediated knockdown of Survivin was verified by western blotting (Figure 10A). Exemplary immunofluorescence staining of  $\gamma$ H2AX and 53BP1 foci is depicted in Figure 10D.

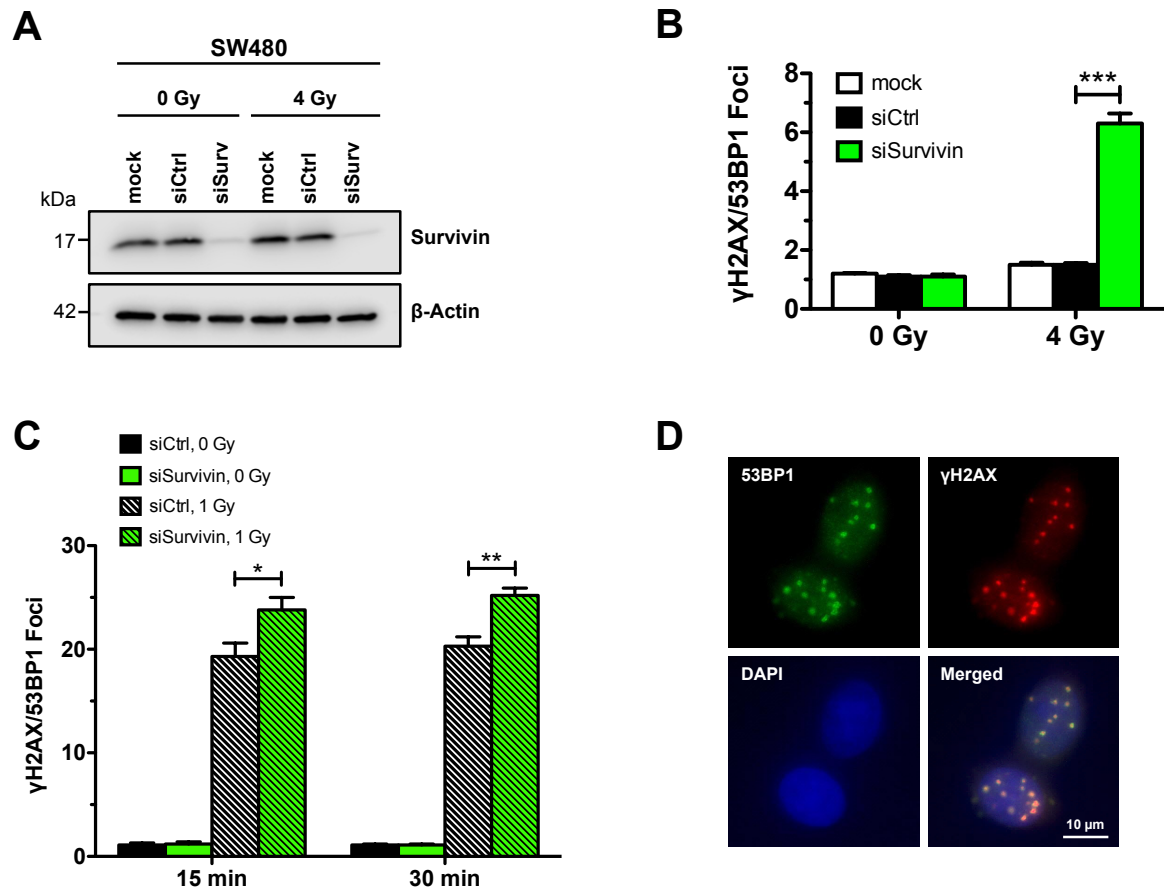


Figure 10: Treatment with Survivin-specific siRNA results in increased numbers of  $\gamma$ H2AX and 53BP1 foci in irradiated SW480 cells. Survivin knockdown was verified by western blotting.  $\beta$ -actin served as a loading control (A). SW480 cells were irradiated 48 h after siRNA transfection with 1 Gy or 4 Gy. At 24 h after IR with 4 Gy (B) as well as 15 min and 30 min after IR with 1 Gy (C), cells were fixed and stained for DAPI,  $\gamma$ H2AX and 53BP1. For each condition,  $\gamma$ H2AX/53BP1 foci were quantified from at least 40 nuclei and combined to a single data point. (D) Exemplary immunofluorescence staining of  $\gamma$ H2AX, 53BP1 and DAPI. Data represent means  $\pm$  SEM from at least three independent experiments. Statistical significances are indicated by asterisks: \*  $p < 0.05$ , \*\*  $p < 0.01$ , \*\*\*  $p < 0.001$ .

In the ovarian cancer cell line A2780, western blotting analysis showed a strong knockdown of Survivin in cells transfected with Survivin siRNA as compared to control siRNA and mock treated cells (Figure 11A). Upon Survivin knockdown and irradiation with 4 Gy, residual DNA damage (24 h) was significantly increased in A2780 cells (Figure 11B). The numbers of  $\gamma$ H2AX/53BP1 foci at early time points (15 min, 30 min) were also increased after irradiation with 1 Gy upon knockdown of Survivin (Figure 11C).



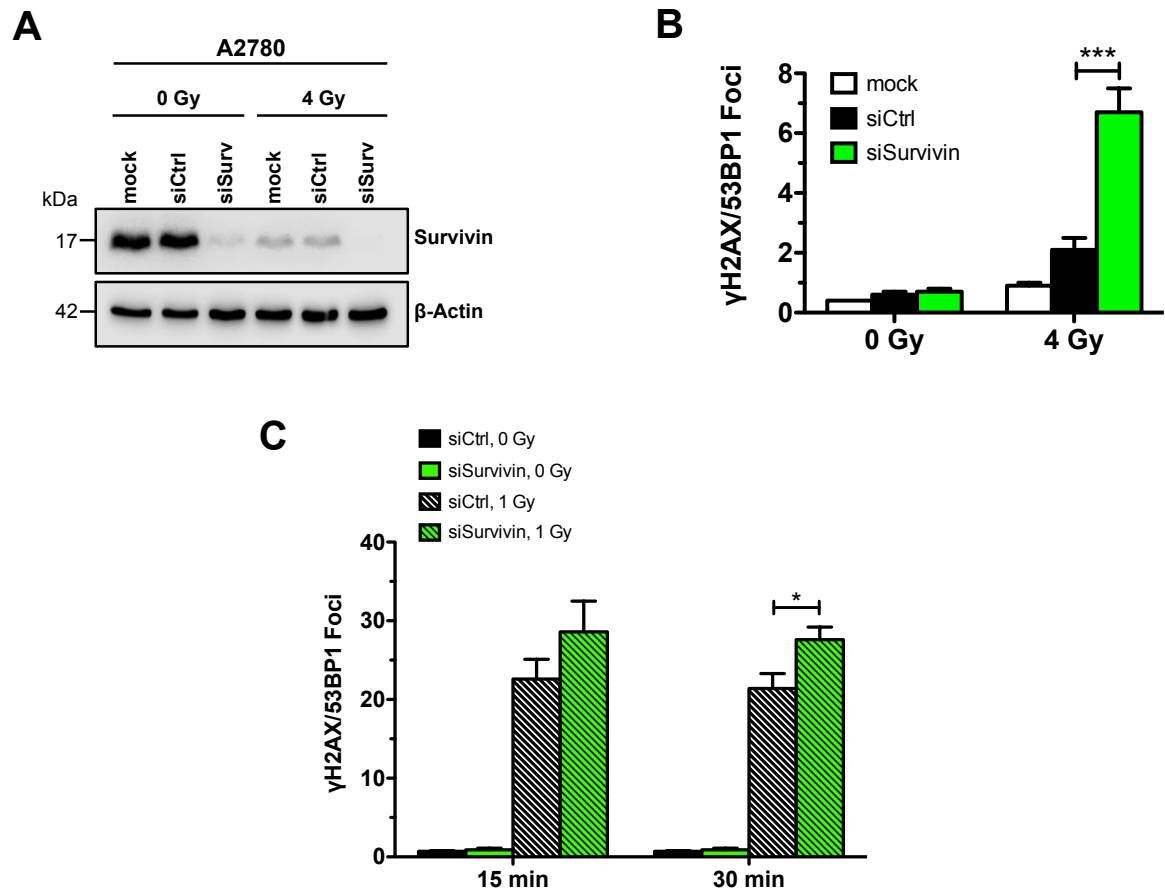


Figure 11: Treatment with Survivin-specific siRNA results in increased numbers of  $\gamma$ H2AX and 53BP1 foci in irradiated A2780 cells. Survivin knockdown was verified by western blotting.  $\beta$ -actin served as a loading control (A). A2780 cells were irradiated 48 h after siRNA transfection with 1 Gy or 4 Gy. At 24 h after IR with 4 Gy (B) as well as 15 min and 30 min after IR with 1 Gy (C), cells were fixed and stained for DAPI,  $\gamma$ H2AX and 53BP1. For each condition,  $\gamma$ H2AX/53BP1 foci were quantified from at least 40 nuclei and combined to a single data point. Data represent means  $\pm$  SEM from at least three independent experiments. Statistical significances are indicated by asterisks: \*  $p < 0.05$ , \*\*\*  $p < 0.001$ .

In summary, Survivin knockdown results in an increased number of DNA DSBs at 15 min and 30 min after irradiation with 1 Gy, in both, colorectal and ovarian cancer cells. Quantification of  $\gamma$ H2AX/53BP1 foci 24 h after irradiation with 4 Gy further indicates an increased modulation of DNA damage repair upon Survivin depletion. These findings thus confirmed an impact of Survivin in radiation-induced DNA double-strand break repair.

#### 4.1.2. Involvement of Survivin in the non-homologous end-joining repair pathway

In order to investigate in which DNA repair pathway Survivin is involved,  $\gamma$ H2AX/53BP1 foci were next quantified in a BRCA2 homozygously deleted ovarian cancer cell line (OVSAHO) (Domcke et al., 2013). By loading Rad51 to the resected DNA regions (Sorensen et al., 2005), BRCA2 has a crucial role in HR and due to the lack of BRCA2, the OVSAHO cell line is incapable in performing HR.

In OVSAHO ovarian cancer cells, western blotting analysis showed an efficient knockdown of Survivin in cells transfected with Survivin siRNA compared to control siRNA and mock treated cells (Figure 12A). Survivin knockdown and irradiation with 4 Gy resulted in significantly increased residual DNA damage (24 h) (Figure 12B). The number of  $\gamma$ H2AX/53BP1 foci at early time points (15 min, 30 min) was also increased significantly after irradiation with 1 Gy upon knockdown of Survivin (Figure 12C).

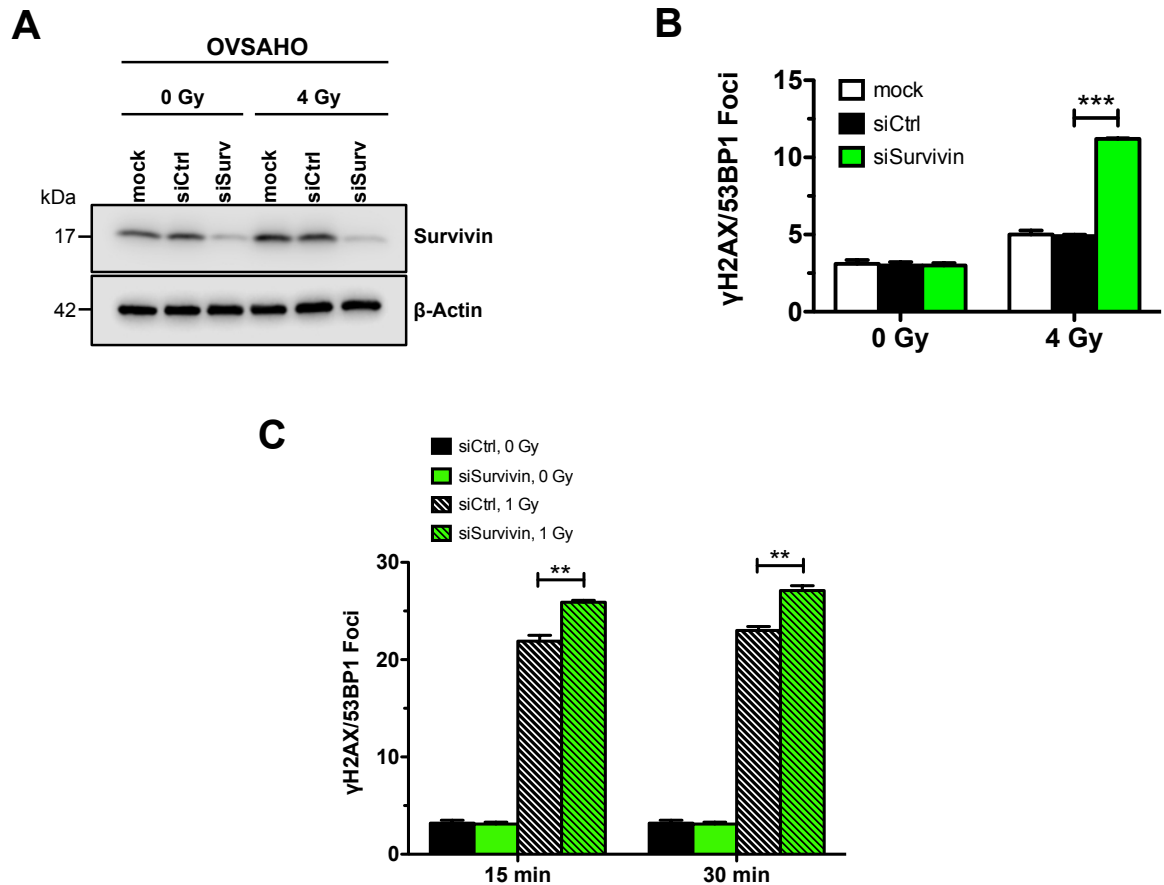


Figure 12: Treatment with Survivin-specific siRNA results in increased numbers of  $\gamma$ H2AX and 53BP1 foci in irradiated OVSAHO cells. Survivin knockdown was verified by western blotting.  $\beta$ -actin served as a loading control (A). OVSAHO cells were irradiated 48 h after siRNA transfection with 1 Gy or 4 Gy. At 24 h after IR with 4 Gy (B) as well as 15 min and 30 min after IR with 1 Gy (C), cells were fixed and stained for DAPI,  $\gamma$ H2AX and 53BP1. For each condition,  $\gamma$ H2AX/53BP1 foci were quantified from at least 40 nuclei and combined to a single data point. Data represent means  $\pm$  SEM from at least three independent experiments. Statistical significances are indicated by asterisks: \*\*  $p < 0.01$ , \*\*\*  $p < 0.001$ .

Data given in Figure 12 indicate a hampered DNA DSB repair in BRCA2 deficient OVSAHO cells upon Survivin knockdown. Since these cells are not able to repair DSBs with HR and consequently use NHEJ to repair DSBs, it is most likely that Survivin does not impact on HR but on the NHEJ repair pathway.

### 4.1.3. Analysis of the involvement of Survivin in the homologous recombination repair pathway

To further confirm, that HR is not involved in Survivin mediated modulation of DNA DSB repair, an additional HR assay was performed. In this assay, HR efficiency was quantified in a non-radioactive, real-time PCR-based approach. The assay is based on the co-transfection of two plasmids, each with a different mutation in its lacZ coding region. A recombination of these two plasmids results in a recombined plasmid with a functional lacZ sequence (Ohba et al., 2014) that can be quantified with specific primers via real-time PCR.

In order to test the applicability of the assay, SW480 cells were transfected with only one lacZ-mutated plasmid as negative control and a plasmid including a functional lacZ sequence as a positive control (Figure 13C). In non-irradiated SW480 cells, Survivin knockdown did not result in a decreased HR efficiency compared to mock and control siRNA treated cells (Figure 13A). Upon irradiation with 4 Gy and siRNA-mediated Survivin depletion, a slight but not significant decrease in HR activity could be measured compared to mock and control siRNA treated cells (Figure 13B).

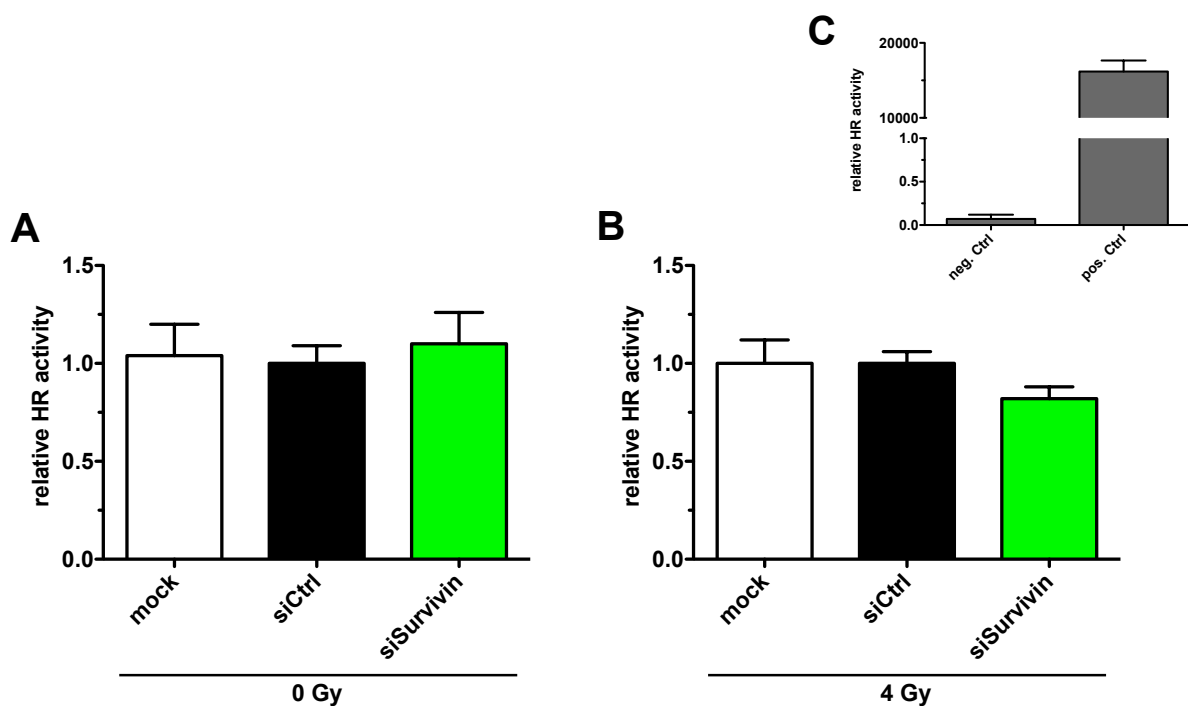


Figure 13: Homologous recombination (HR) assay displays no involvement of Survivin in HR in SW480 cells. To measure HR efficiency, a real-time PCR-based HR assay was used. This assay is based on the homologous recombination of two co-transfected plasmids, each with a different mutation on its lacZ gene. By using specific primers and real-time PCR, the correct recombination of the lacZ sequence can be quantified. Cells were transfected with Survivin siRNA (green), control siRNA (black) or mock treated (white) and partly irradiated with 4 Gy (B). Non-irradiated cells (0 Gy) are shown in (A). (C) Transfection of only one lacZ-mutated plasmid served as negative control and a plasmid including a functional lacZ sequence as a positive control. Data represent means  $\pm$  SEM from at least three independent experiments.

---

In conclusion, these results further indicate that Survivin is probably not involved in the modulation of the HR repair pathway.

---

#### **4.2. Establishment of cell lines, stably expressing a Survivin- $\Delta$ XIAP deletion mutant**

---

To analyse the impact of the XIAP binding site of Survivin on radiation induced DNA double-strand break repair, a colorectal cancer and a glioblastoma cell line were stably transfected with different Survivin constructs expressing the wild type protein (Surv. wt, covering amino acid residues (AA) 1-142) and the deletion mutant of the XIAP binding site ( $\Delta$ XIAP, AA 1-14 and 39-142), each fused in frame to EGFP at the C-terminus of the recombinant proteins (Figure 14A). Cells stably transfected with a sole EGFP construct served as a control. The Survivin constructs and the stably transfected SW480 colorectal cancer cells were kindly provided by Dr. Chrysi Petraki. The glioblastoma cell line LN-229 was stably transfected with the Survivin constructs within this thesis.

In order to ascertain that effects analysed in Survivin mutant cells arise from the recombinant constructs, endogenous Survivin was depleted with Survivin-directed siRNA, targeting only the endogenous and not the recombinant Survivin. The knockdown of endogenous Survivin as well as the expression of EGFP, Surv. wt and Survivin- $\Delta$ XIAP in SW480 cells (Figure 14B) and LN-229 cells (Figure 14C) were confirmed by western blotting.

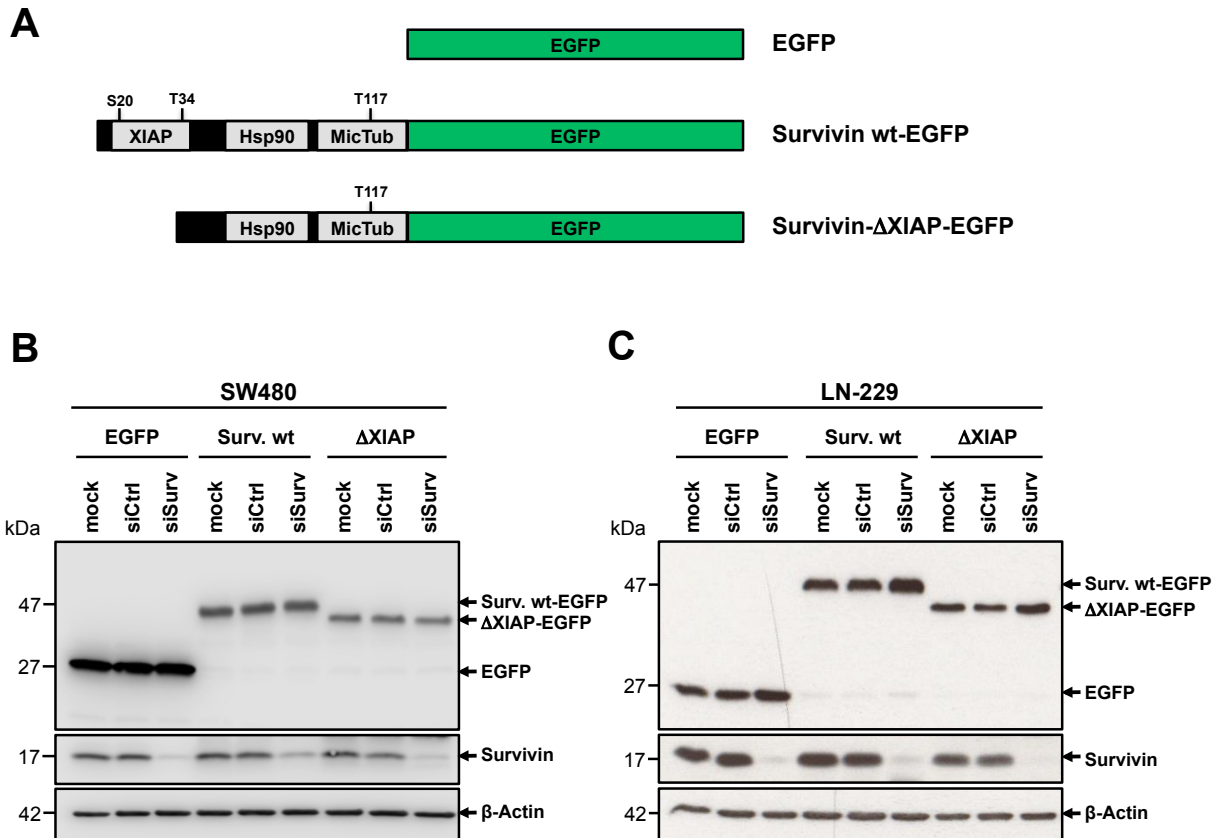


Figure 14: Stable transfection of colorectal cancer (SW480) and glioblastoma (LN-229) cells with Survivin-EGFP fusion constructs. (A) Schematical representation of enhanced green fluorescent protein (EGFP), Survivin wild type-EGFP (Surv. wt) and Survivin XIAP binding site deletion mutant fused to EGFP ( $\Delta$ XIAP). The expression of EGFP, Surv. wt and  $\Delta$ XIAP protein as well as the siRNA-mediated knockdown of endogenous Survivin in SW480 (B) and LN-229 (C) was confirmed by western blotting.  $\beta$ -actin served as a loading control.

### 4.3. Interaction of Survivin with DNA-PKcs, a key player of the non-homologous end-joining DNA repair pathway

Survivin has been shown to participate in the non-homologous end-joining DNA repair pathway by interacting with repair factors such as DNA-PKcs (Capalbo et al., 2010; Reichert et al., 2011). Thus, the following experiments were performed to characterise in more detail the interaction of Survivin with DNA-PKcs.

#### 4.3.1. Interaction of the Survivin- $\Delta$ XIAP mutant with DNA-PKcs

A first set of experiments was performed to analyse whether the deletion of the XIAP binding site impacts on the interaction between Survivin and DNA-PKcs. In line with that, SW480 colorectal cancer and LN-229 glioblastoma cells stably overexpressing the Survivin wt, Survivin- $\Delta$ XIAP and EGFP constructs were used for immunoprecipitation assays to unravel an interaction.

As depicted in Figure 15 and Figure 16, DNA-PKcs was found to precipitate with Surv. wt but not with EGFP or the  $\Delta$ XIAP construct in both SW480 colorectal cancer cells and LN-229 glioblastoma cells.

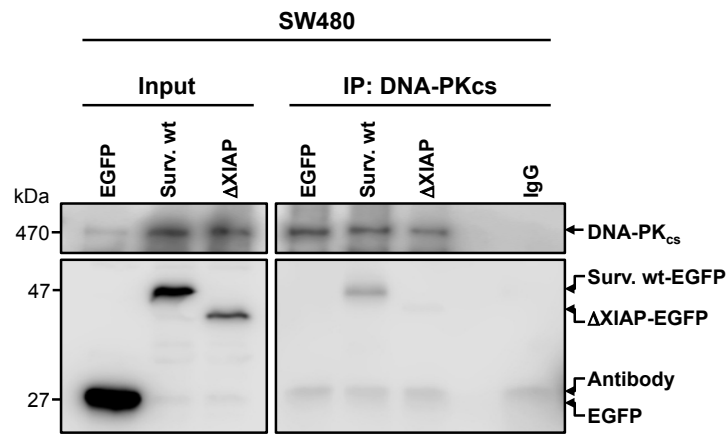


Figure 15: In immunoprecipitation (IP) experiments with SW480 lysates, DNA-PKcs was found to precipitate with recombinant Survivin wt but not with the  $\Delta$ XIAP deletion mutant after irradiation with 4 Gy. DNA-PKcs-IPs were performed with lysates of SW480 cells stably overexpressing EGFP (as a control), recombinant Survivin wt and the  $\Delta$ XIAP deletion mutant after irradiation with 4 Gy. Co-immunoprecipitated proteins were detected via western blotting. Non-specific isotype antibody (immunoglobulin G, IgG) served as additional control. Input showed the respective proteins in cell lysates. DNA-PKcs was detected with an anti-DNA-PKcs antibody while recombinant Survivin-EGFP constructs were detected with an anti-GFP antibody.

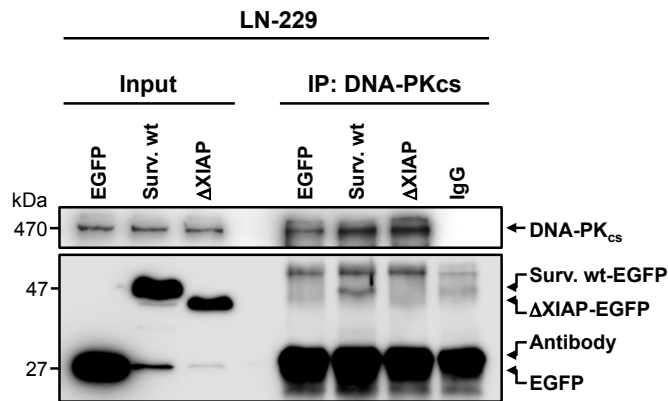


Figure 16: In immunoprecipitation (IP) experiments with LN-229 lysates, DNA-PKcs was found to precipitate with recombinant Survivin wt but not with the  $\Delta$ XIAP deletion mutant after irradiation with 4 Gy. DNA-PKcs-IPs were performed with lysates of LN-229 cells stably overexpressing EGFP (as a control), recombinant Survivin wt and the  $\Delta$ XIAP deletion mutant after irradiation with 4 Gy. Co-immunoprecipitated proteins were detected via western blotting. Non-specific isotype antibody (immunoglobulin G, IgG) served as additional control. Input showed the respective proteins in cell lysates. DNA-PKcs was detected with an anti-DNA-PKcs antibody while recombinant Survivin-EGFP constructs were detected with an anti-GFP antibody.

---

In conclusion, these data indicate that Survivin indeed interacts with the DNA-PKcs on a molecular level. Moreover, the XIAP binding site of Survivin seems to be an essential determinant for the protein-protein interaction between Survivin and DNA-PKcs.

---

### **4.3.2. Interaction of Survivin with the kinase domain (PI3K) of DNA-PKcs**

---

After showing a probable direct involvement of the XIAP binding site of Survivin in the interaction with DNA-PKcs, we next asked on the localisation of the putative binding regions of DNA-PKcs. In 2003, Chen and colleagues reported that Survivin binds directly to the catalytic domain of Aurora-B and thereby stimulates Aurora-B kinase activity (Chen et al., 2003). In analogy, we decided to investigate an interaction of Survivin with the kinase domain of DNA-PKcs, the PI3K domain.

#### **Survivin binds to the PI3K domain of DNA-PKcs in pulldown assay**

At first, the interaction of Survivin with the PI3K domain of DNA-PKcs was analysed by a GST pulldown assay. Experimentally, the PI3K domain was fused to GST and expressed in the IPTG-inducible *E. coli* strain BL21 (Figure 17A). After purification of GST-PI3K protein via glutathione coupled sepharose beads, the production of GST and GST-PI3K was analysed by SDS-PAGE and Coomassie Blue staining (Figure 17B). Finally, GST (as a control) and GST-PI3K were incubated with cell lysates of SW480 cells expressing Survivin-EGFP or FLAG-Survivin fusion constructs.

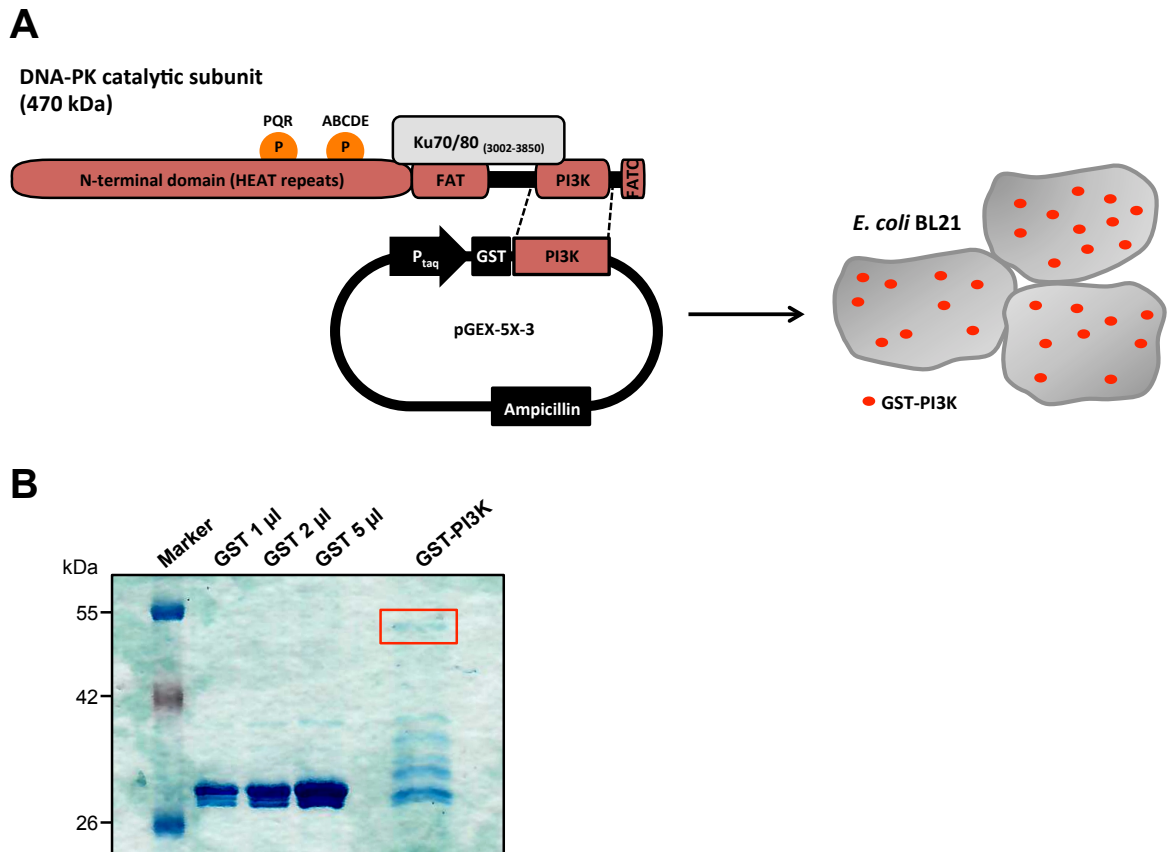


Figure 17: Expression of GST fusion constructs in *E. coli* BL21 for GST pulldown assay. (A) Schematic methodology of the cloning procedure of the DNA-PKcs kinase domain (PI3K) in the pGEX-5X-3 vector and its expression in *E. coli*. (B) GST fusion constructs were purified with glutathione coupled sepharose beads and analysed via SDS-PAGE and Coomassie Blue staining. Different amounts of the GST protein solution (1  $\mu$ l, 2  $\mu$ l and 5  $\mu$ l) and 10  $\mu$ l of the GST-PI3K protein solution were loaded onto the gel. Red frame indicates GST-PI3K fusion construct in the corresponding lane.

After purification of the GST fusion proteins, a very prominent GST band was detected, independently of whether 1  $\mu$ l, 2  $\mu$ l and 5  $\mu$ l were loaded onto the SDS gel. In the GST-PI3K fraction, only a weak band was visible at the correct height of approximately 55 kDa (indicated by a red frame in Figure 17B). After assessing equivalent amounts of GST and GST-PI3K in a specific volume of the protein solution, approximately the same amounts of GST and GST-PI3K were used for incubation with the SW480 lysates.



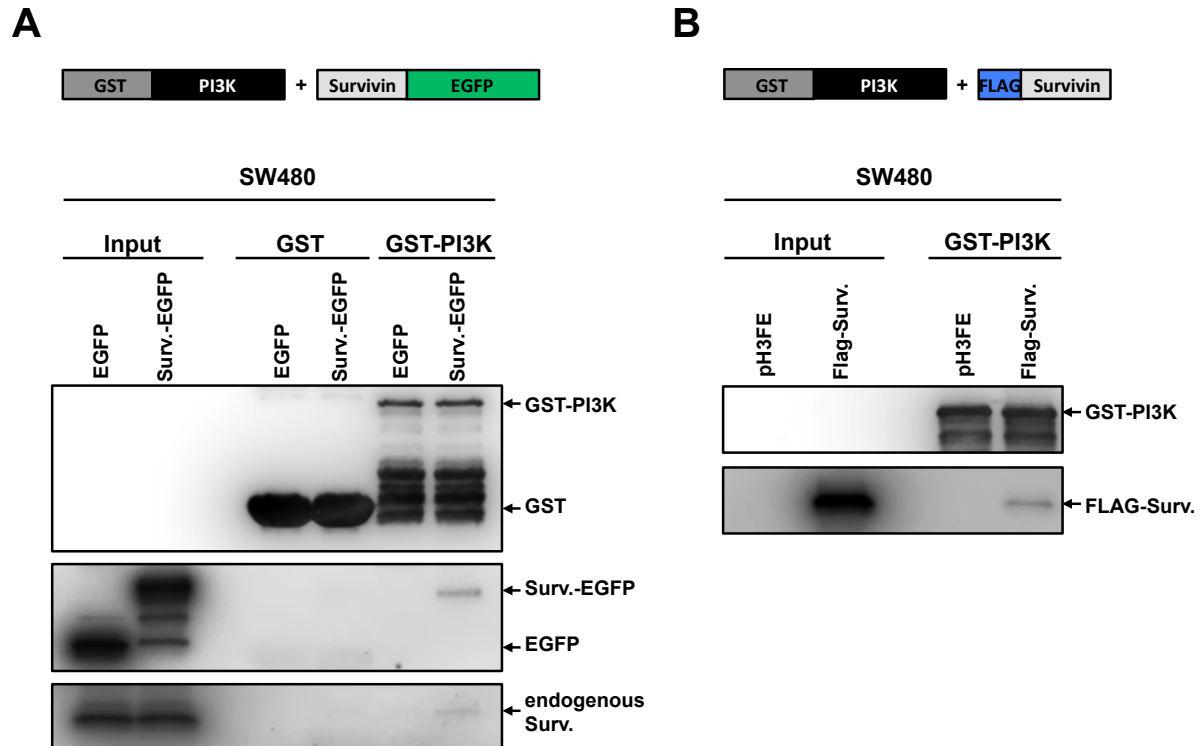


Figure 18: GST pull-down assay in SW480 cells shows binding of Survivin to the PI3K domain of DNA-PKcs. GST (as a control) and GST-PI3K fusion construct were expressed in *E. coli* BL21 and purified with glutathione coupled sepharose beads before incubation with SW480 cells irradiated with 4 Gy, expressing Survivin-EGFP (A) or FLAG-Survivin (B) fusion proteins. Input showed the respective proteins in cell lysates. GST fusion proteins were detected using an anti-GST antibody, Survivin-EGFP with an anti-GFP antibody, endogenous Survivin with an anti-Survivin antibody and FLAG-Survivin with an anti-FLAG antibody.

After incubation of GST-PI3K with cell lysates of SW480 cells irradiated with 4 Gy and pull-down of GST-PI3K via glutathione coupled sepharose beads, both, Survivin-EGFP and endogenous Survivin were detected to interact with the GST-PI3K fusion construct (Figure 18A). By using EGFP and GST controls, one can rule out that the interaction was induced by the presence of the tags (Figure 18A). After incubating GST-PI3K with cell lysates of irradiated SW480 expressing FLAG-Survivin, the latter was confirmed binding to GST-PI3K (Figure 18B).

### Survivin binds to the PI3K domain of DNA-PKcs in NanoBiT complementation assay

To confirm the results from the pull-down assays, interaction analysis with NanoBiT complementation assay was performed. The NanoBiT assay is based on a two-subunit luciferase. Each of the subunits can be fused to an interaction partner. If the fusion constructs are expressed in cells, the two subunits come into close proximity when the proteins are interacting. This leads to a structural complementation of the subunits, generating a functional luciferase that is producing a detectable luminescent signal (Figure 19).

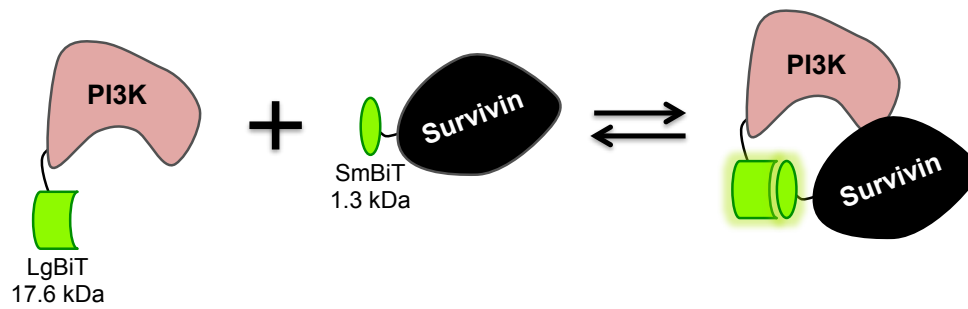


Figure 19: Schematic representation of the NanoBiT complementation assay principle. The large (LgBiT) and the small (SmBiT) subunit of a two-subunit NanoLuc luciferase are fused to two interaction partners (PI3K and Survivin). When expressed in cells, an interaction of the two proteins brings the two subunits into close proximity, leading to the structural complementation of LgBiT and SmBiT. This results in a functional enzyme that is producing a luminescent signal.

To establish the best combinations, plasmid constructs were created encoding LgBiT and SmBiT fusions to the N- and C-termini of Survivin and PI3K kinase domain, resulting in eight different expression constructs. After successful cloning of all constructs, HEK-293T cells were transfected and western blotting was performed in order to check whether the constructs are produced in the cells. Due to a lacking anti-PI3K antibody, only the Survivin constructs were analysed by western blotting (Figure 20).

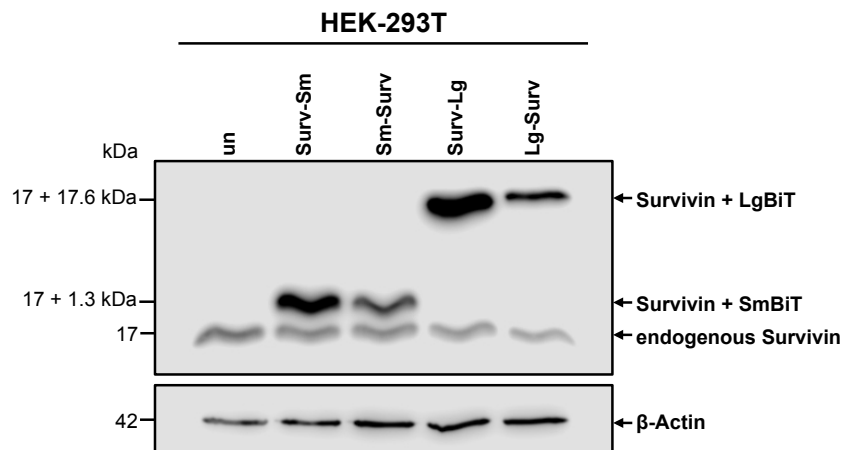


Figure 20: Expression of Survivin-LgBiT and Survivin-SmBiT constructs in HEK-293T cells. Western blot confirmation of Survivin-LgBiT and Survivin-SmBiT expression for NanoBiT complementation assay. Anti-Survivin antibody was used to detect fusion protein expression,  $\beta$ -actin served as loading control.

All four Survivin constructs showed a strong signal in the western blot and were used together with the four PI3K constructs in order to test all combinations of the constructs to determine the optimal orientation for fusing Survivin and PI3K to LgBiT and SmBiT. After testing all combinations in the NanoBiT assay, Survivin-SmBiT and LgBiT-PI3K turned out to be the

optimal construct combination for this assay (data not shown) and accordingly were used for all continuative NanoBiT experiments.

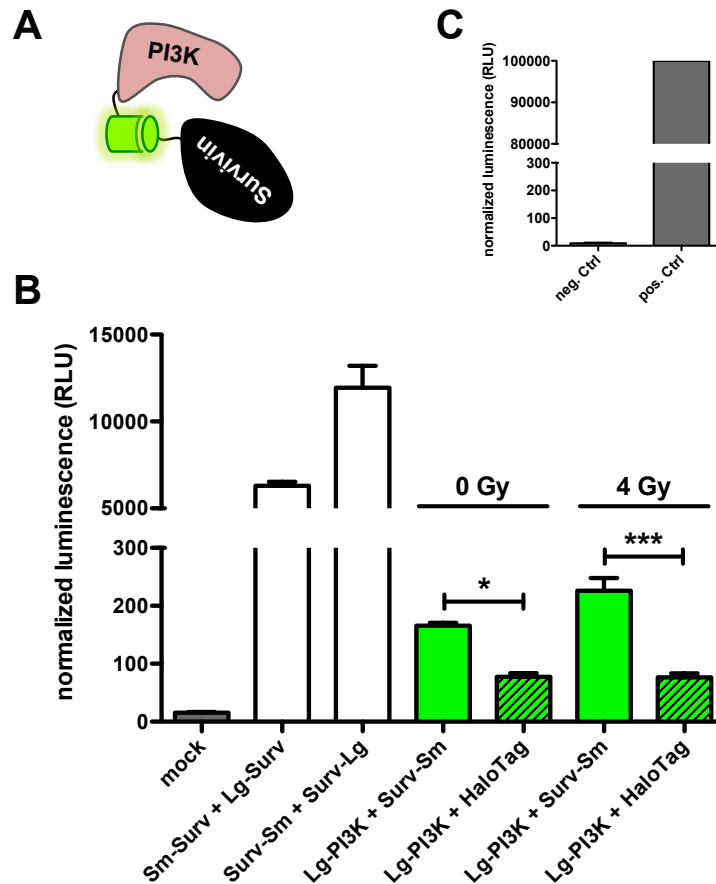


Figure 21: NanoBiT complementation assay for protein-protein interaction analysis indicates an interaction between Survivin and the PI3K domain of DNA-PKcs. To measure an interaction, HEK-293T cells were transiently transfected with Survivin-SmBiT (Surv-Sm) and LgBiT-PI3K (Lg-PI3K). When interacting in the cell, the two subunits form a functional luciferase resulting in a detectable luminescence signal (A). (B) 24 h after transfection with the NanoBiT constructs, cells were irradiated with 4 Gy followed by the addition of Nano-Glo® Live Cell Reagent and luminescence measurement at 1 h after IR. As controls, cells were mock treated (grey) or transfected with HaloTag plasmid instead of the SmBiT construct (green with black stripes). As a positive control, Survivin fused to SmBiT and LgBiT was used to show dimerization of Survivin (white). (C) Internal assay negative and positive controls were used to verify the assay's functionality. Data represent means  $\pm$  SEM from at least three independent experiments. Statistical significances are indicated by asterisks: \*  $p < 0.05$ , \*\*\*  $p < 0.001$ .

Assessment of the well established Survivin-Survivin interaction measurements confirmed the ability of Survivin to form stable homodimers. Besides, an interaction between Survivin and the PI3K domain of DNA-PKcs was evident in non-irradiated and irradiated (4 Gy) cells, indicated by a significantly increased luminescence signal compared to mock treated cells and HaloTag control (Figure 21B). These results thus confirm the findings of the pull-down experiments by showing an interaction between Survivin and the kinase domain of DNA-PKcs in HEK-293T cells.

## Survivin binds to the PI3K domain of DNA-PKcs in flow cytometry-based FRET

As a third method, the interaction of Survivin with the PI3K domain of DNA-PKcs was analysed via Förster resonance energy transfer (FRET). FRET is based on energy transfer between two fluorophores. In this assay, an excited donor fluorophore can transfer energy to an acceptor fluorophore, if the fluorophores are within a distance of 10 nm. Furthermore, it is essential that the emission spectrum of the donor fluorophore and the absorption spectrum of the acceptor fluorophore are overlapping (Clegg, 1995; Jares-Erijman and Jovin, 2003; Sun et al., 2013). YFP and CFP fulfil these requirements and were fused to the potential interaction partners Survivin and the kinase domain (PI3K) of DNA-PKcs (Figure 22).

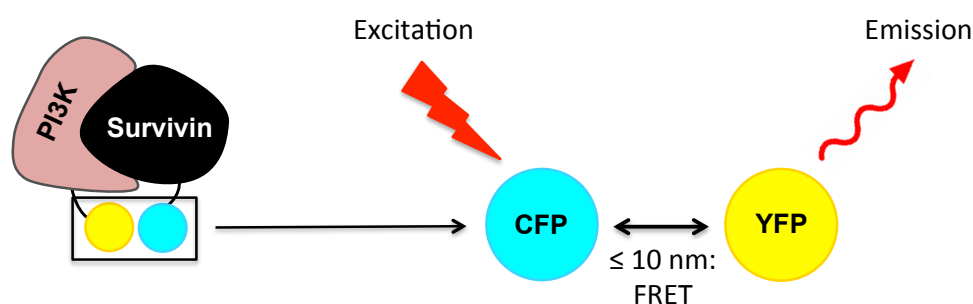


Figure 22: Schematic representation of the Förster resonance energy transfer (FRET) principle. FRET is based on the energy transfer from an excited donor fluorophore to an acceptor fluorophore. The two fluorophores have to be within a distance of 10 nm or less for this energy transfer to work. In addition, the emission spectrum of the donor fluorophore and the absorption spectrum of the acceptor fluorophore must be overlapping. As fluorophores, cyan fluorescent protein (CFP) or yellow fluorescent protein (YFP) were fused to the interaction partners Survivin and PI3K. (Figure modified from (Simkova and Stanek, 2012))

At first, CFP and YFP were fused to the N- and C-termini of Survivin and PI3K to unravel the optimal combination to use in flow cytometry-based FRET. After transfection of the different fusion constructs in HEK-293T cells, their expression was confirmed by western blotting (Figure 23A) and fluorescence microscopy (Figure 23B).

Western blotting confirmed expression of Survivin fusion constructs with signals corresponding to the expected molecular weight (44/45 kDa). In contrast, expression of the PI3K constructs was lower compared to Survivin and only CFP/YFP fused to the N-terminus of PI3K resulted in a band of the correct molecular weight (59 kDa). The C-terminal fusion of CFP and YFP resulted in degradation of the protein, indicated by a second (smaller) protein band in the experiment (Figure 23A). Fluorescence microscopy of the CFP and YFP fusion constructs showed localisation of both constructs in the cytoplasm and in the nucleus (Figure 23B).

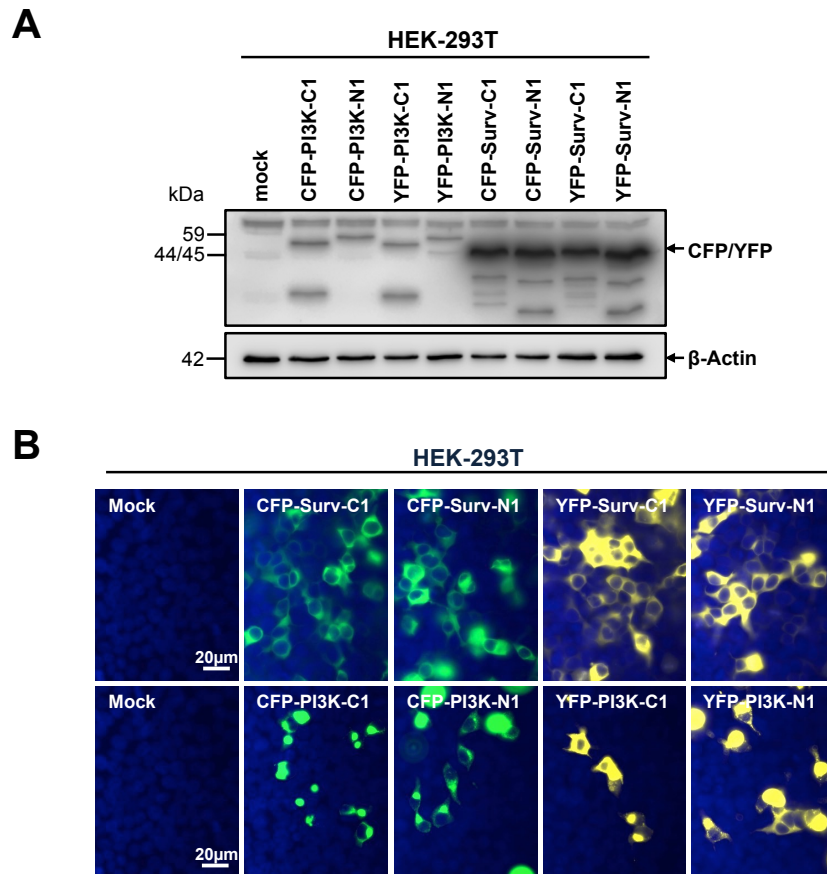


Figure 23: Expression of CFP/YFP-Survivin/-PI3K fusion constructs in HEK-293T cells. (A) Western blot confirmation of expression of N- and C-terminal CFP/YFP-Survivin and CFP/YFP-PI3K constructs. GFP antibodies were used to detect recombinant protein expression,  $\beta$ -actin served as loading control. (B) Immunofluorescence staining of Survivin/PI3K fusion constructs using GFP (for CFP constructs) and YFP antibodies. Nuclei were stained with DAPI (blue).

The gates for flow cytometry-based FRET analyses were set according to Banning and colleagues (Banning et al., 2010) and are exemplarily shown in Figure 24. At first, living cells were separated from cell debris by forward scatter (FSC) and sideward scatter (SSC) (Figure 24A1+B1) followed by separation of the FRET signal from CFP, YFP and background signals (Figure 24A2+B2). The four quadrants in Figure 24A2+B2 separate the four signals of YFP fluorescence (upper-left quadrant), CFP fluorescence (lower-right quadrant), cells that are CFP and YFP positive (upper-right quadrant) and the background signal (lower-left quadrant). Another important gating step was necessary because YFP, when excited at 405 nm, exhibited some emission in the FRET-channel, resulting in false-positive FRET-positive cells (Figure 24A3+B3). Finally, FRET was plotted versus CFP and a triangular gate was created to determine the number of FRET-positive cells (Figure 24A4+B4). In this gate, the actual FRET signal is separated from the CFP signal again, because both are excited at the same wavelength. The gates were set using cells co-transfected with CFP and YFP only, indicating FRET-negative cells as well as cells transfected with a CFP-YFP fusion protein indicating FRET-positive cells.

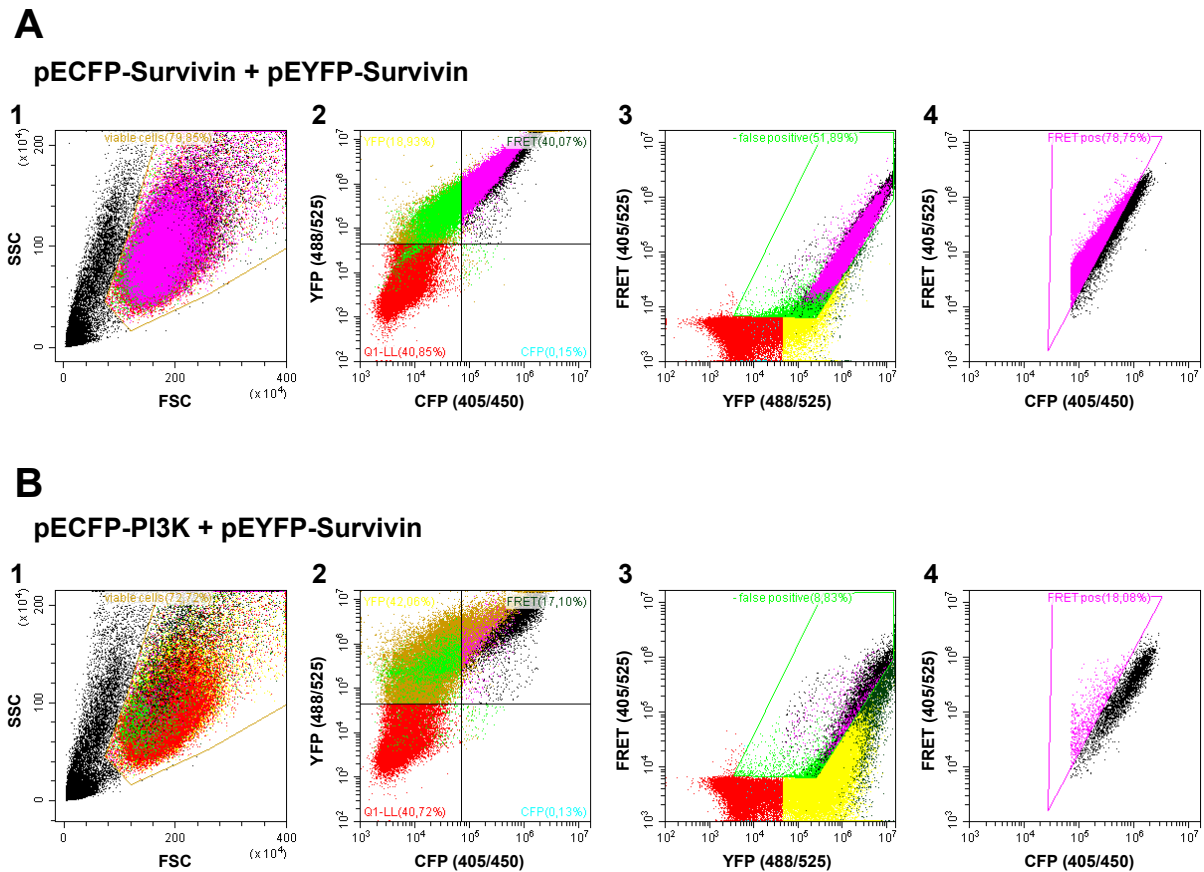


Figure 24: Exemplary gating strategy for FRET interaction analyses with flow cytometry. (A) Gating for the formation of Survivin homodimers. (B) Gating for PI3K-Survivin interaction analysis. SSC: sideward scatter; FSC: forward scatter; YFP: yellow fluorescent protein; CFP: cyan fluorescent protein; FRET: Förster resonance energy transfer.

Transfection of HEK-293T cells with the CFP-YFP fusion construct resulted in 100% FRET-positive cells. In contrast, mock-treated cells and co-transfection of CFP and YFP showed less than 1% FRET-positive cells. Dimerization of Survivin could be confirmed by 75% FRET-positive cells and co-transfection with Survivin and the PI3K domain of DNA-PKcs showed approximately 18% FRET-positive cells. As opposed to this, co-transfection of Survivin and the alternative HEAT1 or FATC domain of DNA-PKcs showed no or very few FRET-positive cells (Figure 25B).

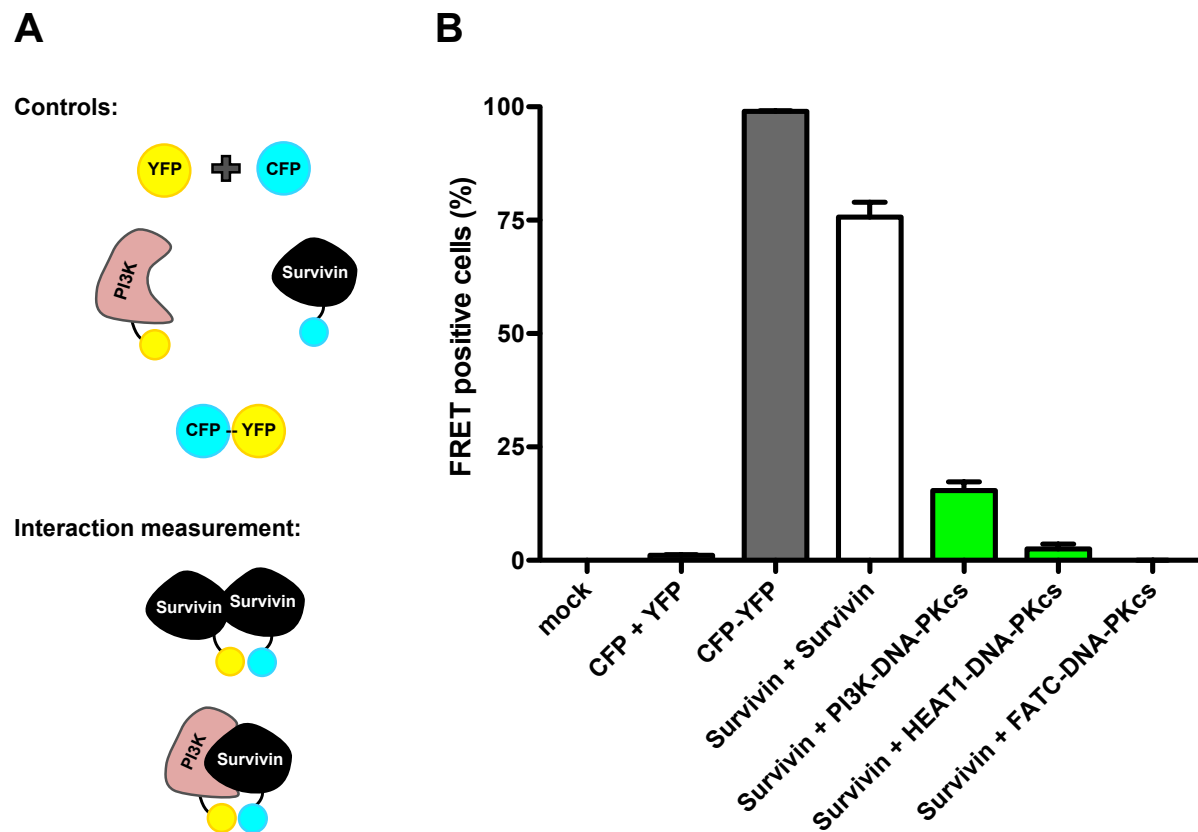


Figure 25: Flow cytometry-based FRET measurements show an interaction between Survivin and the PI3K domain of DNA-PKcs. (A) Schematical representation of the used constructs in the FRET measurements. Negative controls were co-transfections of CFP and YFP as well as transfections of the PI3K or Survivin fusion constructs alone. Positive controls were a CFP-YFP fusion construct and the formation of Survivin homodimers. (B) FRET-positive cells in percent of controls (grey), Survivin dimerization (white) and interactions of Survivin with different domains of DNA-PKcs, including PI3K, HEAT1 and FATC (green). Data represent means  $\pm$  SEM from at least three independent experiments. FRET measurements were performed by Melanie Hoffmann.

In summary, these findings could provide evidence for an interaction of Survivin with the kinase domain (PI3K) of DNA-PKcs with three independent methods, giving further insights in the role of Survivin in the NHEJ DNA double-strand break repair pathway.

#### 4.4. The impact of Survivin on the activity of DNA-PK

After having established that Survivin interacts with the kinase domain of the DNA-PKcs, we finally performed experiments to gain knowledge about the functional properties of this interaction. For the analysis of DNA-PKcs kinase activity, autophosphorylation at serine 2056 (Ser2056, S2056) was assessed by western blotting and phosphorylation of a p53-derived target peptide was tested by a SignaTECT kinase assay.

---

#### 4.4.1. Survivin depletion modulates autophosphorylation of DNA-PKcs on serine 2056

---

As compared to siRNA control transfected cells, autophosphorylation of Ser2056 was decreased after siRNA-mediated knockdown of Survivin in mock irradiated and irradiated (4 Gy) SW480 colorectal cancer cells (Figure 26A). This decrease was further confirmed in LN-229 glioblastoma cells (Figure 26B).

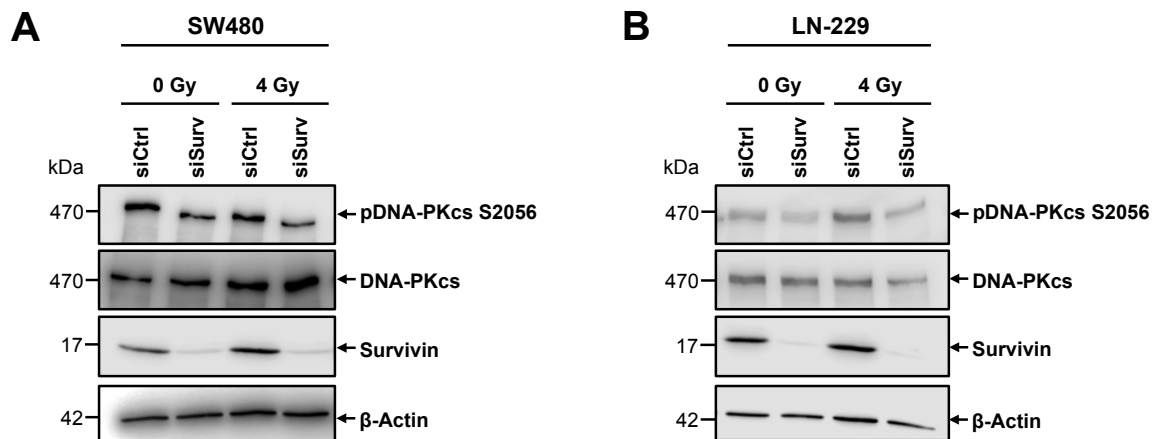


Figure 26: Autophosphorylation of serine 2056 of DNA-PKcs is modulated by Survivin. SW480 (A) and LN-229 (B) cells irradiated with 4 Gy 48 h after transient transfection with control siRNA (siCtrl) or Survivin-directed siRNA (siSurv). 1 h after irradiation, cell lysates were prepared and separated by SDS gels. Western blotting was performed using anti-Survivin, anti-DNA-PKcs and anti-pDNA-PKcs S2056 antibodies.  $\beta$ -actin served as loading control.

These data confirmed former findings on a modulation of DNA-PKcs kinase activity following attenuation of Survivin (Capalbo et al., 2010; Reichert et al., 2011).

---

#### 4.4.2. XIAP binding site of Survivin is crucial for modulation of DNA-PK kinase activity

---

Irradiation of SW480 cells stably expressing EGFP, Survivin wt and  $\Delta$ XIAP deletion mutant of Survivin in the presence of non-specific (control siRNA) resulted in an increased DNA-PK activity compared to non-irradiated cells (Figure 27, black bars). To analyse the effects of the recombinant Survivin constructs, siRNA targeting the endogenous but not the recombinant Survivin was used.

Depletion of endogenous Survivin before irradiation with 4 Gy decreased DNA-PK activity in cells expressing the EGFP and  $\Delta$ XIAP constructs to the level observed in non-irradiated cells. By contrast, expression of recombinant Survivin wt rescued DNA-PK activity after siRNA-mediated knockdown of the endogenous Survivin and irradiation with 4 Gy (Figure 27, green bars).



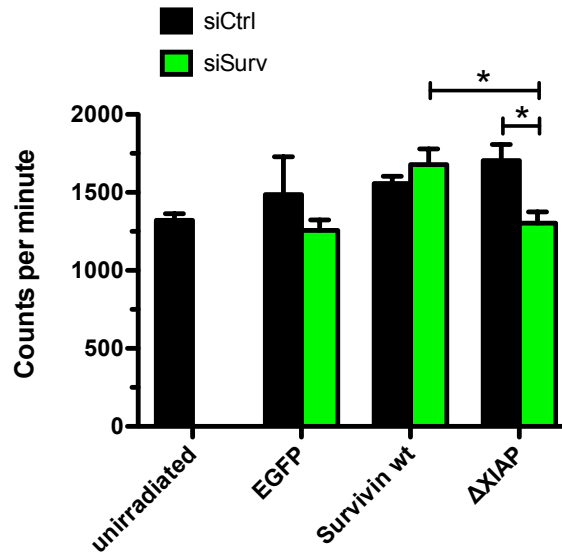


Figure 27: XIAP binding site deletion mutant of Survivin is not able to restore DNA-PK kinase activity upon knockdown of endogenous Survivin. This kinase assay is based on the phosphorylation of a biotinylated p53-derived peptide substrate by DNA-PK with [ $\gamma$ - $^{32}\text{P}$ ] ATP. This biotinylated peptide substrate was then spotted on a biotin capture membrane for detection of the incorporated  $^{32}\text{P}$  into the p53-derived peptide. SW480 cell stably expressing EGFP, Survivin wt and  $\Delta$ XIAP were transiently transfected with control siRNA (black) or Survivin siRNA (green) and 48 h thereafter irradiated with 4 Gy. Nuclear extracts were isolated 1 h after irradiation and SignaTECT kinase assay was performed. Y-axis shows  $^{32}\text{P}$  counts per minute. Data represent means  $\pm$  SEM from four independent experiments. Statistical significances are indicated by asterisks: \*  $p < 0.05$ .

Summing up, in our functional assays we showed that a knockdown of Survivin decreased autophosphorylation of DNA-PKs at Ser2056 as well as the activity of DNA-PK in the Survivin- $\Delta$ XIAP mutant expressing cells. These results indicate that the interaction between DNA-PKs and Survivin is modulating DNA-PK activity in irradiated cells.

---

## 5. Discussion

---

Survivin is dramatically overexpressed in the majority of solid and hematologic human tumours. This has been reported in studies analysing many different tumour entities, whereas the respective normal tissues did not show Survivin expression (Altieri, 2003b; Miura et al., 2011; Rodel et al., 2012). While in non-cancerous cells, Survivin expression is controlled in a cell cycle-dependent manner with a peak in mitosis (Li et al., 1998) and a prominent increase in G2/M phase (Altieri, 2001; Lens et al., 2006), gene expression of Survivin in tumour cells is additionally mediated by cell cycle-independent mechanisms (Li et al., 2010; Xia and Altieri, 2006). These mechanisms can activate transcription, e.g. by demethylation of CpG islands in the promoter region (Hattori et al., 2001) or increased promoter activity by oncologic transcription factors (Li and Altieri, 1999) as well as negatively regulate transcription, for instance by wild type tumour suppressor p53 (Xia and Altieri, 2006). Besides transcriptional regulation, Survivin is also post-transcriptionally regulated by ubiquitylation, de-ubiquitylation (Vong et al., 2005; Zhao et al., 2000) and phosphorylation (Colnaghi and Wheatley, 2010; Dohi et al., 2007; O'Connor et al., 2002; Wheatley et al., 2007).

The elevated levels of Survivin in tumours were not only associated with a higher risk of tumour recurrences and lymph node metastases, but also with a shortened survival of patients with many different tumour entities (Altieri, 2003b; Capalbo et al., 2007; Mita et al., 2008; Rodel et al., 2012; Sprenger et al., 2011). Due to its diagnostic relevance, Survivin has been proposed as prognostic factor (Rodel et al., 2012). Besides, Survivin was reported to be associated with a lowered success to standard anti-cancer therapy and to comprise a chemo- and radiation resistance factor (Asanuma et al., 2000; Chakravarti et al., 2004; Rodel et al., 2003). In line with that, Survivin attenuation resulted in a radiosensitization of tumour cells *in vitro* and *in vivo*. *In vitro* studies using glioblastoma, colorectal carcinoma, hepatocellular carcinoma and non-small cell lung cancer (NSCLC) cells showed a decreased clonogenic survival upon Survivin depletion and ionizing radiation accompanied by increased apoptosis and induction of a G2/M cell cycle arrest (Rodel et al., 2011; Rodel et al., 2012).

Apart from participating in cell division and cytokinesis as a member of the chromosomal passenger complex and its role in apoptosis inhibition, Survivin is a nodal protein that is involved in a multitude of cellular signalling pathways and transcriptional networks in tumour cells (Altieri, 2008). A striking feature of Survivin is its ability to co-operate with a variety of protein partners including other members of the IAP family (Dohi et al., 2004), heat shock proteins (Fortugno et al., 2003; Zhao et al., 2000), microtubules (Giodini et al., 2002; Rosa et al., 2006), p53 (Hoffman et al., 2002) as well as DNA repair proteins (Capalbo et al., 2010). Important for these protein-protein interactions are the different domains and binding sites of Survivin. In order to gain more information about the different protein interactions, further investigation of the different domains and binding sites of Survivin were seriously required. In a recent project in our group, deletion mutants of a multitude of Survivin's domains and binding sites were analysed regarding to cell cycle changes, apoptosis, invasion/transmigration, clonogenic survival and  $\gamma$ H2AX/53BP1 foci detection as a marker for the induction and repair of DNA double-strand breaks. Deletion of the BIR domain as well as XIAP, microtubule and Hsp90 binding sites resulted in an arrest in the G2/M cell cycle phase, increased apoptosis and reduced transmigration ability in SW480 colorectal cancer cells.

---

Moreover, radiation survival was decreased and numbers of residual (24 h)  $\gamma$ H2AX/53BP1 foci were elevated in the XIAP binding site and BIR domain deletion mutant, indicating that the XIAP binding site of Survivin may be essential for clonogenic survival after irradiation as well as the modulation of DNA repair (Petraki, 2014).

The aim of this present study was to further unravel the molecular mechanism underlying a Survivin-mediated modulation of DNA repair. In order to achieve that goal, it was crucial to characterise the interaction between Survivin and DNA-PKcs, which is a major enzyme of the non-homologous end-joining repair pathway (NHEJ).

In a first set of experiments, the impact of Survivin on radiation-induced DNA damage repair was analysed in SW480 colorectal cancer cells by immunofluorescence staining of the phosphorylation of the histone variant H2AX on serine 139 ( $\gamma$ H2AX) and p53-binding protein 1 (53BP1) recruitment as markers for the presence of DNA DSBs.  $\gamma$ H2AX/53BP1 foci were quantified 15 min and 30 min after irradiation with 1 Gy as well as 24 h after irradiation with 4 Gy. Quantification at early time points (15 min, 30 min) showed a significant increase of nuclear foci after irradiation with 1 Gy upon knockdown of Survivin in SW480 cells (Figure 10C). Residual DNA damage (24 h) was also significantly increased upon Survivin depletion and irradiation with 4 Gy (Figure 10B). These findings indicate a hampered double-strand break repair in Survivin-depleted cells, both, at short time points and 24 h after irradiation. These results are consistent with the literature, where a similar effect after Survivin knockdown has been observed in SW480 and LN-229 glioblastoma cells (Capalbo et al., 2010; Reichert et al., 2011). In the present study, a DNA repair modulating effect of Survivin expression was further confirmed using an A2780 ovarian cancer line (Figure 11), indicating that modulation of DNA damage repair by Survivin may comprise a more general functionality of the protein.

In order to identify the DNA DSB repair pathway in which Survivin is involved,  $\gamma$ H2AX/53BP1 foci have been quantified in the BRCA2-deficient ovarian cancer cell line OVSAHO. BRCA2 has a crucial role in the HR repair pathway by loading Rad51 to resected DNA regions (Sorensen et al., 2005) and due to the homozygous deletion of BRCA2 (Domcke et al., 2013), the OVSAHO cell line it is not able to perform HR. Survivin knockdown and irradiation with 4 Gy resulted in significantly increased residual DNA damage after 24 h (Figure 12B). The number of  $\gamma$ H2AX/53BP1 foci at early time points (15 min, 30 min) after IR with 1 Gy was significantly increased in Survivin-depleted cells, too (Figure 12C). The comparable effects, resulting from a Survivin knockdown in HR proficient SW480 and LN-229 cells and the HR-deficient OVSAHO cell line may indicate that Survivin is involved in regulation of a DNA DSB repair pathway other than HR.

These findings are a contradictory to the literature. Survivin has recently been shown to participate in HR. By using the small-molecule Survivin inhibitor YM155, Qin and colleagues were able to show a suppressed HR repair in human esophageal squamous cell carcinoma (ESCC) (Qin et al., 2014). Besides, Survivin was found to participate in HR by modulating the protein expression of Rad51 and MUS81 in breast cancer cells (Vequaud et al., 2016). In the present study, a contribution of Survivin in HR was thus further analysed by a real-time PCR-based HR assay, which is often used to measure HR efficiency in cells upon different treatments (Christmann et al., 2017; Maachani et al., 2015; Ohba et al., 2014). In this assay,

---

HR efficiency was quantified by co-transfection of two plasmids, each with a different mutation in its lacZ coding region. A recombination of these two plasmids leads to a recombined plasmid with a functional lacZ sequence which can be quantified with specific primers via real-time PCR (Ohba et al., 2014). In contrast to the literature cited above, a significantly decreased HR efficiency after Survivin knockdown and DSB induction by irradiation with 4 Gy could not be observed in SW480 colorectal cancer cells (Figure 13). These discrepancies could result from the different cell lines that were used in these studies. Moreover, in these studies the Survivin suppressant YM155 was used. This molecule, however, is also reported to directly impact on DNA double-strand break repair (Hong et al., 2017) and thus may facilitate some of the effects reported.

According to preceding studies, Survivin accumulates in the nucleus following irradiation. During the regulation of DNA repair it interacts with DNA-PKcs and Ku70, two important proteins of the NHEJ DSB repair pathway (Capalbo et al., 2010; Reichert et al., 2011). In this study, immunoprecipitation experiments confirmed the binding of recombinant Survivin wt to DNA-PKcs in both SW480 colorectal cancer (Figure 15) and LN-229 glioblastoma cells (Figure 16). By contrast, Survivin lacking the XIAP binding site did not precipitate with DNA-PKcs. As a result, the XIAP binding site of Survivin is not only important for the formation of a Survivin-XIAP complex that is inhibiting apoptosis (Dohi et al., 2004), but also for the interaction with DNA-PKcs in order to regulate DNA double-strand break repair via NHEJ. The decreased radiation survival and the elevated numbers of residual  $\gamma$ H2AX/53BP1 foci in the XIAP binding site deletion mutant of Survivin that was described earlier (Petraki, 2014), might at least in part, be explained by the inability of this mutant to interact with DNA-PKcs. Since the XIAP binding site is a part of the larger BIR domain of Survivin, this is in line with the general function of the BIR domains of all IAPs as mediator of protein-protein interactions (Srinivasula and Ashwell, 2008).

Methodically, immunoprecipitations were performed with anti-DNA-PKcs antibodies. However, the vice versa experiment using anti-Survivin antibodies did not work. The reason for this may be the huge molecular weight of DNA-PKcs. Regarding its considerable weight of 470 kDa compared to smaller Survivin-EGFP construct (44 kDa) it is possible that during an interaction, DNA-PKcs sterically hinders the binding of the antibody to the protein. Therefore, precipitation of the Survivin-EGFP/DNA-PKcs complex with an anti-Survivin antibody might not be possible. In order to make sure that the interaction of Survivin and DNA-PKcs is not EGFP-mediated, EGFP-expressing cells were used as a control. In the immunoprecipitation experiment in SW480 cells, EGFP in the input runs slightly below the light chain of the antibody that is present in the IP lanes. However, EGFP did not bind to precipitated DNA-PKcs (Figure 15).

After showing a direct involvement of the XIAP binding site of Survivin in the interaction with DNA-PKcs, the next step was to investigate possible binding regions of DNA-PKcs mediating the interaction with Survivin. For Aurora-B, another well-established interaction partner of Survivin in terms of cell cycle regulation, it was shown that Survivin binds to its catalytic domain (Chen et al., 2003). In the presence of Survivin, histone H3 is phosphorylated more efficiently by Aurora-B than in the absence of Survivin. Furthermore, a decreased Aurora-B kinase activity in cells lacking Survivin indicates that Survivin stimulates Aurora-B kinase activity in order to help Aurora-B targeting its substrates during the cell cycle (Chen et al.,

---

2003). In analogy, we next analysed a putative interaction of Survivin with the kinase domain of DNA-PKcs. Indeed, by using GST pulldown assay (Figure 18), NanoLuc Binary Technology (NanoBiT®) complementation assay (Figure 21) and flow cytometry-based Förster resonance energy transfer (Figure 25), binding of Survivin to the kinase domain (PI3K) of DNA-PKcs was observed. Furthermore, *in silico* docking analysis was used to gain a bioinformatic perspective on the interaction between Survivin and DNA-PKcs.

At first, a glutathione S-transferase (GST) pulldown assay was performed using lysates of SW480 colorectal cancer cells. After pulldown of GST-PI3K, both Survivin-EGFP and endogenous Survivin were found binding to the GST-PI3K fusion construct (Figure 18A). By using EGFP and GST controls, it was ruled out that the interaction was induced by the presence of the tags (Figure 18A). However, endogenous Survivin was expected being pulled down by GST-PI3K also in cells expressing EGFP, which did not. The reason for this remains unclear, but the amount of GST-PI3K-bound endogenous Survivin might have been under the detectable minimum of the western blot. In GST control pulldown assays, Survivin was not detectable, hence, we suggest a specific interaction between Survivin and the PI3K domain of DNA-PKcs. These results were confirmed by using FLAG-tagged Survivin (Figure 18B). The bacterial expression of GST-PI3K turned out to be fairly weak, instead several degradation products could be detected (Figure 17B). The fact that an interaction of the Survivin fusion constructs with PI3K was found although expression of GST-PI3K was weak, suggests that it is indeed a specific interaction.

To confirm the results of the GST pulldown assay, the two-subunit luciferase-based NanoBiT complementation assay was performed but in contrast to the GST pulldown assay, the NanoBiT assay was performed in HEK-293T cells. In preliminary experiments using different transfection reagents, transfection efficiency in HEK-293T cells was found to be substantially higher than in SW480 cells and therefore this cell line was chosen for this interaction assay. Since it measures the luciferase signal generated only from double-transfected cells, a high transfection efficiency is essential for obtaining reproducible results. A discrimination of non-transfected cells was not possible prior to measuring luminescence. To verify the specificity of the NanoBiT assay, a negative control using co-transfection of the LgBiT fusion construct and a HaloTag construct was used. Interaction of Survivin-SmBiT and LgBiT-PI3K was significantly increased compared to HaloTag and single fusion controls, therefore the interaction can be considered specific (Figure 21B).

Lastly, the interaction of Survivin with the PI3K domain of DNA-PKcs was analysed via Förster resonance energy transfer. Here, YFP and CFP fluorescence tags were fused to the interaction partners Survivin and the kinase domain (PI3K) of DNA-PKcs. When measuring the CFP-YFP fusion construct as well as CFP and YFP negative controls for the establishment of the flow cytometric based FRET assay, the results were as expected. The CFP-YFP fusion construct resulted in nearly 100% FRET-positive cells, proving the functionality of this assay. False positive cells created by a co-localisation of the fluorophores in the cell without protein interactions could be ruled out because co-transfection of the CFP and YFP plasmids did not show any interaction (Figure 25). Another proof of principle control was the co-transfection of Survivin fused to CFP and YFP, resulting in approximately 75% FRET-positive cells. This confirms the published ability of Survivin forming homodimers (Chantalat et al., 2000; Verdecia et al., 2000). The decreased number of FRET-positive cells compared to the CFP-YFP

---

fusion construct, suggests that not all Survivin proteins are forming homodimers. Another explanation could be that endogenous Survivin forms dimers with CFP- or YFP-tagged Survivin, which would not be detected as a FRET-positive signal. The analysis of the interaction between Survivin and the kinase domain of DNA-PKcs (PI3K) resulted in approximately 18% FRET-positive cells. As opposed to this, co-transfection of Survivin and the HEAT1 or FATC domain of DNA-PKcs showed no or very few FRET-positive cells (Figure 25). These findings support the assumption that the interaction of Survivin with DNA-PKcs is indeed mainly mediated by the kinase domain of DNA-PKcs.

One remaining question is why the interaction between Survivin and the PI3K domain of DNA-PKcs was rather weak in both, NanoBiT and FRET, compared to the positive controls of the respective assay. One explanation for the weak interaction might be the cellular localisation of the two fusion proteins. Fluorescence microscopy of the CFP and YFP fusion constructs indicated localisation of both constructs in the cytoplasm and in the nucleus (Figure 23B). Since DNA-PKcs is a DNA repair protein, it is mainly localised in the nucleus (Koike et al., 1999) and accordingly the interaction with Survivin is considered most likely in the nucleus as well. It is known that Survivin accumulates in the nucleus shortly after irradiation (Capalbo et al., 2010), which supports this hypothesis. The mechanism behind the accumulation of Survivin in the nucleus is not yet fully understood, however, it could be hampered by the fusion of Survivin to the fluorescence tags. Additionally, the PI3K-DNA-PKcs fusion protein is not actively transported to the nucleus because its sequence does not contain a nuclear localisation signal (NLS). As a result, both, the PI3K and the Survivin fusion proteins are only partly present in the nucleus. An interaction in the cytoplasm is probably not possible due to lack of nuclear co-factors that are involved in or needed for the interaction. Another factor that could negatively affect the interaction between Survivin and the PI3K domain of DNA-PKcs is the absence of the neighbouring FAT and FATC domains as well as the HEAT repeats. Although Survivin does not bind to other tested single domains of DNA-PKcs (HEAT1 and FATC, Figure 25B) except PI3K, these other domains could be beneficial for an interaction of Survivin with the PI3K domain. According to the literature, the different parts of DNA-PKcs have a different role on its activity (Davis et al., 2013). The HEAT repeats probably mediate protein-protein interactions (Andrade and Bork, 1995; Brewerton et al., 2004; Jiang et al., 2006) and the FATC domain was found to be required for kinase activity (Beamish et al., 2000). The presence of these domains may further increase the ability of the PI3K domain and Survivin to form a complex.

A bioinformatic modelling approach for the interaction of Survivin with DNA-PKcs was performed using the programs Schrödinger Suite and PatchDock. Before the docking analysis, pre-processing steps were performed to obtain more native structures of the proteins. After the docking analysis, the best-docked poses were post-processed and refined by side-chain optimization and rigid-body minimization. Interactions between residues were determined according to their binding energies ( $\Delta G$ ) and distances. Interaction pairs with higher  $\Delta G$  values and distances  $< 5 \text{ \AA}$  between side chain hydrogen atoms were qualified as potential interactors (see chapter 3.2.21 for a more detailed description of the docking analysis).

The protein docking analysis confirmed binding of Survivin to the PI3K kinase domain of DNA-PKcs. However, for this interaction Survivin must be present in its dimerized form. In order to mimic more natural conditions of the interaction, we aimed to find out whether the

---

interaction of Survivin with the kinase domain of DNA-PKcs is also happening in the presence of the whole DNA-PKcs protein. Therefore, protein docking analysis was performed, investigating the interaction of Survivin with the entire DNA-PKcs protein (Figure 28).

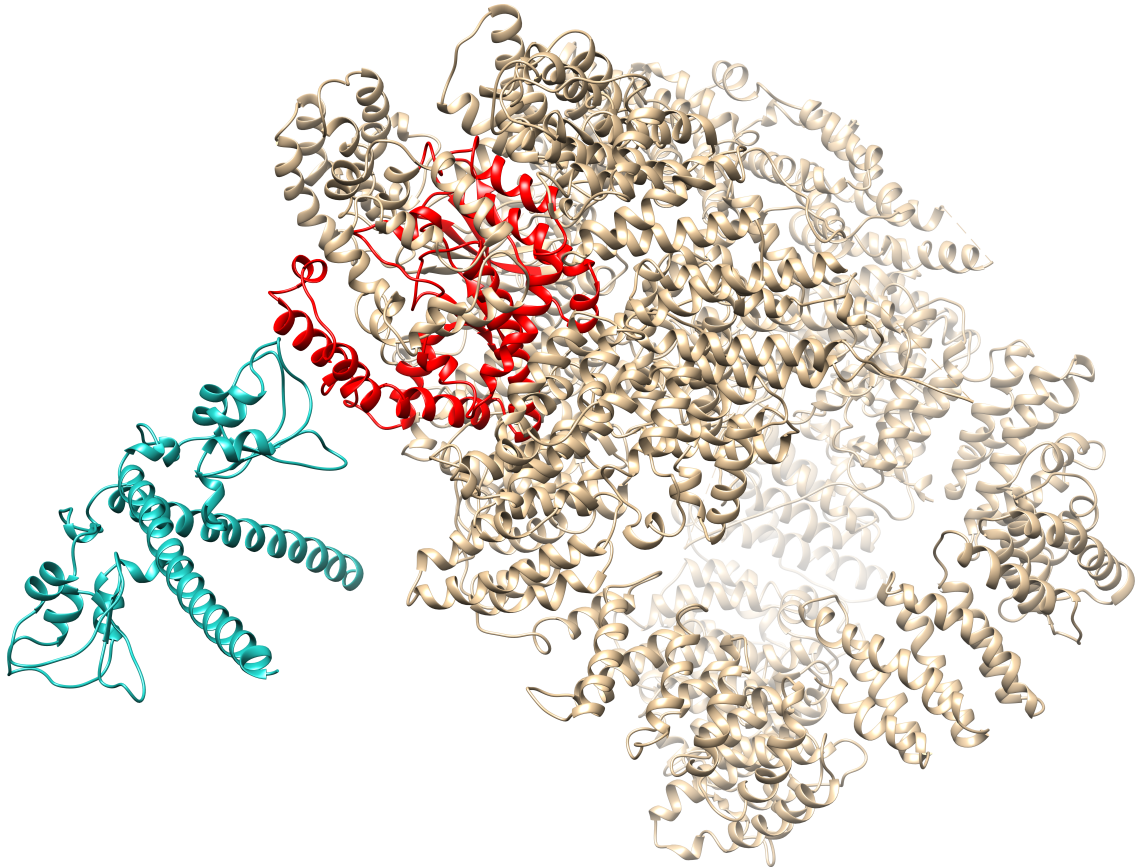


Figure 28: Protein docking analysis show an interaction between Survivin and DNA-PKcs. Before the docking analysis, pre-processing steps were performed to obtain more native structures of the proteins. After the docking analysis, the best-docked poses were then post-processed and refined by side-chain optimization and rigid-body minimization. After that, interactions between residues were determined according to their binding energies ( $\Delta G$ ) and their distances. Interaction pairs with higher  $\Delta G$  values and distances  $<5 \text{ \AA}$  between side chain hydrogen atoms were qualified as potential interactors. Cyan: Survivin; red: kinase domain (PI3K) of DNA-PKcs; light brown: the rest of DNA-PKcs. Protein model was created using the Chimera program (University of California, San Francisco, CA, USA). Protein docking analysis was performed by Ömer Güllülü.

The protein docking analysis resulted in the hypothesis that Survivin is only able to bind to DNA-PKcs in its dimerized form (Figure 28), although this assumption has not yet been analysed experimentally.

For the dimerization of Survivin, its N-terminal region including the BIR domain is sufficient (Chantalat et al., 2000). The exact function of the Survivin dimerization is not yet fully understood, however, it could have a potential role in stabilizing Survivin. In terms of its role in the organisation of the microtubule organizing centres (MTOC), the orientation and length

---

of the two C-terminal helices of the Survivin dimer suggest that Survivin could bridge proteins participating in the organization of the MTOC (Verdecia et al., 2000). Considering the need of dimerized Survivin for the interaction with DNA-PKcs, it could possibly have a similar bridging function in DNA double-strand break repair. Dimerization is also important for Survivin to remain in the nucleus. The reason for that is the monomer-specific NES of Survivin, whose hydrophobic residues are occupied in its homodimer form. With these occupied residues, Crm1, the main export protein in mammalian cells that facilitates the transport of RNA and proteins across the nuclear membrane to the cytoplasm, is no longer able to shuttle Survivin (Engelsma et al., 2007; Knauer et al., 2007; Stauber et al., 2006). In summary, dimerization of Survivin modulates cytoplasmic access of the protein and by being present in its dimerized form Survivin is able to accumulate in the nucleus where it can interact with DNA-PKcs.

Functionally, Survivin has been shown to impact on Ser2056 autophosphorylation of DNA-PKcs as well as DNA-PK kinase activity after irradiation (Capalbo et al., 2010; Reichert et al., 2011). In this study, a reduction of Ser2056 autophosphorylation after siRNA-mediated Survivin attenuation followed by irradiation was confirmed in SW480 colorectal cancer and LN-229 glioblastoma cells (Figure 26). Besides, irradiation of SW480 cells stably expressing EGFP, Survivin wt and  $\Delta$ XIAP deletion mutant of Survivin resulted in an increased DNA-PK activity compared to non-irradiated cells (Figure 27). Additionally, siRNA targeting the endogenous Survivin was used to analyse the effects of the recombinant Survivin mutants on the DNA-PK activity. Depletion of endogenous Survivin followed by irradiation decreased DNA-PK kinase activity to the level observed in non-irradiated cells expressing the EGFP and  $\Delta$ XIAP construct. Only the recombinant Survivin wt was able to rescue DNA-PK activity after siRNA-mediated attenuation of endogenous Survivin and irradiation (Figure 27). These results indicate the importance of the XIAP binding site of Survivin for DNA-PK kinase activity in irradiated cells. Without its XIAP binding site, Survivin is not able to interact with DNA-PKcs in order to increase DNA-PK activity after irradiation.

In this study we show that Survivin is not only interacting with DNA-PKcs but directly binds to its kinase domain (Figure 29). This interaction between Survivin and DNA-PKcs is important for DNA-PK kinase activity in irradiated cells. However, this does not mean that Survivin depletion leads to a loss of the NHEJ repair pathway. Knockdown of Survivin only modulates DNA repair capacity. Also, DNA-PK activity is just decreased after Survivin knockdown and not completely depleted. All in all, the role of Survivin in the NHEJ repair of irradiation-induced DSBs is more of modulating nature, comparable to its role in the chromosomal passenger complex where it enhances the kinase activity of Aurora-B and targets it to its substrate (Chen et al., 2003). Depletion of Survivin in HeLa cells causes mislocalisation of Aurora-B followed by a decreased Aurora-B activity and increased cytokinesis defects (Chen et al., 2003). This fits to the impact of Survivin knockdown on DNA-PKcs with decreased kinase activity and a hampered DNA DSB repair. Regarding this, the role of Survivin might be very similar for both kinases, as a bridging protein targeting both, Aurora-B and DNA-PKcs to its substrates.



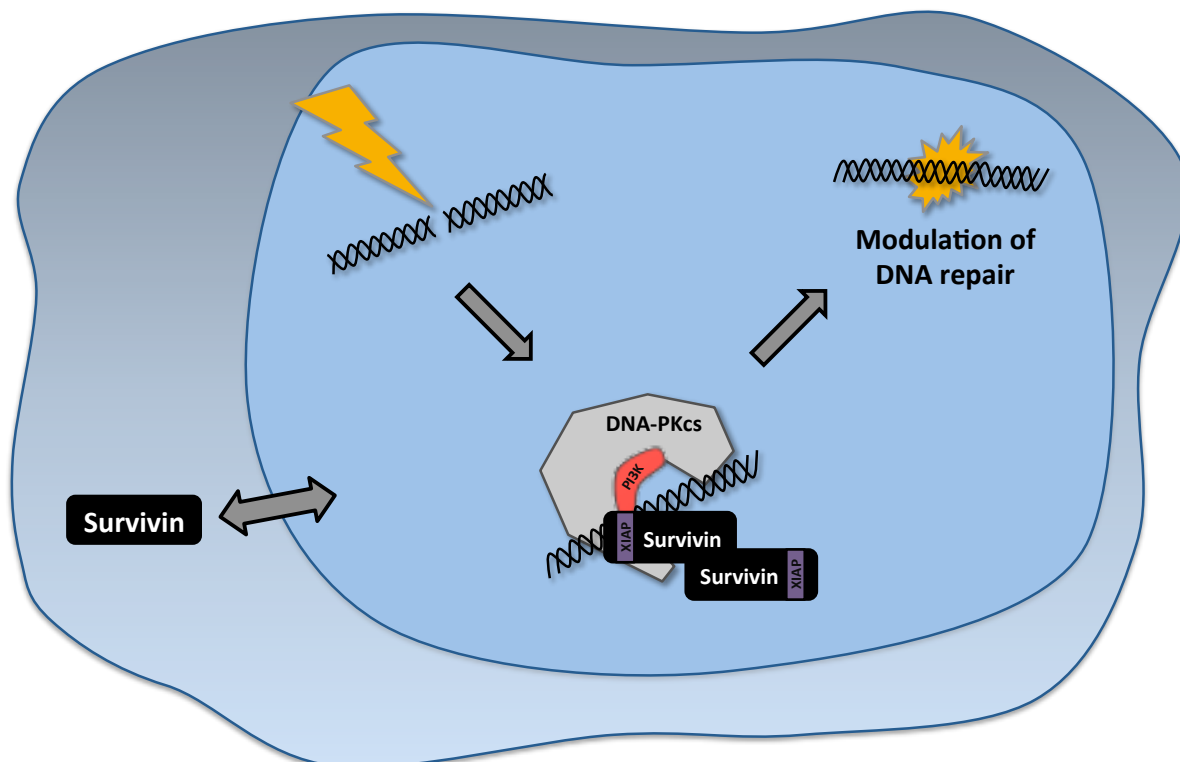


Figure 29: Survivin as a modulator of the NHEJ double-strand break repair pathway. In this schematic illustration Survivin is shown to translocate to the nucleus following irradiation in order to modulate the NHEJ double-strand break repair pathway via binding to the kinase domain (PI3K) of DNA-PKcs in its dimerized form. Thereby, the XIAP binding site of Survivin is crucial for binding to DNA-PKcs and its kinase activity.

The different expression in tumours compared to their respective normal tissue as well as the involvement in apoptosis inhibition, maintaining cancer cell viability and its robust correlation with poor patient prognosis, renders Survivin a promising target for molecular cancer therapy (Mita et al., 2008; Peery et al., 2017; Pennati et al., 2008). In line with that, a variety of Survivin-targeting strategies such as mRNA antagonization, siRNAs, small molecule inhibitors or Survivin-based immunotherapy have been developed (Mita et al., 2008; Peery et al., 2017). Despite strong preclinical data for some inhibitors, only limited response of currently available therapeutics targeting Survivin in clinical trials was found (Peery et al., 2017).

The improved understanding of Survivin's role in the NHEJ repair of radiation-induced DSBs shows once more the importance of Survivin for tumour cells. Targeting Survivin and thereby achieving hampered DNA repair in the tumour tissue could, especially in combination with radiotherapy, may improve the clinical outcome of the patients. One key for successful targeting of Survivin in order to inhibit DNA repair could be a homodimerization inhibitor. By using such an inhibitor, dimerization could be prevented and Survivin would be exported from the nucleus to the cytoplasm. By preventing the interaction between Survivin and DNA-PKcs using an inhibitor targeting the exact interacting amino acids, a benefit for the patients may be achieved. Although the exact interacting amino acids are yet to be identified.

---

In conclusion these findings for the first time indicate that Survivin not only interacts with DNA-PKcs but directly binds to its kinase domain. Besides it modulates DNA-PKcs kinase activity and as a consequence repair of radiation induced DNA double-strand breaks. These results add a further facet to the plethora of functions exerted by the nodal protein Survivin in the cellular radiation response in cancer cells.

### **Future prospects**

For future perspectives, the interaction between Survivin and DNA-PKcs must be further investigated by looking more closely at the sites of interaction of the two proteins. By using a bioinformatic protein docking approach, the exact amino acids of Survivin that are involved in its interaction with DNA-PKcs, more specifically its PI3K domain could be identified. In the next step, single amino acids or a combination of various amino acids within the binding site could be mutated to check whether an interaction of the two proteins would still be possible. Ideally, one or a combination of several mutations would eliminate the interaction while wild type Survivin could still interact.

Preliminary data including mass spectrometry-based quantitative proteomics following stable isotope labelling with amino acids in cell culture (SILAC) further revealed potential interaction partners of Survivin, such as Parp1 and XRCC1. Both of these proteins are important factors in the MMEJ (also called alternative end-joining) (Iliakis et al., 2015). An interaction between Survivin and Parp1 and/or XRCC1 could imply its involvement in a second end-joining DSB repair pathway. Interaction with two factors of this pathway would suggest once more a protein bridging function of Survivin. First immunoprecipitation analysis already confirmed binding of Survivin to Parp1, although this interaction does not seem to be dependent of Survivin's XIAP binding site (data not shown). Considering this, Survivin's role could go beyond NHEJ double-strand break repair, which could be worth further investigation.

---

## 6. References

---

- Altieri, D.C. (2001). The molecular basis and potential role of survivin in cancer diagnosis and therapy. *Trends in molecular medicine* 7, 542-547.
- Altieri, D.C. (2003a). Survivin, versatile modulation of cell division and apoptosis in cancer. *Oncogene* 22, 8581-8589.
- Altieri, D.C. (2003b). Validating survivin as a cancer therapeutic target. *Nature reviews Cancer* 3, 46-54.
- Altieri, D.C. (2008). Survivin, cancer networks and pathway-directed drug discovery. *Nature reviews Cancer* 8, 61-70.
- Altieri, D.C. (2010). Survivin and IAP proteins in cell-death mechanisms. *The Biochemical journal* 430, 199-205.
- Ambrosini, G., Adida, C., and Altieri, D.C. (1997). A novel anti-apoptosis gene, survivin, expressed in cancer and lymphoma. *Nature medicine* 3, 917-921.
- Andersen, M.H., and Thor, S.P. (2002). Survivin - a universal tumor antigen. *Histology and histopathology* 17, 669-675.
- Andrade, M.A., and Bork, P. (1995). HEAT repeats in the Huntington's disease protein. *Nature genetics* 11, 115-116.
- Andrusier, N., Nussinov, R., and Wolfson, H.J. (2007). FireDock: fast interaction refinement in molecular docking. *Proteins* 69, 139-159.
- Arora, V., Cheung, H.H., Plenchette, S., Micali, O.C., Liston, P., and Korneluk, R.G. (2007). Degradation of survivin by the X-linked inhibitor of apoptosis (XIAP)-XAF1 complex. *The Journal of biological chemistry* 282, 26202-26209.
- Asanuma, K., Moriai, R., Yajima, T., Yagihashi, A., Yamada, M., Kobayashi, D., and Watanabe, N. (2000). Survivin as a radioresistance factor in pancreatic cancer. *Japanese journal of cancer research : Gann* 91, 1204-1209.
- Badran, A., Yoshida, A., Ishikawa, K., Goi, T., Yamaguchi, A., Ueda, T., and Inuzuka, M. (2004). Identification of a novel splice variant of the human anti-apoptosis gene survivin. *Biochemical and biophysical research communications* 314, 902-907.
- Bakkenist, C.J., and Kastan, M.B. (2003). DNA damage activates ATM through intermolecular autophosphorylation and dimer dissociation. *Nature* 421, 499-506.
- Banning, C., Votteler, J., Hoffmann, D., Koppensteiner, H., Warmer, M., Reimer, R., Kirchhoff, F., Schubert, U., Hauber, J., and Schindler, M. (2010). A flow cytometry-based FRET assay to identify and analyse protein-protein interactions in living cells. *PloS one* 5, e9344.

---

Baumann, P., Benson, F.E., and West, S.C. (1996). Human Rad51 protein promotes ATP-dependent homologous pairing and strand transfer reactions in vitro. *Cell* 87, 757-766.

Beamish, H.J., Jessberger, R., Riballo, E., Priestley, A., Blunt, T., Kysela, B., and Jeggo, P.A. (2000). The C-terminal conserved domain of DNA-PKcs, missing in the SCID mouse, is required for kinase activity. *Nucleic acids research* 28, 1506-1513.

Beardmore, V.A., Ahonen, L.J., Gorbsky, G.J., and Kallio, M.J. (2004). Survivin dynamics increases at centromeres during G2/M phase transition and is regulated by microtubule-attachment and Aurora B kinase activity. *Journal of cell science* 117, 4033-4042.

Beucher, A., Birraux, J., Tchouandong, L., Barton, O., Shibata, A., Conrad, S., Goodarzi, A.A., Krempler, A., Jeggo, P.A., and Lobrich, M. (2009). ATM and Artemis promote homologous recombination of radiation-induced DNA double-strand breaks in G2. *The EMBO journal* 28, 3413-3427.

Bishop, J.M. (1987). The molecular genetics of cancer. *Science* 235, 305-311.

Bishop, J.M. (1991). Molecular themes in oncogenesis. *Cell* 64, 235-248.

Bolderson, E., Tomimatsu, N., Richard, D.J., Boucher, D., Kumar, R., Pandita, T.K., Burma, S., and Khanna, K.K. (2010). Phosphorylation of Exo1 modulates homologous recombination repair of DNA double-strand breaks. *Nucleic acids research* 38, 1821-1831.

Bosotti, R., Isacchi, A., and Sonnhammer, E.L. (2000). FAT: a novel domain in PIK-related kinases. *Trends in biochemical sciences* 25, 225-227.

Bourhis, E., Hymowitz, S.G., and Cochran, A.G. (2007). The mitotic regulator Survivin binds as a monomer to its functional interactor Borealin. *The Journal of biological chemistry* 282, 35018-35023.

Branzei, D., and Foiani, M. (2008). Regulation of DNA repair throughout the cell cycle. *Nature reviews Molecular cell biology* 9, 297-308.

Brewerton, S.C., Dore, A.S., Drake, A.C., Leuther, K.K., and Blundell, T.L. (2004). Structural analysis of DNA-PKcs: modelling of the repeat units and insights into the detailed molecular architecture. *Journal of structural biology* 145, 295-306.

Caldas, H., Honsey, L.E., and Altura, R.A. (2005). Survivin 2alpha: a novel Survivin splice variant expressed in human malignancies. *Molecular cancer* 4, 11.

Capalbo, G., Dittmann, K., Weiss, C., Reichert, S., Hausmann, E., Rodel, C., and Rodel, F. (2010). Radiation-induced survivin nuclear accumulation is linked to DNA damage repair. *International journal of radiation oncology, biology, physics* 77, 226-234.

Capalbo, G., Rodel, C., Stauber, R.H., Knauer, S.K., Bache, M., Kappler, M., and Rodel, F. (2007). The role of survivin for radiation therapy. Prognostic and predictive factor and therapeutic target. *Strahlentherapie und Onkologie : Organ der Deutschen Rontgenesellschaft [et al]* 183, 593-599.

---

Celeste, A., Petersen, S., Romanienko, P.J., Fernandez-Capetillo, O., Chen, H.T., Sedelnikova, O.A., Reina-San-Martin, B., Coppola, V., Meffre, E., Difilippantonio, M.J., *et al.* (2002). Genomic instability in mice lacking histone H2AX. *Science* 296, 922-927.

Chakravarti, A., Zhai, G.G., Zhang, M., Malhotra, R., Latham, D.E., Delaney, M.A., Robe, P., Nestler, U., Song, Q., and Loeffler, J. (2004). Survivin enhances radiation resistance in primary human glioblastoma cells via caspase-independent mechanisms. *Oncogene* 23, 7494-7506.

Chan, D.W., and Lees-Miller, S.P. (1996). The DNA-dependent protein kinase is inactivated by autophosphorylation of the catalytic subunit. *The Journal of biological chemistry* 271, 8936-8941.

Chantalat, L., Skoufias, D.A., Kleman, J.P., Jung, B., Dideberg, O., and Margolis, R.L. (2000). Crystal structure of human survivin reveals a bow tie-shaped dimer with two unusual alpha-helical extensions. *Molecular cell* 6, 183-189.

Chen, B.P., Chan, D.W., Kobayashi, J., Burma, S., Asaithamby, A., Morotomi-Yano, K., Botvinick, E., Qin, J., and Chen, D.J. (2005). Cell cycle dependence of DNA-dependent protein kinase phosphorylation in response to DNA double strand breaks. *The Journal of biological chemistry* 280, 14709-14715.

Chen, J., Jin, S., Tahir, S.K., Zhang, H., Liu, X., Sarthy, A.V., McGonigal, T.P., Liu, Z., Rosenberg, S.H., and Ng, S.C. (2003). Survivin enhances Aurora-B kinase activity and localizes Aurora-B in human cells. *The Journal of biological chemistry* 278, 486-490.

Chen, J., Wu, W., Tahir, S.K., Kroeger, P.E., Rosenberg, S.H., Cowser, L.M., Bennett, F., Krajewski, S., Krajewska, M., Welsh, K., *et al.* (2000). Down-regulation of survivin by antisense oligonucleotides increases apoptosis, inhibits cytokinesis and anchorage-independent growth. *Neoplasia* 2, 235-241.

Christmann, M., Diesler, K., Majhen, D., Steigerwald, C., Berte, N., Freund, H., Stojanovic, N., Kaina, B., Osmak, M., Ambriovic-Ristov, A., *et al.* (2017). Integrin alphaVbeta3 silencing sensitizes malignant glioma cells to temozolomide by suppression of homologous recombination repair. *Oncotarget* 8, 27754-27771.

Ciccia, A., and Elledge, S.J. (2010). The DNA damage response: making it safe to play with knives. *Molecular cell* 40, 179-204.

Clegg, R.M. (1995). Fluorescence resonance energy transfer. *Current opinion in biotechnology* 6, 103-110.

Collis, S.J., DeWeese, T.L., Jeggo, P.A., and Parker, A.R. (2005). The life and death of DNA-PK. *Oncogene* 24, 949-961.

Colnaghi, R., Connell, C.M., Barrett, R.M., and Wheatley, S.P. (2006). Separating the anti-apoptotic and mitotic roles of survivin. *The Journal of biological chemistry* 281, 33450-33456.

Colnaghi, R., and Wheatley, S.P. (2010). Liaisons between survivin and Plk1 during cell division and cell death. *The Journal of biological chemistry* 285, 22592-22604.

---

Conze, D.B., Albert, L., Ferrick, D.A., Goeddel, D.V., Yeh, W.C., Mak, T., and Ashwell, J.D. (2005). Posttranscriptional downregulation of c-IAP2 by the ubiquitin protein ligase c-IAP1 in vivo. *Molecular and cellular biology* 25, 3348-3356.

Critchlow, S.E., and Jackson, S.P. (1998). DNA end-joining: from yeast to man. *Trends in biochemical sciences* 23, 394-398.

Crook, N.E., Clem, R.J., and Miller, L.K. (1993). An apoptosis-inhibiting baculovirus gene with a zinc finger-like motif. *Journal of virology* 67, 2168-2174.

Cui, X., Yu, Y., Gupta, S., Cho, Y.M., Lees-Miller, S.P., and Meek, K. (2005). Autophosphorylation of DNA-dependent protein kinase regulates DNA end processing and may also alter double-strand break repair pathway choice. *Molecular and cellular biology* 25, 10842-10852.

Davis, A.J., Chen, B.P., and Chen, D.J. (2014). DNA-PK: a dynamic enzyme in a versatile DSB repair pathway. *DNA repair* 17, 21-29.

Davis, A.J., Lee, K.J., and Chen, D.J. (2013). The N-terminal region of the DNA-dependent protein kinase catalytic subunit is required for its DNA double-stranded break-mediated activation. *The Journal of biological chemistry* 288, 7037-7046.

de la Torre-Ruiz, M., and Lowndes, N.F. (2000). The *Saccharomyces cerevisiae* DNA damage checkpoint is required for efficient repair of double strand breaks by non-homologous end joining. *FEBS letters* 467, 311-315.

Ditchfield, C., Johnson, V.L., Tighe, A., Ellston, R., Haworth, C., Johnson, T., Mortlock, A., Keen, N., and Taylor, S.S. (2003). Aurora B couples chromosome alignment with anaphase by targeting BubR1, Mad2, and Cenp-E to kinetochores. *The Journal of cell biology* 161, 267-280.

Dohi, T., Okada, K., Xia, F., Wilford, C.E., Samuel, T., Welsh, K., Marusawa, H., Zou, H., Armstrong, R., Matsuzawa, S., *et al.* (2004). An IAP-IAP complex inhibits apoptosis. *The Journal of biological chemistry* 279, 34087-34090.

Dohi, T., Xia, F., and Altieri, D.C. (2007). Compartmentalized phosphorylation of IAP by protein kinase A regulates cytoprotection. *Molecular cell* 27, 17-28.

Domcke, S., Sinha, R., Levine, D.A., Sander, C., and Schultz, N. (2013). Evaluating cell lines as tumour models by comparison of genomic profiles. *Nature communications* 4, 2126.

Du, C., Fang, M., Li, Y., Li, L., and Wang, X. (2000). Smac, a mitochondrial protein that promotes cytochrome c-dependent caspase activation by eliminating IAP inhibition. *Cell* 102, 33-42.

Duffy, M.J., O'Donovan, N., Brennan, D.J., Gallagher, W.M., and Ryan, B.M. (2007). Survivin: a promising tumor biomarker. *Cancer letters* 249, 49-60.

Engelsma, D., Rodriguez, J.A., Fish, A., Giaccone, G., and Fornerod, M. (2007). Homodimerization antagonizes nuclear export of survivin. *Traffic* 8, 1495-1502.

---

Esteve, P.O., Chin, H.G., and Pradhan, S. (2005). Human maintenance DNA (cytosine-5)-methyltransferase and p53 modulate expression of p53-repressed promoters. *Proceedings of the National Academy of Sciences of the United States of America* *102*, 1000-1005.

Fang, Z.H., Dong, C.L., Chen, Z., Zhou, B., Liu, N., Lan, H.F., Liang, L., Liao, W.B., Zhang, L., and Han, Z.C. (2009). Transcriptional regulation of survivin by c-Myc in BCR/ABL-transformed cells: implications in anti-leukaemic strategy. *Journal of cellular and molecular medicine* *13*, 2039-2052.

Förster, T. (1948). Zwischenmolekulare Energiewanderung und Fluoreszenz. *Annalen der Physik* *437*, 55-75.

Fortugno, P., Beltrami, E., Plescia, J., Fontana, J., Pradhan, D., Marchisio, P.C., Sessa, W.C., and Altieri, D.C. (2003). Regulation of survivin function by Hsp90. *Proceedings of the National Academy of Sciences of the United States of America* *100*, 13791-13796.

Fukuda, S., and Pelus, L.M. (2006). Survivin, a cancer target with an emerging role in normal adult tissues. *Molecular cancer therapeutics* *5*, 1087-1098.

Garcia, V., Phelps, S.E., Gray, S., and Neale, M.J. (2011). Bidirectional resection of DNA double-strand breaks by Mre11 and Exo1. *Nature* *479*, 241-244.

Gassmann, R., Carvalho, A., Henzing, A.J., Ruchaud, S., Hudson, D.F., Honda, R., Nigg, E.A., Gerloff, D.L., and Earnshaw, W.C. (2004). Borealin: a novel chromosomal passenger required for stability of the bipolar mitotic spindle. *The Journal of cell biology* *166*, 179-191.

Giodini, A., Kallio, M.J., Wall, N.R., Gorbisky, G.J., Tognin, S., Marchisio, P.C., Symons, M., and Altieri, D.C. (2002). Regulation of microtubule stability and mitotic progression by survivin. *Cancer research* *62*, 2462-2467.

Goodwin, J.F., and Knudsen, K.E. (2014). Beyond DNA repair: DNA-PK function in cancer. *Cancer discovery* *4*, 1126-1139.

Gritsko, T., Williams, A., Turkson, J., Kaneko, S., Bowman, T., Huang, M., Nam, S., Eweis, I., Diaz, N., Sullivan, D., *et al.* (2006). Persistent activation of stat3 signaling induces survivin gene expression and confers resistance to apoptosis in human breast cancer cells. *Clinical cancer research : an official journal of the American Association for Cancer Research* *12*, 11-19.

Guex, N., and Peitsch, M.C. (1997). SWISS-MODEL and the Swiss-PdbViewer: an environment for comparative protein modeling. *Electrophoresis* *18*, 2714-2723.

Guha, M., and Altieri, D.C. (2009). Survivin as a global target of intrinsic tumor suppression networks. *Cell cycle* *8*, 2708-2710.

Guha, M., Plescia, J., Leav, I., Li, J., Languino, L.R., and Altieri, D.C. (2009). Endogenous tumor suppression mediated by PTEN involves survivin gene silencing. *Cancer research* *69*, 4954-4958.

Hanahan, D., and Weinberg, R.A. (2000). The hallmarks of cancer. *Cell* *100*, 57-70.

---

Hanahan, D., and Weinberg, R.A. (2011). Hallmarks of cancer: the next generation. *Cell* *144*, 646-674.

Hattori, M., Sakamoto, H., Satoh, K., and Yamamoto, T. (2001). DNA demethylase is expressed in ovarian cancers and the expression correlates with demethylation of CpG sites in the promoter region of c-erbB-2 and survivin genes. *Cancer letters* *169*, 155-164.

Hauf, S., Cole, R.W., LaTerra, S., Zimmer, C., Schnapp, G., Walter, R., Heckel, A., van Meel, J., Rieder, C.L., and Peters, J.M. (2003). The small molecule Hesperadin reveals a role for Aurora B in correcting kinetochore-microtubule attachment and in maintaining the spindle assembly checkpoint. *The Journal of cell biology* *161*, 281-294.

Hill, R., and Lee, P.W. (2010). The DNA-dependent protein kinase (DNA-PK): More than just a case of making ends meet? *Cell cycle* *9*, 3460-3469.

Hinds, M.G., Norton, R.S., Vaux, D.L., and Day, C.L. (1999). Solution structure of a baculoviral inhibitor of apoptosis (IAP) repeat. *Nature structural biology* *6*, 648-651.

Hoffman, W.H., Biade, S., Zilfou, J.T., Chen, J., and Murphy, M. (2002). Transcriptional repression of the anti-apoptotic survivin gene by wild type p53. *The Journal of biological chemistry* *277*, 3247-3257.

Holliday, R. (1979). A new theory of carcinogenesis. *British journal of cancer* *40*, 513-522.

Honda, R., Korner, R., and Nigg, E.A. (2003). Exploring the functional interactions between Aurora B, INCENP, and survivin in mitosis. *Molecular biology of the cell* *14*, 3325-3341.

Hong, M., Ren, M.Q., Silva, J., Paul, A., Wilson, W.D., Schroeder, C., Weinberger, P., Janik, J., and Hao, Z. (2017). YM155 inhibits topoisomerase function. *Anti-cancer drugs* *28*, 142-152.

Hunter, A.M., LaCasse, E.C., and Korneluk, R.G. (2007). The inhibitors of apoptosis (IAPs) as cancer targets. *Apoptosis : an international journal on programmed cell death* *12*, 1543-1568.

Iliakis, G., Murmann, T., and Soni, A. (2015). Alternative end-joining repair pathways are the ultimate backup for abrogated classical non-homologous end-joining and homologous recombination repair: Implications for the formation of chromosome translocations. *Mutation research Genetic toxicology and environmental mutagenesis* *793*, 166-175.

Inagaki, H. (2007). Mucosa-associated lymphoid tissue lymphoma: molecular pathogenesis and clinicopathological significance. *Pathology international* *57*, 474-484.

Iwasa, T., Okamoto, I., Suzuki, M., Nakahara, T., Yamanaka, K., Hatashita, E., Yamada, Y., Fukuoka, M., Ono, K., and Nakagawa, K. (2008). Radiosensitizing effect of YM155, a novel small-molecule survivin suppressant, in non-small cell lung cancer cell lines. *Clinical cancer research : an official journal of the American Association for Cancer Research* *14*, 6496-6504.

Jackson, S.P., and Bartek, J. (2009). The DNA-damage response in human biology and disease. *Nature* *461*, 1071-1078.



---

Jares-Erijman, E.A., and Jovin, T.M. (2003). FRET imaging. *Nature biotechnology* *21*, 1387-1395.

Jette, N., and Lees-Miller, S.P. (2015). The DNA-dependent protein kinase: A multifunctional protein kinase with roles in DNA double strand break repair and mitosis. *Progress in biophysics and molecular biology* *117*, 194-205.

Jiang, X., Sun, Y., Chen, S., Roy, K., and Price, B.D. (2006). The FATC domains of PIKK proteins are functionally equivalent and participate in the Tip60-dependent activation of DNA-PKcs and ATM. *The Journal of biological chemistry* *281*, 15741-15746.

Jiang, Y., Saavedra, H.I., Holloway, M.P., Leone, G., and Altura, R.A. (2004). Aberrant regulation of survivin by the RB/E2F family of proteins. *The Journal of biological chemistry* *279*, 40511-40520.

Jones, P.A., and Laird, P.W. (1999). Cancer epigenetics comes of age. *Nature genetics* *21*, 163-167.

Kawakami, H., Tomita, M., Matsuda, T., Ohta, T., Tanaka, Y., Fujii, M., Hatano, M., Tokuhisa, T., and Mori, N. (2005). Transcriptional activation of survivin through the NF-kappaB pathway by human T-cell leukemia virus type I tax. *International journal of cancer* *115*, 967-974.

Kelly, R.J., Lopez-Chavez, A., Citrin, D., Janik, J.E., and Morris, J.C. (2011). Impacting tumor cell-fate by targeting the inhibitor of apoptosis protein survivin. *Molecular cancer* *10*, 35.

Khanna, K.K., and Jackson, S.P. (2001). DNA double-strand breaks: signaling, repair and the cancer connection. *Nature genetics* *27*, 247-254.

Kim, P.J., Plescia, J., Clevers, H., Fearon, E.R., and Altieri, D.C. (2003). Survivin and molecular pathogenesis of colorectal cancer. *Lancet* *362*, 205-209.

Kinzler, K.W., and Vogelstein, B. (1996). Lessons from hereditary colorectal cancer. *Cell* *87*, 159-170.

Knauer, S.K., Bier, C., Habtemichael, N., and Stauber, R.H. (2006). The Survivin-Crm1 interaction is essential for chromosomal passenger complex localization and function. *EMBO reports* *7*, 1259-1265.

Knauer, S.K., Kramer, O.H., Knosel, T., Engels, K., Rodel, F., Kovacs, A.F., Dietmaier, W., Klein-Hitpass, L., Habtemichael, N., Schweitzer, A., *et al.* (2007). Nuclear export is essential for the tumor-promoting activity of survivin. *FASEB journal : official publication of the Federation of American Societies for Experimental Biology* *21*, 207-216.

Koike, M., Awaji, T., Kataoka, M., Tsujimoto, G., Kartasova, T., Koike, A., and Shiomi, T. (1999). Differential subcellular localization of DNA-dependent protein kinase components Ku and DNA-PKcs during mitosis. *Journal of cell science* *112 ( Pt 22)*, 4031-4039.

Krieg, A., Mahotka, C., Krieg, T., Grabsch, H., Muller, W., Takeno, S., Suschek, C.V., Heydthausen, M., Gabbert, H.E., and Gerharz, C.D. (2002). Expression of different survivin

---

variants in gastric carcinomas: first clues to a role of survivin-2B in tumour progression. *British journal of cancer* *86*, 737-743.

Kuranaga, E., Kanuka, H., Tonoki, A., Takemoto, K., Tomioka, T., Kobayashi, M., Hayashi, S., and Miura, M. (2006). *Drosophila* IKK-related kinase regulates nonapoptotic function of caspases via degradation of IAPs. *Cell* *126*, 583-596.

Lechler, P., Wu, X., Bernhardt, W., Campean, V., Gastiger, S., Hackenbeck, T., Klanke, B., Weidemann, A., Warnecke, C., Amann, K., *et al.* (2007). The tumor gene survivin is highly expressed in adult renal tubular cells: implications for a pathophysiological role in the kidney. *The American journal of pathology* *171*, 1483-1498.

Lee, C.W., Raskett, C.M., Prudovsky, I., and Altieri, D.C. (2008). Molecular dependence of estrogen receptor-negative breast cancer on a notch-survivin signaling axis. *Cancer research* *68*, 5273-5281.

Lens, S.M., Vader, G., and Medema, R.H. (2006). The case for Survivin as mitotic regulator. *Current opinion in cell biology* *18*, 616-622.

Li, F., Ackermann, E.J., Bennett, C.F., Rothermel, A.L., Plescia, J., Tognin, S., Villa, A., Marchisio, P.C., and Altieri, D.C. (1999). Pleiotropic cell-division defects and apoptosis induced by interference with survivin function. *Nature cell biology* *1*, 461-466.

Li, F., and Altieri, D.C. (1999). Transcriptional analysis of human survivin gene expression. *The Biochemical journal* *344 Pt 2*, 305-311.

Li, F., Ambrosini, G., Chu, E.Y., Plescia, J., Tognin, S., Marchisio, P.C., and Altieri, D.C. (1998). Control of apoptosis and mitotic spindle checkpoint by survivin. *Nature* *396*, 580-584.

Li, F., Cheng, Q., Ling, X., Stablewski, A., Tang, L., Foster, B.A., Johnson, C.S., Rustum, Y.M., and Porter, C.W. (2010). Generation of a novel transgenic mouse model for bioluminescent monitoring of survivin gene activity in vivo at various pathophysiological processes: survivin expression overlaps with stem cell markers. *The American journal of pathology* *176*, 1629-1638.

Lieber, M.R. (2008). The mechanism of human nonhomologous DNA end joining. *The Journal of biological chemistry* *283*, 1-5.

Lieber, M.R. (2010). The mechanism of double-strand DNA break repair by the nonhomologous DNA end-joining pathway. *Annual review of biochemistry* *79*, 181-211.

Liston, P., Fong, W.G., Kelly, N.L., Toji, S., Miyazaki, T., Conte, D., Tamai, K., Craig, C.G., McBurney, M.W., and Korneluk, R.G. (2001). Identification of XAF1 as an antagonist of XIAP anti-Caspase activity. *Nature cell biology* *3*, 128-133.

Livak, K.J., and Schmittgen, T.D. (2001). Analysis of relative gene expression data using real-time quantitative PCR and the 2<sup>-</sup>(Delta Delta C(T)) Method. *Methods* *25*, 402-408.

---

Lorick, K.L., Jensen, J.P., Fang, S., Ong, A.M., Hatakeyama, S., and Weissman, A.M. (1999). RING fingers mediate ubiquitin-conjugating enzyme (E2)-dependent ubiquitination. *Proceedings of the National Academy of Sciences of the United States of America* *96*, 11364-11369.

Lou, Z., Minter-Dykhouse, K., Franco, S., Gostissa, M., Rivera, M.A., Celeste, A., Manis, J.P., van Deursen, J., Nussenzweig, A., Paull, T.T., *et al.* (2006). MDC1 maintains genomic stability by participating in the amplification of ATM-dependent DNA damage signals. *Molecular cell* *21*, 187-200.

Maachani, U.B., Kramp, T., Hanson, R., Zhao, S., Celiku, O., Shankavaram, U., Colombo, R., Caplen, N.J., Camphausen, K., and Tandle, A. (2015). Targeting MPS1 Enhances Radiosensitization of Human Glioblastoma by Modulating DNA Repair Proteins. *Molecular cancer research : MCR* *13*, 852-862.

Mahaney, B.L., Meek, K., and Lees-Miller, S.P. (2009). Repair of ionizing radiation-induced DNA double-strand breaks by non-homologous end-joining. *The Biochemical journal* *417*, 639-650.

Mahotka, C., Liebmann, J., Wenzel, M., Suschek, C.V., Schmitt, M., Gabbert, H.E., and Gerharz, C.D. (2002). Differential subcellular localization of functionally divergent survivin splice variants. *Cell death and differentiation* *9*, 1334-1342.

Mahotka, C., Wenzel, M., Springer, E., Gabbert, H.E., and Gerharz, C.D. (1999). Survivin-deltaEx3 and survivin-2B: two novel splice variants of the apoptosis inhibitor survivin with different antiapoptotic properties. *Cancer research* *59*, 6097-6102.

Makharashvili, N., Tubbs, A.T., Yang, S.H., Wang, H., Barton, O., Zhou, Y., Deshpande, R.A., Lee, J.H., Lobrich, M., Sleckman, B.P., *et al.* (2014). Catalytic and noncatalytic roles of the CtIP endonuclease in double-strand break end resection. *Molecular cell* *54*, 1022-1033.

Mandel, M., and Higa, A. (1970). Calcium-dependent bacteriophage DNA infection. *Journal of molecular biology* *53*, 159-162.

Marusawa, H., Matsuzawa, S., Welsh, K., Zou, H., Armstrong, R., Tamm, I., and Reed, J.C. (2003). HBXIP functions as a cofactor of survivin in apoptosis suppression. *The EMBO journal* *22*, 2729-2740.

Mashiach, E., Schneidman-Duhovny, D., Andrusier, N., Nussinov, R., and Wolfson, H.J. (2008). FireDock: a web server for fast interaction refinement in molecular docking. *Nucleic acids research* *36*, W229-232.

Meek, K., Douglas, P., Cui, X., Ding, Q., and Lees-Miller, S.P. (2007). trans Autophosphorylation at DNA-dependent protein kinase's two major autophosphorylation site clusters facilitates end processing but not end joining. *Molecular and cellular biology* *27*, 3881-3890.

Mehrotra, S., Languino, L.R., Raskett, C.M., Mercurio, A.M., Dohi, T., and Altieri, D.C. (2010). IAP regulation of metastasis. *Cancer cell* *17*, 53-64.

---

Merkle, D., Douglas, P., Moorhead, G.B., Leonenko, Z., Yu, Y., Cramb, D., Bazett-Jones, D.P., and Lees-Miller, S.P. (2002). The DNA-dependent protein kinase interacts with DNA to form a protein-DNA complex that is disrupted by phosphorylation. *Biochemistry* *41*, 12706-12714.

Mirza, A., McGuirk, M., Hockenberry, T.N., Wu, Q., Ashar, H., Black, S., Wen, S.F., Wang, L., Kirschmeier, P., Bishop, W.R., *et al.* (2002). Human survivin is negatively regulated by wild-type p53 and participates in p53-dependent apoptotic pathway. *Oncogene* *21*, 2613-2622.

Mita, A.C., Mita, M.M., Nawrocki, S.T., and Giles, F.J. (2008). Survivin: key regulator of mitosis and apoptosis and novel target for cancer therapeutics. *Clinical cancer research : an official journal of the American Association for Cancer Research* *14*, 5000-5005.

Miura, K., Fujibuchi, W., Ishida, K., Naitoh, T., Ogawa, H., Ando, T., Yazaki, N., Watanabe, K., Haneda, S., Shibata, C., *et al.* (2011). Inhibitor of apoptosis protein family as diagnostic markers and therapeutic targets of colorectal cancer. *Surgery today* *41*, 175-182.

O'Connor, D.S., Wall, N.R., Porter, A.C., and Altieri, D.C. (2002). A p34(cdc2) survival checkpoint in cancer. *Cancer cell* *2*, 43-54.

Ochi, T., Blackford, A.N., Coates, J., Jhujh, S., Mehmood, S., Tamura, N., Travers, J., Wu, Q., Draviam, V.M., Robinson, C.V., *et al.* (2015). DNA repair. PAXX, a paralog of XRCC4 and XLF, interacts with Ku to promote DNA double-strand break repair. *Science* *347*, 185-188.

Ohba, S., Mukherjee, J., See, W.L., and Pieper, R.O. (2014). Mutant IDH1-driven cellular transformation increases RAD51-mediated homologous recombination and temozolomide resistance. *Cancer research* *74*, 4836-4844.

Orth, M., Lauber, K., Niyazi, M., Friedl, A.A., Li, M., Maihofer, C., Schuttrumpf, L., Ernst, A., Niemoller, O.M., and Belka, C. (2014). Current concepts in clinical radiation oncology. *Radiation and environmental biophysics* *53*, 1-29.

Oshima, K., Takeda, M., Kuranaga, E., Ueda, R., Aigaki, T., Miura, M., and Hayashi, S. (2006). IKK epsilon regulates F actin assembly and interacts with Drosophila IAP1 in cellular morphogenesis. *Current biology : CB* *16*, 1531-1537.

Patterson, G.H., Piston, D.W., and Barisas, B.G. (2000). Forster distances between green fluorescent protein pairs. *Analytical biochemistry* *284*, 438-440.

Peery, R.C., Liu, J.Y., and Zhang, J.T. (2017). Targeting survivin for therapeutic discovery: past, present, and future promises. *Drug discovery today* *22*, 1466-1477.

Pennati, M., Folini, M., and Zaffaroni, N. (2008). Targeting survivin in cancer therapy. *Expert opinion on therapeutic targets* *12*, 463-476.

Petraki, C. (2014). The role of the inhibitor of apoptosis protein Survivin in cellular radiation response (Technical University Darmstadt).

---

Pfeiffer, P., Goedecke, W., Kuhfittig-Kulle, S., and Obe, G. (2004). Pathways of DNA double-strand break repair and their impact on the prevention and formation of chromosomal aberrations. *Cytogenetic and genome research* *104*, 7-13.

Plenchette, S., Cheung, H.H., Fong, W.G., LaCasse, E.C., and Korneluk, R.G. (2007). The role of XAF1 in cancer. *Current opinion in investigational drugs* *8*, 469-476.

Qin, Q., Cheng, H., Lu, J., Zhan, L., Zheng, J., Cai, J., Yang, X., Xu, L., Zhu, H., Zhang, C., *et al.* (2014). Small-molecule survivin inhibitor YM155 enhances radiosensitization in esophageal squamous cell carcinoma by the abrogation of G2 checkpoint and suppression of homologous recombination repair. *Journal of hematology & oncology* *7*, 62.

Ranjha, L., Howard, S.M., and Cejka, P. (2018). Main steps in DNA double-strand break repair: an introduction to homologous recombination and related processes. *Chromosoma*.

Reichert, S., Rodel, C., Mirsch, J., Harter, P.N., Tomicic, M.T., Mittelbronn, M., Kaina, B., and Rodel, F. (2011). Survivin inhibition and DNA double-strand break repair: a molecular mechanism to overcome radioresistance in glioblastoma. *Radiotherapy and oncology : journal of the European Society for Therapeutic Radiology and Oncology* *101*, 51-58.

Renkawitz, J., Lademann, C.A., and Jentsch, S. (2014). Mechanisms and principles of homology search during recombination. *Nature reviews Molecular cell biology* *15*, 369-383.

Riballo, E., Kuhne, M., Rief, N., Doherty, A., Smith, G.C., Recio, M.J., Reis, C., Dahm, K., Fricke, A., Krempler, A., *et al.* (2004). A pathway of double-strand break rejoining dependent upon ATM, Artemis, and proteins locating to gamma-H2AX foci. *Molecular cell* *16*, 715-724.

Risk Factors Collaborators, G.B.D. (2016). Global, regional, and national comparative risk assessment of 79 behavioural, environmental and occupational, and metabolic risks or clusters of risks, 1990-2015: a systematic analysis for the Global Burden of Disease Study 2015. *Lancet* *388*, 1659-1724.

Rodel, C., Haas, J., Groth, A., Grabenbauer, G.G., Sauer, R., and Rodel, F. (2003). Spontaneous and radiation-induced apoptosis in colorectal carcinoma cells with different intrinsic radiosensitivities: survivin as a radioresistance factor. *International journal of radiation oncology, biology, physics* *55*, 1341-1347.

Rodel, F., Frey, B., Leitmann, W., Capalbo, G., Weiss, C., and Rodel, C. (2008). Survivin antisense oligonucleotides effectively radiosensitize colorectal cancer cells in both tissue culture and murine xenograft models. *International journal of radiation oncology, biology, physics* *71*, 247-255.

Rodel, F., Hoffmann, J., Distel, L., Herrmann, M., Noisternig, T., Papadopoulos, T., Sauer, R., and Rodel, C. (2005). Survivin as a radioresistance factor, and prognostic and therapeutic target for radiotherapy in rectal cancer. *Cancer research* *65*, 4881-4887.

Rodel, F., Reichert, S., Sprenger, T., Gaipl, U.S., Mirsch, J., Liersch, T., Fulda, S., and Rodel, C. (2011). The role of survivin for radiation oncology: moving beyond apoptosis inhibition. *Current medicinal chemistry* *18*, 191-199.

---

Rodel, F., Sprenger, T., Kaina, B., Liersch, T., Rodel, C., Fulda, S., and Hehlhans, S. (2012). Survivin as a prognostic/predictive marker and molecular target in cancer therapy. *Current medicinal chemistry* 19, 3679-3688.

Rogakou, E.P., Pilch, D.R., Orr, A.H., Ivanova, V.S., and Bonner, W.M. (1998). DNA double-stranded breaks induce histone H2AX phosphorylation on serine 139. *The Journal of biological chemistry* 273, 5858-5868.

Rosa, J., Canovas, P., Islam, A., Altieri, D.C., and Doxsey, S.J. (2006). Survivin modulates microtubule dynamics and nucleation throughout the cell cycle. *Molecular biology of the cell* 17, 1483-1493.

Ruchaud, S., Carmena, M., and Earnshaw, W.C. (2007). The chromosomal passenger complex: one for all and all for one. *Cell* 131, 230-231.

Samuel, T., Okada, K., Hyer, M., Welsh, K., Zapata, J.M., and Reed, J.C. (2005). cIAP1 Localizes to the nuclear compartment and modulates the cell cycle. *Cancer research* 65, 210-218.

San Filippo, J., Sung, P., and Klein, H. (2008). Mechanism of eukaryotic homologous recombination. *Annual review of biochemistry* 77, 229-257.

Sancar, A., Lindsey-Boltz, L.A., Unsal-Kacmaz, K., and Linn, S. (2004). Molecular mechanisms of mammalian DNA repair and the DNA damage checkpoints. *Annual review of biochemistry* 73, 39-85.

Scheithauer, H., Belka, C., Lauber, K., and Gaipl, U.S. (2014). Immunological aspects of radiotherapy. *Radiation oncology* 9, 185.

Schmidt, S.M., Schag, K., Muller, M.R., Weck, M.M., Appel, S., Kanz, L., Grunebach, F., and Brossart, P. (2003). Survivin is a shared tumor-associated antigen expressed in a broad variety of malignancies and recognized by specific cytotoxic T cells. *Blood* 102, 571-576.

Schneidman-Duhovny, D., Inbar, Y., Nussinov, R., and Wolfson, H.J. (2005). PatchDock and SymmDock: servers for rigid and symmetric docking. *Nucleic acids research* 33, W363-367.

Selvin, P.R. (2000). The renaissance of fluorescence resonance energy transfer. *Nature structural biology* 7, 730-734.

Shibata, A., Conrad, S., Birraux, J., Geuting, V., Barton, O., Ismail, A., Kakarougkas, A., Meek, K., Taucher-Scholz, G., Lobrich, M., *et al.* (2011). Factors determining DNA double-strand break repair pathway choice in G2 phase. *The EMBO journal* 30, 1079-1092.

Shiloh, Y. (2003). ATM and related protein kinases: safeguarding genome integrity. *Nature reviews Cancer* 3, 155-168.

Sibanda, B.L., Chirgadze, D.Y., and Blundell, T.L. (2010). Crystal structure of DNA-PKcs reveals a large open-ring cradle comprised of HEAT repeats. *Nature* 463, 118-121.

---

Silke, J., Kratina, T., Chu, D., Ekert, P.G., Day, C.L., Pakusch, M., Huang, D.C., and Vaux, D.L. (2005). Determination of cell survival by RING-mediated regulation of inhibitor of apoptosis (IAP) protein abundance. *Proceedings of the National Academy of Sciences of the United States of America* *102*, 16182-16187.

Simkova, E., and Stanek, D. (2012). Probing nucleic acid interactions and pre-mRNA splicing by Forster Resonance Energy Transfer (FRET) microscopy. *International journal of molecular sciences* *13*, 14929-14945.

Skoufias, D.A., Mollinari, C., Lacroix, F.B., and Margolis, R.L. (2000). Human survivin is a kinetochore-associated passenger protein. *The Journal of cell biology* *151*, 1575-1582.

Smith, P.K., Krohn, R.I., Hermanson, G.T., Mallia, A.K., Gartner, F.H., Provenzano, M.D., Fujimoto, E.K., Goeke, N.M., Olson, B.J., and Klenk, D.C. (1985). Measurement of protein using bicinchoninic acid. *Analytical biochemistry* *150*, 76-85.

Sommer, K.W., Schamberger, C.J., Schmidt, G.E., Sasgary, S., and Cerni, C. (2003). Inhibitor of apoptosis protein (IAP) survivin is upregulated by oncogenic c-H-Ras. *Oncogene* *22*, 4266-4280.

Sorensen, C.S., Hansen, L.T., Dziegielewska, J., Syljuasen, R.G., Lundin, C., Bartek, J., and Helleday, T. (2005). The cell-cycle checkpoint kinase Chk1 is required for mammalian homologous recombination repair. *Nature cell biology* *7*, 195-201.

Sprenger, T., Rodel, F., Beissbarth, T., Conradi, L.C., Rothe, H., Homayounfar, K., Wolff, H.A., Ghadimi, B.M., Yildirim, M., Becker, H., *et al.* (2011). Failure of downregulation of survivin following neoadjuvant radiochemotherapy in rectal cancer is associated with distant metastases and shortened survival. *Clinical cancer research : an official journal of the American Association for Cancer Research* *17*, 1623-1631.

Srinivasula, S.M., and Ashwell, J.D. (2008). IAPs: what's in a name? *Molecular cell* *30*, 123-135.

Stauber, R.H., Rabenhorst, U., Reikik, A., Engels, K., Bier, C., and Knauer, S.K. (2006). Nucleocytoplasmic shuttling and the biological activity of mouse survivin are regulated by an active nuclear export signal. *Traffic* *7*, 1461-1472.

Sun, C., Cai, M., Gunasekera, A.H., Meadows, R.P., Wang, H., Chen, J., Zhang, H., Wu, W., Xu, N., Ng, S.C., *et al.* (1999). NMR structure and mutagenesis of the inhibitor-of-apoptosis protein XIAP. *Nature* *401*, 818-822.

Sun, C., Cai, M., Meadows, R.P., Xu, N., Gunasekera, A.H., Herrmann, J., Wu, J.C., and Fesik, S.W. (2000). NMR structure and mutagenesis of the third Bir domain of the inhibitor of apoptosis protein XIAP. *The Journal of biological chemistry* *275*, 33777-33781.

Sun, Y., Rombola, C., Jyothikumar, V., and Periasamy, A. (2013). Forster resonance energy transfer microscopy and spectroscopy for localizing protein-protein interactions in living cells. *Cytometry Part A : the journal of the International Society for Analytical Cytology* *83*, 780-793.

Symington, L.S., and Gautier, J. (2011). Double-strand break end resection and repair pathway choice. *Annual review of genetics* *45*, 247-271.

---

Terasawa, M., Ogawa, H., Tsukamoto, Y., Shinohara, M., Shirahige, K., Kleckner, N., and Ogawa, T. (2007). Meiotic recombination-related DNA synthesis and its implications for cross-over and non-cross-over recombinant formation. *Proceedings of the National Academy of Sciences of the United States of America* 104, 5965-5970.

Torre, L.A., Bray, F., Siegel, R.L., Ferlay, J., Lortet-Tieulent, J., and Jemal, A. (2015). Global cancer statistics, 2012. *CA: a cancer journal for clinicians* 65, 87-108.

Uematsu, N., Weterings, E., Yano, K., Morotomi-Yano, K., Jakob, B., Taucher-Scholz, G., Mari, P.O., van Gent, D.C., Chen, B.P., and Chen, D.J. (2007). Autophosphorylation of DNA-PKCS regulates its dynamics at DNA double-strand breaks. *The Journal of cell biology* 177, 219-229.

Uren, A.G., Wong, L., Pakusch, M., Fowler, K.J., Burrows, F.J., Vaux, D.L., and Choo, K.H. (2000). Survivin and the inner centromere protein INCENP show similar cell-cycle localization and gene knockout phenotype. *Current biology : CB* 10, 1319-1328.

Uziel, T., Lerenthal, Y., Moyal, L., Andegeko, Y., Mittelman, L., and Shiloh, Y. (2003). Requirement of the MRN complex for ATM activation by DNA damage. *The EMBO journal* 22, 5612-5621.

Vader, G., Kauw, J.J., Medema, R.H., and Lens, S.M. (2006). Survivin mediates targeting of the chromosomal passenger complex to the centromere and midbody. *EMBO reports* 7, 85-92.

Vaira, V., Lee, C.W., Goel, H.L., Bosari, S., Languino, L.R., and Altieri, D.C. (2007). Regulation of survivin expression by IGF-1/mTOR signaling. *Oncogene* 26, 2678-2684.

van Gent, D.C., Hoeijmakers, J.H., and Kanaar, R. (2001). Chromosomal stability and the DNA double-stranded break connection. *Nature reviews Genetics* 2, 196-206.

Velculescu, V.E., Madden, S.L., Zhang, L., Lash, A.E., Yu, J., Rago, C., Lal, A., Wang, C.J., Beaudry, G.A., Ciriello, K.M., *et al.* (1999). Analysis of human transcriptomes. *Nature genetics* 23, 387-388.

Vequaud, E., Desplanques, G., Jezequel, P., Juin, P., and Barille-Nion, S. (2016). Survivin contributes to DNA repair by homologous recombination in breast cancer cells. *Breast cancer research and treatment* 155, 53-63.

Verdecia, M.A., Huang, H., Dutil, E., Kaiser, D.A., Hunter, T., and Noel, J.P. (2000). Structure of the human anti-apoptotic protein survivin reveals a dimeric arrangement. *Nature structural biology* 7, 602-608.

Vong, Q.P., Cao, K., Li, H.Y., Iglesias, P.A., and Zheng, Y. (2005). Chromosome alignment and segregation regulated by ubiquitination of survivin. *Science* 310, 1499-1504.

Walker, A.I., Hunt, T., Jackson, R.J., and Anderson, C.W. (1985). Double-stranded DNA induces the phosphorylation of several proteins including the 90 000 mol. wt. heat-shock protein in animal cell extracts. *The EMBO journal* 4, 139-145.



---

Wang, R.H., Zheng, Y., Kim, H.S., Xu, X., Cao, L., Luhasen, T., Lee, M.H., Xiao, C., Vassilopoulos, A., Chen, W., *et al.* (2008). Interplay among BRCA1, SIRT1, and Survivin during BRCA1-associated tumorigenesis. *Molecular cell* 32, 11-20.

Wechsler, T., Chen, B.P., Harper, R., Morotomi-Yano, K., Huang, B.C., Meek, K., Cleaver, J.E., Chen, D.J., and Wabl, M. (2004). DNA-PKcs function regulated specifically by protein phosphatase 5. *Proceedings of the National Academy of Sciences of the United States of America* 101, 1247-1252.

Weissman, A.M. (2001). Themes and variations on ubiquitylation. *Nature reviews Molecular cell biology* 2, 169-178.

Weterings, E., and van Gent, D.C. (2004). The mechanism of non-homologous end-joining: a synopsis of synapsis. *DNA repair* 3, 1425-1435.

Wheatley, S.P., Barrett, R.M., Andrews, P.D., Medema, R.H., Morley, S.J., Swedlow, J.R., and Lens, S.M. (2007). Phosphorylation by aurora-B negatively regulates survivin function during mitosis. *Cell cycle* 6, 1220-1230.

Wheatley, S.P., Carvalho, A., Vagnarelli, P., and Earnshaw, W.C. (2001). INCENP is required for proper targeting of Survivin to the centromeres and the anaphase spindle during mitosis. *Current biology : CB* 11, 886-890.

WHO (2018). Cancer - Fact sheet (World Health Organization).

Wright, C.W., and Duckett, C.S. (2005). Reawakening the cellular death program in neoplasia through the therapeutic blockade of IAP function. *The Journal of clinical investigation* 115, 2673-2678.

Wu, X.Y., Fu, Z.X., and Wang, X.H. (2010). Effect of hypoxia-inducible factor 1-alpha on Survivin in colorectal cancer. *Molecular medicine reports* 3, 409-415.

Xia, F., and Altieri, D.C. (2006). Mitosis-independent survivin gene expression in vivo and regulation by p53. *Cancer research* 66, 3392-3395.

Yang, D., Welm, A., and Bishop, J.M. (2004). Cell division and cell survival in the absence of survivin. *Proceedings of the National Academy of Sciences of the United States of America* 101, 15100-15105.

Yin, X., Liu, M., Tian, Y., Wang, J., and Xu, Y. (2017). Cryo-EM structure of human DNA-PK holoenzyme. *Cell research* 27, 1341-1350.

Zender, L., Spector, M.S., Xue, W., Flemming, P., Cordon-Cardo, C., Silke, J., Fan, S.T., Luk, J.M., Wigler, M., Hannon, G.J., *et al.* (2006). Identification and validation of oncogenes in liver cancer using an integrative oncogenomic approach. *Cell* 125, 1253-1267.

Zhang, T., Otevrel, T., Gao, Z., Ehrlich, S.M., Fields, J.Z., and Boman, B.M. (2001). Evidence that APC regulates survivin expression: a possible mechanism contributing to the stem cell origin of colon cancer. *Cancer research* 61, 8664-8667.

---

Zhao, J., Tenev, T., Martins, L.M., Downward, J., and Lemoine, N.R. (2000). The ubiquitin-proteasome pathway regulates survivin degradation in a cell cycle-dependent manner. *Journal of cell science* 113 Pt 23, 4363-4371.

Zhu, Z., Chung, W.H., Shim, E.Y., Lee, S.E., and Ira, G. (2008). Sgs1 helicase and two nucleases Dna2 and Exo1 resect DNA double-strand break ends. *Cell* 134, 981-994.

---

## 7. Appendix

---

### 7.1. DNA sequences

---

#### Survivin wt

GGTGCCCCGACGTTGCCCCCTGCCTGGCAGCCCTTTCTCAAGGACCACCGCATCTCTACATTCA  
AGAAGTGGCCCTTCTTGGAGGGCTGCGCCTGCACCCCGGAGCGGATGGCCGAGGCTGGCTTCA  
TCCACTGCCCCACTGAGAACGAGCCAGACTTGGCCCAGTGTTTCTTCTGCTTCAAGGAGCTGGA  
AGGCTGGGAGCCAGATGACGACCCCATAGAGGAACATAAAAAGCATTCGTCCGTTGCGCTTT  
CCTTTCTGTCAAGAAGCAGTTTGAAGAATTAACCCTTGGTGAATTTTTGAAACTGGACAGAGAA  
AGAGCCAAGAACAAAATTGCAAAGGAAACCAACAATAAGAAGAAAGAATTTGAGGAAACTGCG  
GAGAAAGTGCGCCGTGCCATCGAGCAGCTGGCTGCCATGGAT

#### Survivin- $\Delta$ XIAP

ATGGGTGCCCCGACGTTGCCCCCTGCCTGGCAGCCCTTTCTCTCTAGAGCCGAGGCTGGCTTCA  
TCCACTGCCCCACTGAGAACGAGCCAGACTTGGCCCAGTGTTTCTTCTGCTTCAAGGAGCTGGA  
AGGCTGGGAGCCAGATGACGACCCCATAGAGGAACATAAAAAGCATTCGTCCGTTGCGCTTT  
CCTTTCTGTCAAGAAGCAGTTTGAAGAATTAACCCTTGGTGAATTTTTGAAACTGGACAGAGAA  
AGAGCCAAGAACAAAATTGCAAAGGAAACCAACAATAAGAAGAAAGAATTTGAGGAAACTGCG  
GAGAAAGTGCGCCGTGCCATCGAGCAGCTGGCTGCCATGGAT

#### PI3K-DNA-PKcs

ATGGAACACCCTTTCCTGGTGAAGGGTGGCGAGGACCTGCGGCAGGACCAGCGCGTGGAGCAG  
CTCTTCCAGGTCATGAATGGGATCCTGGCCCAAGACTCCGCCTGCAGCCAGAGGGCCCTGCAG  
CTGAGGACCTATAGCGTTGTGCCATGACCTCCAGGTTAGGATTAATTGAGTGGCTTGGAAATA  
CTGTTACCTTGAAGGACCTTCTTTTGAACACCATGTCCCAAGAGGAGAAGGCGGCTTACCTGAG  
TGATCCCAGGGCACCGCCGTGTGAATATAAAGATTGGCTGACAAAATGTCAGGAAAACATGAT  
GTTGGAGCTTACATGCTAATGTATAAGGGCGCTAATCGTACTGAAACAGTCACGTCTTTTAGAA  
AACGAGAAAAGTAAAGTGCCTGCTGATCTCTTAAAGCGGGCCTTCGTGAGGATGAGTACAAGCC  
CTGAGGCTTTCCTGGCGCTCCGCTCCCACTTCGCCAGCTCTCACGCTCTGATATGCATCAGCCA  
CTGGATCCTCGGGATTGGAGACAGACATCTGAACAACCTTATGGTGGCCATGGAGACTGGCGG  
CGTGATCGGGATCGACTTTGGGCATGCGTTTGGATCCGCTACACAGTTTCTGCCAGTCCCTGAG  
TTGATGCCTTTTCGGCTAACTCGCCAGTTTATCAATCTGATGTTACCAATGAAAGAAACGGGCC  
TTATGTACAGCATCATGGTACACGCACTCCGGGCCTTCGGCTCAGACCCTGGCCTGCTCACCAA  
CACCATGGATGTGTTTGTCAAGGAGCCCTCCTTTGATTGGAAAAAT

---

### HEAT1-DNA-PKcs

ATGGCGGGCTCCGGAGCCGGTGTGCGTTGCTCCCTGCTGCGGCTGCAGGAGACCTTGTCCGCT  
GCGGACCGCTGCGGTGCTGCCCTGGCCGGTCATCAACTGATCCGCGGCCTGGGGCAGGAATGC  
GTCCTGAGCAGCAGCCCCGCGGTGCTGGCATTACAGACATCTTTAGTTTTTTCCAGAGATTTCCG  
GTTTGCTTGTATTTGTCCGGAAGTCACTCAACAGTATTGAATTCGTGAATGTAGAGAAGAAAT  
CCTAAAGTTTTTATGTATTTTCTTAGAAAAAATGGGCCAGAAGATCGCACCTTACTCTGTTGAAA  
TTAAGAACACTTGTACCAGTGTATAACAAAAGATAGAGCTGCTAAATGTAAAATTCCAGCCCT  
GGACCTTCTTATTAAGTTACTTCAGACTTTTAGAAGTTCTAGACTCATGGATGAATTTAAAATTG  
GAGAATTATTTAGTAAATCTATGGAGAAGTTGCATTGAAAAAAAAAATACCAGATACAGTTTTA  
GAAAAAGTATATGAGCTCCTAGGATTATTGGGTGAAGTTCATCCTAGTGAGATGATAAATAATG  
CAGAAAACCTGTCCGCGCTTTTCTGGGTGAACTTAAGACCCAGATGACATCAGCAGTAAGAGA  
GCCCAAACCTACCTGTTCTGGCAGGATGTCTGAAGGGGTTGTCTCACTTCTGTGCAACTTCACT  
AAGTCCATGGAAGAAGATCCCAGACTTCAAGGGAGATTTTTAATTTTGTACTAAAGGCAATTC  
GTCCTCAGATTGATCTGAAGAGATATGCTGTGCCCTCAGCTGGCTTGCGCCTATTTGCCCTGCA  
TGCATCTCAGTTTAGCACCTGCCTTCTGGACAACCTACGTGTCTCTATTTGAAGTCTTGTTAAAGT  
GGTGTGCCACACAAATGTAGAATTGAAAAAGCTGCACTTTCAGCCCTGGAATCCTTTCTGAA  
ACAGGTTTCTAATATGGTGGCGAAAAATGCAGAAATGCATAAAAAATAAACTGCAGTACTTTATG  
GAGCAGTTTTATGGAATCATCAGAAATGTGGATTCGAACAACAAGGAGTTATCTATTGCTATCC  
GTGGATATGGACTTTTTTGCAGGACCGTGCAAGGTTATAAAC

### FATC-DNA-PKcs

ATGCTGAAAAAAGGAGGGTCATGGATTCAAGAAATAAATGTTGCTGAAAAAATTTGGTACCCCC  
GACAGAAAATATGTTACGCTAAGAGAAAGTTAGCAGGTGCCAATCCAGCAGTCATTACTTGTGA  
TGAGCTACTCCTGGGTCATGAGAAGGCCCTGCCTTACAGAGACTATGTGGCTGTGGCACGAGG  
AAGCAAAGATCACAACATTCGTGCCAAGAACCAGAGAGTGGGCTTTCAGAAGAGACTCAAGT  
GAAGTGCCTGATGGACCAGGCAACAGACCCCAACATCCTTGGCAGAACCTGGGAAGGATGGGA  
GCCCTG

---

---

## 7.2. Curriculum Vitae

---

**Name:** Fabian Weipert  
**Day of birth:** 10.06.1988  
**Place of birth:** Tübingen, Germany  
**Nationality:** German

### Education and Employment:

04/2014 – 03/2018      Technical University of Darmstadt, Germany  
PhD student and scholarship holder within the GRK 1657  
Subject: Studies on the interaction of the inhibitor of apoptosis protein Survivin with DNA-dependent protein kinase to modulate DNA double-strand break repair  
Project accomplished at the Molecular Radiation Biology research group, Department of Radiotherapy and Oncology, Goethe-University Frankfurt, Germany, Principal investigator: Prof. Franz Rödel

10/2011 – 02/2014      Goethe-University Frankfurt, Germany  
Master of Science Molecular Biosciences

08/2012 – 12/2012      University of Tromsø, Norway  
Department of Tumourbiology

10/2008 – 08/2011      University of Applied Sciences Darmstadt, Germany  
Bachelor of Science Biotechnology

10/2007 – 06/2008      Alternative civilian services at the KBF Neckar-Alb (work with handicapped people)

1998 – 2007              School education at St. Meinrad Gymnasium Rottenburg am Neckar, Germany. Degree: Abitur

During my PhD I had the opportunity to present my work at different conferences:  
EACR 2015 in Essen (Poster); DEGRO 2015 in Hamburg (Talk); GBS 2015 in Dresden (Poster); ERR 2016 in Amsterdam (Poster); GBS 2016 in Erlangen (Talk).

---

### 7.3. Own Work

---

Experiments, data analysis and writing of this thesis were all done by myself with exception of the following items:

Flow cytometry-based FRET assays in Figure 25 were performed by Melanie Hoffmann (Department of Radiotherapy and Oncology, Goethe-University Frankfurt, Germany) within her master thesis under my supervision.

Protein docking analysis in Figure 28 was performed by Ömer Güllülü (Department of Radiotherapy and Oncology, Goethe-University Frankfurt, Germany).

---

## 7.4. Acknowledgements

---

First of all, I want to thank Prof. Dr. Franz Rödel for his supervision and the chance to work on one of his research projects. I am very thankful for his guidance, patience and for his help with my dissertation.

Additionally, I want to thank Prof. Dr. Claus Rödel for the opportunity to write my thesis in his department and to use the facilities. A big thank to the medical physics department for the daily dosimetry and the MTAs for their help with the linear accelerator.

I am grateful to Prof. Dr. Bodo Laube and Prof. Dr. Markus Löbrich, my reviewers from the TU Darmstadt. Their support, comments and suggestions concerning this project during our graduate school retreats and thesis committee meetings were a big help.

Special thanks go to PD Dr. Stephanie Hehlhans for being a great help on countless occasions and for always having an open ear for all my questions. Thanks to Melanie Hoffmann for being a great master student. Thank you also for the careful proofreading of my thesis.

I would also like to express my gratitude to all former and present members of the radiation biology lab for the constructive discussions, their generous assistance throughout my whole PhD and for creating a very enjoyable working environment. Thank you all for such a great time in such a lovely team with lots of coffee, cake and frozen yoghurt. Thanks a million to Julius Oppermann and Jeannie Peifer for their great technical assistance and Ömer Güllülü for his help with the protein docking analysis (which I would never have understood without him).

Thanks to all scholars, fellows, professors and other members of the GRK 1657 graduate school at the TU Darmstadt, for their helpful discussions in our meetings and the great time we had during our retreats. The financial support given from the GRK 1657 is gratefully acknowledged.

Last but not least, I want to thank my family for their help during all of my studies. I would not have made it this far without your support.

Lisa, I am forever grateful for having you by my side. Thank you so much for your patience and support whenever I needed it.